SPHERICAL t_ϵ-DESIGN AND APPROXIMATION ON THE SPHERE: THEORY AND ALGORITHMS

YANG ZHOU

Ph.D

The Hong Kong Polytechnic University

2014

The Hong Kong Polytechnic University

Department of Applied Mathematics

Spherical t_ϵ-Design and Approximation on the Sphere: Theory and Algorithms

Yang Zhou

A thesis submitted in partial fulfilment of the requirements

for the degree of Doctor of Philosophy

July 2014

Certificate of Originality

I hereby declare that this thesis is my own work and that, to the best of my knowledge and belief, it reproduces no material previously published or written, nor material that has been accepted for the award of any other degree or diploma, except where due acknowledgement has been made in the text.

_____(Signed)

ZHOU Yang (Name of student)

Dedicate to my parents.

Abstract

This thesis concentrates on the spherical t_ϵ-designs on the two-sphere, numerical algorithms for finding spherical t_ϵ-designs and numerical approximation on the sphere using spherical t_ϵ-designs.

A set of points on the unit sphere is called a spherical t-design if the average value of any polynomial of degree at most t over the set is equal to the average value of the polynomial over the sphere. Spherical t-designs have many important applications in geophysics and bioengineering, and provide many challenging problems in computational mathematics. As a generalization of spherical t-design, we define a spherical t_ϵ-design with $0 \leqslant \epsilon < 1$ which provides an integration rule with a set of points on the unit sphere and positive weights satisfying $(1-\epsilon)^2 \leqslant \frac{\min \text{weight}}{\max \text{weight}} \leqslant 1$. The integration rule also gives the exact integral for any polynomial of degree at most t. Due to the flexibility of choice for the weights, the number of points in the integration rule can be less for making the exact integral for any polynomial of degree at most t. To our knowledge, so far there is no theoretical result which proves the existence of a spherical t-design with $(t+1)^2$ points for arbitrary t. In 2010 Chen, Frommer and Lang developed a computation-assist proof for the existence of spherical t-designs for $t = 1, \ldots, 100$ with $(t+1)^2$ points. Based on the algorithm proposed in that paper, a series of interval enclosures for spherical t-design was computed. In this thesis we prove that all the point sets arbitrarily chosen in these interval enclosures are spherical t_ϵ-designs and give an upper bound of ϵ. We then study the variational characterization and the worst-case error of spherical t_ϵ-design. Based on the reproducing kernel theory and its relationship with the geodesic distance, we propose a way to compute the worst-case error for numerical integration using spherical t_ϵ-design in Sobolev space.

Moreover, we propose an approach for finding spherical t_ϵ-designs. We show that finding a spherical t_ϵ-design can be reformulated as a system of polynomial equations with box constraints. Using the projection operator, the system can be written as a nonsmooth nonconvex least squares problem with zero residual. We propose a smoothing trust region filter algorithm for solving such problems. We present convergence theorems of the proposed algorithm to a Clarke stationary point or a global minimizer of the problem under certain conditions. Preliminary numerical experiments show the efficiency of the proposed algorithm for finding spherical t_ϵ-designs.

Another contribution in this thesis is the numerical approximation on the sphere using regularized least squares approaches. We consider two regularized least squares problems using spherical t_ϵ-designs: regularized polynomial approximation on the sphere, and regularized hybrid approximation on the sphere using both radial basis functions and spherical polynomials. For the first approach we apply the ℓ_2 regularized form and give an approximation quality estimation. For the second approach we study its ℓ_1 regularized form and solve the problem using alternating direction method with multipliers. Numerical experiments are given to demonstrate the effectiveness of these two models.

Acknowledgements

The endeavor of carrying out research is a fascinatingly non-isolated activity. This thesis would not have been possible without the support, encouragement, input and ideas of many people. I am grateful to the several individuals who have supported me in various ways during the PhD program and would like to hereby acknowledge their assistance.

First and foremost, I wish to express my deep thanks to my supervisor, Prof. Chen Xiaojun, for her enlightening guidance, invaluable discussions, insightful ideas and generous support throughout the years. Without her valuable advice and motherly patient guidance, I can not make this study possible.

I would like to thank Prof. Huang Tingzhu, Prof. Xiang Shuhuang, Dr. Du Shouqiang and Dr. Wang Zhengyu for their great encouragement and accompany. I own multiple thanks to my academic brothers and sisters, Dr. Bian Wei, Dr. An Congpei, Dr. Liu Xin, Dr. Zhang Yanfang, Dr. Sun Hailin, Ms. Wang Qiyu, Mr. Wang Hong and Mr. Yang Lei for their spiritual and substantial support. To Dr. Qiao Zhonghua, Dr. Ma Cheng, Dr. Bian Chuanxin, Dr. Tian boshi, Mr. Yang Jin, Mr. Jin Haiyang, Mr. Zhang Hu, Ms. Wei Yan, Dr. Hu Yaohua and Mr. Wang Shujun I am grateful for their help and friendship. The help from the members in DE405, DE407, HJ609 and P115 (Department of Applied Mathematics) are deeply acknowledged. I gratefully acknowledge The Hong Kong Polytechnic University for the financial support during the entire period of my candidature. I also express my gratitude to the supporting status in Department of Applied Mathematics for their kindly help.

Last but far from least, I would like to express my special thanks to my parents, my sister and my fiancee for their love, encouragement and support to me.

Contents

List of Figures

List of Tables

List of Notations

$\mathbb{N}$	set of natrual numbers
$\mathbb{R}$	set of real numbers
$\mathbb{R}^n$	set of n-dimensional real vectors
$\mathbb{R}^{m\times n}$	set of $m \times n$ real matrices
$\mathbb{S}^d$	unit d-sphere
$\mathbb{S}^2$	unit 2-sphere
X_N	point set on the unit sphere
Δ	Laplace operator
Δ^*	Laplace-Beltrami operator
$\omega_d(\mathbf{x})$	normalized surface measure on $\mathbb{S}^d$
$\omega(\mathbf{x})$	normalized surface measure on $\mathbb{S}^2$
$\mathbb{P}_t$	space of spherical polynomials with degree not over t
$\rho(\cdot)$	separate distance of a point set
$\sigma(\cdot,\cdot)$	Hausdorff distance between two point sets
∇	gradient operator
$\mathbb{L}_2(\Omega)$	space of real square integrable functions defined on the region Ω
$\deg(p)$	degree of a polynomial p
$C(\Omega)$	set of real continuous functions defined on the region Ω
$\mathbb{H}^s(\Omega)$	Sobolev space defined on Ω
$F : X \to Y$	a mapping with domain X and range in Y

$\mathbb{P}_t$	polynomial space with degree t on 2-sphere
$\mathfrak{U}^n$	space of n-dimensional rotationally invariant operator
P_ℓ	ℓ-order Legendre polynomial
h_{X_N}	mesh norm of point set X_N
$\mathbb{T}_t$	space of real trigonometric polynomials with order at most t
∂f	subdifferential of the nondifferentiable function f
$\lceil \cdot \rceil$	rounding up to next integer of a real number
$\lfloor \cdot \rfloor$	rounding down to last integer of a real number
$A^\dagger$	generalized inverse of a matrix
$\mathrm{con}\{\cdot\}$	convex hull of a set
$\Gamma(\cdot)$	Gamma function

Chapter 1

Introduction

As a long-standing difficult problem, distribution of points on the sphere is widely studied in recent years. In 1998 Steve Smale proposed a list of eighteen unsolved problems in mathematics, in which distribution of points on the two-sphere is the ranked 7th problem among them.

There are numerous applications of distribution of points on the two-sphere. This problem appears in plenty of academic areas which is relative to numerical integration and approximation on the sphere. For instance, the earth's surface is an approximate sphere $\mathbb{S}^2$, and distribution of points is relevant to many problems of geophysics, including climate modeling, geodetic engineering and global navigation. Especially, polynomial approximation on $\mathbb{S}^2$ has wide applications in coding communications, scattering and inverse scattering problem, viruses analysis and surface reconstruction.

Based on different purposes and strategies, various kinds of point systems are proposed in recent decades, such as minimal energy points [46], extremal points [55, 63] and equal area partitioning points [54, 57]. As an important type of point systems, spherical t-design is a set of points with the average value of any polynomial of degree at most t over the set equal to the average value of the polynomial over the sphere.

In this thesis we investigate a new concept called spherical t_ϵ-design with $0 \leqslant \epsilon < 1$, which is a generalization of spherical t-design. The organization of this thesis is as follows.

In the rest of Chapter 1 we will introduce some backgrounds about the distribution of points on the two-sphere, and its applications to numerical approximation and integration

on the two-sphere.

In Chapter 2 we study the relationship between interval enclosures containing fundamental spherical t-designs and spherical t_ϵ-designs. We prove that all the point sets arbitrarily chosen in the interval enclosures proposed in [25] are spherical t_ϵ-designs and give an upper bound of ϵ. We then study the variational characterization and the worst-case error of spherical t_ϵ-design. Based on the reproducing kernel theory and its relationship with the geodesic distance, we propose a way to compute the worst-case error for numerical integration using spherical t_ϵ-design in Sobolev space.

In Chapter 3 we propose an approach for finding spherical t_ϵ-designs. We show that finding a spherical t_ϵ-design can be reformulated as a system of polynomial equations with box constraints. Using the projection operator, the system can be written as a nonsmooth nonconvex least squares problem with zero residual. We propose a smoothing trust region filter algorithm for solving such problems. We present convergence theorems of the proposed algorithm to a Clarke stationary point or a global minimizer of the problem under certain conditions. Preliminary numerical experiments show the efficiency of the proposed algorithm for finding spherical t_ϵ-designs.

In Chapter 4 we apply the spherical t_ϵ-designs to the numerical approximation on the sphere using regularized least squares approaches. We consider two regularized least squares problems using spherical t_ϵ-designs: regularized polynomial approximation on the sphere, and regularized hybrid approximation on the sphere using both radial basis functions and spherical polynomials. For the first approach we apply the l_2 regularized form and give an approximation quality estimation. For the second approach we study its l_1 regularized form and solve the problem using alternating direction method with multipliers.

We implement relative algorithms and models in MATLAB 2012b on a Lenovo Thinkcenter PC equipped with Intel Core i7-3770 3.4G Hz CPU, 8 GB RAM running Windows 7. Numerical experiments are given to demonstrate the effectiveness of these two models.

1.1 Spherical harmonics

1.1.1 Unit sphere and spherical geometry

The unit sphere is a nonempty compact subset of $\mathbb{R}^{d+1}$ defined by

$$\mathbb{S}^d := \{\mathbf{x} = (x_1, \ldots, x_{d+1})^T \in \mathbb{R}^{d+1} \mid \|\mathbf{x}\|_2 = 1\},$$

where $\|\cdot\|_2$ means the Euclidean norm, i.e.,

$$\|\mathbf{x}\|_2 = \mathbf{x}^T\mathbf{x} = \sum_{i=1}^{d+1} x_i^2.$$

The unit sphere $\mathbb{S}^2 = \{\mathbf{x} = (x, y, z)^T \in \mathbb{R}^3 \ : \ x^2 + y^2 + z^2 = 1\}$ can be parameterized by spherical polar coordinates (θ, φ), where θ and φ are the polar and azimuthal angles respectively, satisfying $0 \leqslant \theta \leqslant \pi$ and $0 \leqslant \varphi \leqslant 2\pi$. That is to say,

$$\mathbf{x} = \begin{pmatrix} \sin\theta\cos\varphi \\ \sin\theta\sin\varphi \\ \cos\theta \end{pmatrix}. \tag{1.1}$$

One significant property of $\mathbb{S}^d$ is that it can be generated from one single point by application of elements of the group of all (proper) rotations $\mathbb{R}^{d+1} \to \mathbb{R}^{d+1}$. Note that with respect to the standard basis in $\mathbb{R}^{d+1}$, the elements of this group are represented by the elements of

$$\mathfrak{U}^{d+1} := \{S \in \mathbb{R}^{(d+1)\times(d+1)} \mid SS^T = I, \det(S) = 1\}. \tag{1.2}$$

For multivariate continuous functions on the sphere

$$f : \mathbb{S}^d \to \mathbb{R},$$

denote the space of all these functions by $C(\mathbb{S}^d)$, provided with the maximum norm, i.e.,

$$\|f\|_{C(\mathbb{S}^d)} = \|f\|_\infty := \sup_{\mathbf{x}\in\mathbb{S}^d} |f(\mathbf{x})|.$$

For $f \in C(\mathbb{S}^d)$ and $S \in \mathfrak{U}^{d+1}$, define $f_S \in C(\mathbb{S}^d)$ by

$$f_S(\mathbf{x}) := f(S\mathbf{x}), \ \mathbf{x} \in \mathbb{S}^d.$$

If $f \in \mathbb{V}$ and $\mathbb{V}$ is a subspace of $C(\mathbb{S}^d)$, f_S needs not to be located in $\mathbb{V}$ for arbitrary S.

Definition 1.1. (Rotationally invariant) *A subspace $\mathbb{V}$ of $C(\mathbb{S}^d)$ is called rotationally invariant if $\mathbf{x} \in \mathbb{S}^d$ implies $S\mathbf{x} \in \mathbb{S}^d$ for all $S \in \mathfrak{U}^{d+1}$ and if $f_S \in \mathbb{V}$ holds for arbitrary $f \in \mathbb{V}$, $S \in \mathfrak{U}^{d+1}$.*

Obviously, $C(\mathbb{S}^d)$ is rotationally invariant. Moreover, there are elements in $C(\mathbb{S}^d)$ with the property that $f_S = f$ for some rotations S. For instance, if f is defined by

$$f(\mathbf{x}) = g(\mathbf{t} \cdot \mathbf{x}), \ \mathbf{x} \in \mathbb{S}^d,$$

for some $g \in C[-1, 1]$ and $\mathbf{t} \in \mathbb{S}^d$, then $f_S = f$ holds for arbitrary $S \in \mathfrak{U}^{d+1}$ which keep $\mathbf{t}$ fixed.

In this thesis we will concentrate on studying the point sets on the two-sphere $\mathbb{S}^2$. Denote a point set on $\mathbb{S}^2$ by $X_N = \{\mathbf{x}_1, \ldots, \mathbf{x}_N\}$, the mesh norm of X_N describes the radius of the largest "hole" on the surface of the sphere with none of $\mathbf{x}_i$ in it.

Definition 1.2. (Mesh norm) *The mesh norm h_{X_N} of a set $X_N \subset \mathbb{S}^d$ is defined by*

$$h_{X_N} := \max_{\mathbf{x} \in \mathbb{S}^d} \min_{\mathbf{y} \in X_N} \cos^{-1}(\mathbf{x} \cdot \mathbf{y}). \tag{1.3}$$

The reproducing kernel is a very useful tool to deal with the representation for approximation schemes. For detail, we refer to the classical article [4]. Let $\mathbb{B}(\mathbb{S}^2)$ be a class of functions defined in $\mathbb{S}^2$, forming a Hilbert space with inner product $\langle \cdot, \cdot \rangle_{\mathbb{B}}$ and norm $\| \cdot \|_{\mathbb{B}}$. The function $\phi(\mathbf{x}, \mathbf{y})$ of $\mathbf{x}, \mathbf{y} \in \mathbb{S}^2$ is called a reproducing kernel of $\mathbb{B}$ if

1. For every $\mathbf{y}$, $\phi(\mathbf{x}, \mathbf{y})$ as function of $\mathbf{x}$ belongs to $\mathbb{B}$.

2. For every $\mathbf{y} \in \mathbb{S}^2$ and every $f \in \mathbb{B}$,

$$f(\mathbf{y}) = \langle f(\cdot), \phi(\cdot, \mathbf{y}) \rangle_{\mathbb{B}}. \tag{1.4}$$

From the definition we can see that $\phi(\cdot, \cdot)$ is invariant under rotation, and is bizonal following the definition below.

Definition 1.3. [67] *A function $\phi(\cdot, \cdot) \in C(\mathbb{S}^2 \times \mathbb{S}^2)$ is called bizonal if for arbitrary points $\mathbf{x}, \mathbf{y} \in \mathbb{S}^2$, the following holds*

$$\phi(\mathbf{x}, \mathbf{y}) = \psi(\mathbf{x} \cdot \mathbf{y})$$

for some univariate function $\psi : [-1, 1] \to \mathbb{R}$.

1.1.2 Spherical harmonic polynomials

The restriction of a homogeneous polynomial in 3-dimension of degree $\ell \geqslant 0$ to the sphere $\mathbb{S}^2$ is called a spherical polynomial of degree ℓ. Denote the space of all spherical polynomials on $\mathbb{S}^2$ of degree $\ell \geqslant 0$ by $\mathbb{Y}_\ell := \mathbb{Y}_\ell(\mathbb{S}^2)$ and it is well known that the dimension of $\mathbb{Y}_\ell$ is

$$\dim(\mathbb{Y}_\ell) = 2\ell + 1. \tag{1.5}$$

Denote the space of square integrable functions on $\mathbb{S}^2$ by $\mathbb{L}_2(\mathbb{S}^2)$. Then it is a Hilbert space with the inner product defined as

$$(f, g)_{\mathbb{L}_2(\mathbb{S}^d)} = \int_{\mathbb{S}^d} f(\mathbf{x})g(\mathbf{x})d\omega(\mathbf{x}), \quad f, g \in \mathbb{L}_2(\mathbb{S}^2), \tag{1.6}$$

and the induced norm

$$\|f\|_{\mathbb{L}_2(\mathbb{S}^d)} = \left(\int_{\mathbb{S}^d} |f(\mathbf{x})|^2 d\omega(\mathbf{x})\right)^{\frac{1}{2}}, \quad f \in \mathbb{L}_2(\mathbb{S}^2), \tag{1.7}$$

where $\omega(\mathbf{x})$ denotes the normalized surface measure on $\mathbb{S}^2$. By Corollary 2.15 in [5], we have that for $\ell \neq \ell'$,

$$\mathbb{Y}_\ell \perp \mathbb{Y}_{\ell'}, \tag{1.8}$$

with respect to the $\mathbb{L}_2(\mathbb{S}^2)$ inner product.

If p is a polynomial, then we denote its restriction to $\mathbb{S}^2$ by $p|_{\mathbb{S}^2}$, and we define

$$\mathbb{P}_t = \mathbb{P}_t(\mathbb{S}^2) = \{p|_{\mathbb{S}^2} \ : \ \deg(p) \leqslant t\}, \tag{1.9}$$

as the space of spherical polynomials of degree $\leqslant t$. Thus together with (1.8) we can have that

$$\mathbb{P}_t = \mathbb{Y}_0 \oplus \mathbb{Y}_1 \ldots \oplus \mathbb{Y}_t, \tag{1.10}$$

is a decomposition of $\mathbb{P}_t$ into orthogonal subspaces, with the orthogonality based on the $\mathbb{L}_2(\mathbb{S}^2)$ inner product. Therefore, a basis for $\mathbb{P}_t$ can be introduced by giving a basis for each

of the subspaces $\mathbb{Y}_\ell,\ \ell > 0$. Denote an $\mathbb{L}_2$-orthogonal basis of $\mathbb{Y}_\ell$ by $\{Y_{\ell,k},\ k = 1, \ldots, 2\ell+1\}$ for a fixed ℓ. We call $Y_{\ell,k}$ a spherical harmonic (polynomial) with degree ℓ and order k. The spherical harmonics is also the eigenfunction of the Laplace's equation with the form as

$$\Delta u = 0 \quad \text{or} \quad \nabla^2 u = 0, \tag{1.11}$$

where $\Delta = \nabla^2$ is the Laplace operator and u is a scalar function. As their name suggests, the spherical harmonics arise from solving the angular portion of Laplace's equation in spherical coordinates using separation of variables. For $d = 2$, $\{Y_{\ell,k}, \ell = 0, \ldots, \infty, k = 1, \ldots, 2\ell + 1\}$ is the eigenvalue function set of the Laplace operator. Then from (1.8) we know that all $Y_{\ell,k}$ are $\mathbb{L}_2$-orthogonal to each other, in the sense that

$$\int_{\mathbb{S}^2} Y_{\ell,k} Y_{\ell',k'} d\omega(\mathbf{x}) = \delta_{\ell,\ell'}\delta_{k,k'}, \quad \ell, \ell' = 0, \ldots, t;\ k, k' = 1, \ldots, 2\ell + 1, \tag{1.12}$$

where $\delta_{\ell,\ell'}$ is the Kronecker delta. Therefore, $\{Y_{\ell,k},\ \ell = 1, \ldots, t,\ k = 1, \ldots, 2\ell + 1\ \}$ is a $\mathbb{L}_2$-orthonormal basis of the space $\mathbb{P}_t$. And it is easy to see that

$$d_t = \dim(\mathbb{P}_t) = \sum_{\ell=0}^{t} 2\ell + 1 = (t + 1)^2. \tag{1.13}$$

The spherical harmonic basis functions derived in this fashion take on complex values, but a complementary, strictly real-valued set of harmonics can also be defined. The close form of real spherical harmonic polynomials $Y_{\ell,k},\ \ell = 0, \ldots, \infty,\ k = 1, \ldots, 2\ell + 1$ on $\mathbb{S}^2$ is [1, 5]

$$Y_{\ell,k}(\theta, \varphi) = \begin{cases} N_{\ell,k} P_\ell^{\ell+1-k}(\cos\theta)\cos k\varphi, & k = 1, \ldots, \ell, \\ N_{\ell,k} P_\ell^0(\cos\theta), & k = \ell + 1, \\ N_{\ell,k} P_\ell^{k-\ell-1}(\cos\theta)\sin k\varphi, & k = \ell + 2, \ldots, 2\ell + 1, \end{cases} \tag{1.14}$$

where $N_{\ell,k}$ are the normalization coefficients

$$N_{\ell,k} = \sqrt{\frac{2\ell + 1}{4\pi} \frac{(\ell - |k - \ell - 1|)!}{(\ell + |k - \ell - 1|)!}}, \quad k = 1, \ldots, 2\ell + 1,$$

and $P_\ell : [-1, 1] \to \mathbb{R}$ are the associated Legendre polynomials. Furthermore, the spherical gradient $\nabla^*(\cdot)$ of $Y_{\ell,k}$ could be represented as [42, 70]

$$\frac{\partial}{\partial\varphi}Y_{\ell,k}(\theta,\varphi) = \begin{cases} -kN_{\ell,k}P_\ell^{|k|}(\cos\theta)\sin k\varphi, & k = -\ell,\ldots,-1, \\ 0, & k = 0, \\ kN_{\ell,k}P_\ell^{k}(\cos\theta)\cos k\varphi, & k = 1,\ldots,\ell, \end{cases} \tag{1.15}$$

$$\sin\theta\frac{\partial}{\partial\theta}Y_{\ell,k}(\theta,\varphi) = \ell\sqrt{\frac{(\ell+1)^2-k^2}{(2\ell+1)(2\ell+3)}}Y_{\ell+1,k}(\theta,\varphi) - (\ell+1)\sqrt{\frac{\ell^2-k^2}{(2\ell+1)(2\ell-1)}}Y_{\ell-1,k}(\theta,\varphi). \tag{1.16}$$

Moreover, for any given $Y_{\ell,k}$, we have

1. $Y_{\ell,k}(\theta,\varphi+2\pi) = Y_{\ell,k}(\theta,\varphi)$,
2. $|Y_{\ell,k}(0,\varphi)| < \infty$,
3. $|Y_{\ell,k}(\pi,\varphi)| < \infty$,
4. $\|Y_{\ell,k}\|_\infty \leqslant \sqrt{\frac{2\ell+1}{4\pi}}$ for $k = 1,\ldots,2\ell+1$, $\ell = 0,\ldots,\infty$.

Another important result about spherical harmonics is the addition theorem, which is concerned with the relationship between spherical harmonics and Legendre polynomials. The addition theorem holds on $\mathbb{S}^d$ with $d \geqslant 1$. Similar with what is defined in $\mathbb{S}^2$ case, we define $\mathbb{Y}_\ell^d$ as the space of all spherical polynomials with degree ℓ on $\mathbb{S}^d$, and let $P_{\ell,d}$ be the normalized Gegenbauer polynomial [1], then the addition theorem can be represented as follows.

Theorem 1.4. [5] **(Addition Theorem)** *Let $\{Y_{\ell,k}^{(d)} : k = 1,\ldots,M(d,\ell)\}$ be an orthogonal basis of $\mathbb{Y}_\ell^d$, i.e.,*

$$\int_{\mathbb{S}^d} Y_{\ell,k}^{(d)}(\mathbf{x})Y_{\ell,k'}^{(d)}(\mathbf{x})d\omega_d(\mathbf{x}) = \delta_{kk'}, \quad 1 \leqslant k,k' \leqslant M(d,\ell).$$

Then

$$\sum_{k=1}^{M(d,\ell)} Y_{\ell,k}^{(d)}(\mathbf{x})Y_{\ell,k}^{(d)}(\mathbf{y}) = M(d,\ell)P_{\ell,d}(\mathbf{x}\cdot\mathbf{y}) \quad \forall\mathbf{x},\mathbf{y}\in\mathbb{S}^d. \tag{1.17}$$

Another important result is Berstein's inequality. Define the set of trigonometric polynomials $\mathbb{T}_t^c$ by

$$\mathbb{T}_t^c = \left\{ p \ : \ p(\theta) := \sum_{k=-t}^{t} a_k e^{ik\theta}, \ a_k \in \mathbb{C} \right\}. \tag{1.18}$$

A real trigonometric polynomial of degree at most t is an element of $\mathbb{T}_t^c$ taking only real values on the real line. We denote by $\mathbb{T}_t$ the set of all real trigonometric polynomials of degree at most t.

Theorem 1.5. [16] **(Bernstein's Inequality)** *The inequality*

$$\|p^{(m)}\|_{C^m(\mathbb{R})} \leqslant t^m \|p\|_{C^m(\mathbb{R})} \tag{1.19}$$

holds for every $p \in \mathbb{T}_t$, where $\|\cdot\|_{C^m(\mathbb{R})}$ denotes the uniform norm on $C^m(\mathbb{R})$.

1.2 Distribution of points on the sphere

1.2.1 Spherical t-designs

Firstly, we show the definition of spherical t-design which was first introduced in the groundbreaking paper [36] by Delsarte, Goethals and Seidel.

Definition 1.6. (Spherical t-design) *Let $X_N = \{\mathbf{x}_1, \dots, \mathbf{x}_N\}$ be a set of N points on the unit sphere $\mathbb{S}^d$, and let $\mathbb{P}_t := \mathbb{P}_t(\mathbb{S}^d)$ be the linear space of restrictions of polynomials of degree at most t in $d+1$ variables to $\mathbb{S}^d$. The set X_N is a spherical t-design if*

$$\frac{1}{N}\sum_{j=1}^{N} p(\mathbf{x}_j) = \frac{1}{|\mathbb{S}^d|}\int_{\mathbb{S}^d} p(\mathbf{x}) d\omega_d(\mathbf{x}) \tag{1.20}$$

holds for all spherical polynomials $p \in \mathbb{P}_t$, where $d\omega_d(\mathbf{x})$ denotes the normalized surface measure on $\mathbb{S}^d$.

In the past decades, spherical t-designs have been extremely studied, see [2, 3, 6, 7, 8, 9, 25, 43, 47, 64]. The existence of spherical designs for all values t was proved by Seymour and Zaslavsky [60] in 1984. However, the number of points N needed to construct a spherical t-design is a long-standing open problem.

For each $t, d \in \mathbb{N}$ denote by $N(d,t)$ the minimal number of points in a spherical t-design in $\mathbb{S}^d$. The following lower bound

$$N(d,t) \geqslant \begin{cases} \binom{d+k}{d} + \binom{d+k-1}{d} & \text{if } t = 2k, \\ 2\binom{d+k}{d} & \text{if } t = 2k+1, \end{cases} \tag{1.21}$$

is proved in [36]. Spherical t-designs attaining this bound are called tight. It has been proved that the vertices of a regular $t+1$-gon form a tight spherical t-design on the circle $\mathbb{S}^1$, so we have $N(1,t) = t+1$, see [36]. Exactly eight tight spherical designs are known for $d \geqslant 2$ and $t \geqslant 4$. All such configurations of points are highly symmetrical and optimal from many different points of view, see [33, 35]. Unfortunately, tight designs rarely exist.

In particular, Bannai and Damerell [7, 10] have shown that tight spherical designs with $d \geqslant 2$ and $t \geqslant 4$ may exist only for $t = 4, 5, 7$ or 11.

In [50, 61] a well known lower bound of the number of positive weight quadrature points was established for general regions. Denote $\Omega \subseteq \mathbb{R}^d$ by a region which is either the closure of a connected open domain, or a smooth closed lower-dimensional manifold in region $\mathbb{R}^d$.

Lemma 1.7. [61] *If a quadrature rule is exact for all polynomials of degree $\leqslant 2t$ on the region Ω, then the number of quadrature points N satisfies $N \geqslant d_t(\Omega)$, where $d_t(\Omega)$ is the dimension of $\mathbb{P}_t(\Omega)$.*

Recently, a lot of remarkable work for the value of $N(d, t)$ has been raised. In 1993, Korevaar and Meyers [47] proved that $N(d, t) \leqslant C_d t^{(d^2+d)/2}$ and conjectured that $N(d, t) \leqslant C_d t^d$, where C_d is a sufficient large positive constant depending only on d. This conjecture have been proved by Bondarenko, Radchenko and Viazovska [14] in 2011. In addition, Bondarenko, Radchenko and Viazovska [15] proved the existence of well separated spherical t-designs for all $N \geqslant C_d t^d$ for some unknown $C_d > 0$.

Theorem 1.8. [14] *For $d \geqslant 2$, there exists a constant C_d depending only on d such that for every $N \geqslant C_d t^d$ there exists a spherical t-design on $\mathbb{S}^d$ with N points.*

For $d = 2$, there is an even stronger conjecture by Hardin and Sloane [43] saying that $N(2, t) \leqslant \frac{1}{2}t^2 + o(t^2)$ as $t \to \infty$. Numerical evidence supporting the conjecture was also given [43, 64].

In 2011, Chen, Frommer and Lang [25] proposed a computational-assisted proof for the existence of spherical designs on $\mathbb{S}^2$ with $N = (t + 1)^2$ for all values of $t \leqslant 100$. In [25], an algorithm based on interval arithmetic is proposed to calculate a series of sets of small interval enclosures containing spherical designs.

It is well known that there are many equivalent conditions for a set $X_N \subset \mathbb{S}^2$ to be a spherical t-design. Among them the following proposition plays a significant role in the study of this problem:

Proposition 1.9. [36, 64] *A finite set* $X_N = \{\mathbf{x}_1, \ldots, \mathbf{x}_N\}$ *is a spherical* t*-design if and only if the Weyl sums*

$$\sum_{i=1}^{N} Y_{\ell,k}(\mathbf{x}_i) = 0, \quad k = 1, \ldots, 2\ell + 1, \ \ell = 1, \ldots, t. \tag{1.22}$$

Based on this proposition, Chen and Womersley [28] reformulated the problem of finding a spherical t-design with $N = (t+1)^2$ points as a system of underdetermined nonlinear equations. A generalized result was then proved in [2] for the case $N \geqslant (t+1)^2$. Define the function $\mathbf{C}_t : \underbrace{\mathbb{S}^2 \times \cdots \times \mathbb{S}^2}_{N \ times} \to \mathbb{R}^{N-1}$ by

$$\mathbf{C}_t(X_N) := \mathbf{E}\mathbf{G}_t(X_N)\mathbf{e}, \tag{1.23}$$

where

$$\begin{aligned} \mathbf{E} &:= [\mathbf{1}, -\mathbf{I}_{N-1}] \in \mathbb{R}^{(N-1)\times N}, && (1.24)\\ \mathbf{G}_t(X_N) &:= \mathbf{Y}_t(X_N)^T \mathbf{Y}_t(X_N), && (1.25)\\ \mathbf{e} &:= (1, 1, \ldots, 1)^T \in \mathbb{R}^{(t+1)^2}, && (1.26)\\ \text{and } \mathbf{1} &:= (1, \ldots, 1)^T \in \mathbb{R}^{N-1}, && (1.27) \end{aligned}$$

and

$$(\mathbf{Y}_t)_{i,\ell^2+k}(X_N) = Y_{\ell,k}(\mathbf{x}_i), \quad i = 1, \ldots, N, \ k = 1, \ldots, 2\ell + 1, \ \ell = 0, \ldots, t.$$

Proposition 1.10. [2] *Let* $N \geqslant (t+1)^2$*, and suppose that* $X_N = \{\mathbf{x}_1, \ldots, \mathbf{x}_N\}$ *is a fundamental system of* $\mathbb{P}_t$*. Then* X_N *is a spherical* t*-design if and only if* $\mathbf{C}_t(X_N) = \mathbf{0}$*.*

By Proposition 1.9 we can guess that for any fixed t and $N = (t+1)^2$, spherical t-design is not unique, since equation (1.22) is nonlinear with respect to the points with maximal degree t. The matrix $\mathbf{G}_t(X_N)$ which is constructed by some spherical t-designs may be singular, or ill-conditioned, which is not suitable for polynomial approximation and interpolation. To overcome this challenge, a new concept called well-conditioned (extremal) spherical t-design was proposed in [2].

Definition 1.11. (Extremal spherical designs) *A set* $X_N = \{\mathbf{x}_1, \ldots, \mathbf{x}_N\} \subset \mathbb{S}^2$ *of* $N \geqslant (t+1)^2$ *points is an extremal spherical* t*-design if the determinant of the matrix* $\mathbf{H}_t(X_N) := \mathbf{Y}_t(X_N)\mathbf{Y}_t(X_N)^T \in \mathbb{R}^{(t+1)^2 \times (t+1)^2}$ *is maximal subject to the constraint that* X_N *is a spherical* t*-design.*

In [2], the well conditioned spherical t-designs with $N \geqslant (t+1)^2$ points are constructed by maximizing the determinant of a Gram matrix which satisfies undetermined nonlinear equations. Interval methods are then used to prove the existence of a true spherical t-design and to provide a guaranteed interval containing the true spherical t-design. The well-conditioned spherical designs are proved to have well separated properties.

Some other noteworthy work is that Sloan and Womersley [64] analyzed some variational characterization of spherical designs and proposed another approach to find spherical t-design with $N \leqslant (t+1)^2$ using the found variational characterization. Furthermore, Brauchart, Saff, Sloan, and Womersley studied the worst-case error of numerical integration for functions in Sobolev spaces using spherical designs in [19], and demonstrated the effectiveness numerical integration using spherical designs compared to some other point systems.

1.2.2 QMC designs

Denote the space of square integrable functions on $\mathbb{S}^d$ by $\mathbb{L}_2(\mathbb{S}^d)$. It is a Hilbert space with the inner product

$$\langle f, g \rangle_{\mathbb{L}_2(\mathbb{S}^d)} = \int_{\mathbb{S}^d} f(\mathbf{x}) g(\mathbf{x}) d\omega_d(\mathbf{x}), \quad f, g \in \mathbb{L}_2(\mathbb{S}^d), \tag{1.28}$$

and the induced norm

$$\|f\|_{\mathbb{L}_2(\mathbb{S}^d)} = \left(\int_{\mathbb{S}^d} |f(\mathbf{x})|^2 d\omega_d(\mathbf{x}) \right)^{\frac{1}{2}}, \quad f \in \mathbb{L}_2(\mathbb{S}^d). \tag{1.29}$$

The Sobolev space $\mathbb{H}^s(\mathbb{S}^d)$ can be defined for $s \geqslant 0$ as the set of all functions $f \in \mathbb{L}_2(\mathbb{S}^d)$ whose Laplace-Fourier coefficients

$$\hat{f}_{\ell,k} = \langle f, Y_{\ell,k} \rangle_{\mathbb{L}_2(\mathbb{S}^d)} = \int_{\mathbb{S}^d} f(\mathbf{x}) Y_{\ell,k}(\mathbf{x}) d\omega_d(\mathbf{x}) \tag{1.30}$$

satisfy

$$\sum_{\ell=0}^{\infty} \sum_{k=1}^{M(d,\ell)} (1+\lambda_\ell)^s \left| \hat{f}_{\ell,k} \right|^2 < \infty, \tag{1.31}$$

where the $\lambda_\ell = \ell(\ell+d-1)$. Obviously, by letting $s=0$ we can obtain $\mathbb{H}^0(\mathbb{S}^d) = \mathbb{L}_2(\mathbb{S}^d)$.

Define the norm of $\mathbb{H}^s(\mathbb{S}^2)$ as

$$\|f\|_{\mathbb{H}^s} = \left[\sum_{\ell=0}^{\infty} \sum_{k=1}^{2\ell+1} \frac{1}{\alpha_\ell^{(s)}} \hat{f}_{\ell,k}^2 \right]^{\frac{1}{2}}, \tag{1.32}$$

where the sequence of positive parameters $\alpha_\ell^{(s)}$ should satisfy

$$\alpha_\ell^{(s)} \sim (1+\lambda_\ell)^{-s} \sim (\ell+1)^{-2s}. \tag{1.33}$$

Correspondingly, we define the inner product in $\mathbb{H}^s(\mathbb{S}^2)$ as

$$\langle f, g \rangle_{\mathbb{H}^s} = \sum_{\ell=0}^{\infty} \sum_{k=1}^{2\ell+1} \frac{1}{\alpha_\ell^{(s)}} \hat{f}_{\ell,k} \hat{g}_{\ell,k}. \tag{1.34}$$

The results in this section are based on the explicit expression for the "worst-case error" in [19]. In [19] the worst-case integration error is established based on the concept of reproducing kernel. Using the relationship between reproducing kernel and point distance, an efficient way to calculate the the worst-case error is found.

Definition 1.12. [19] **(Worst-case error)** *For a Banach space $\mathbb{B}$ of continuous functions on $\mathbb{S}^d$ and denote its norm by $\|\cdot\|_{\mathbb{B}}$, the worst-case error for the integration rule $Q[X_N]$ with node set $X_N = \{\mathbf{x}_1, \ldots, \mathbf{x}_N\}$ approximating the integral $I(f)$, with $Q[X_N](f)$ and $I(f)$ defined by*

$$Q[X_N](f) := \frac{1}{N} \sum_{j=1}^{N} f(\mathbf{x}_j), \quad I(f) := \int_{\mathbb{S}^d} f(\mathbf{x}) d\omega_d(\mathbf{x}), \tag{1.35}$$

is given by

$$E_{\mathbb{B}}(Q[X_N]) := \sup\big\{|Q[X_N](f) - I(f)| : f \in \mathbb{B}, \|f\|_{\mathbb{B}} \leqslant 1\big\}. \tag{1.36}$$

In [19] Brauchart, Saff, Sloan and Womersley studied the equal weight numerical integration and raised a concept called QMC (Quasi-Monte Carlo) designs. They discussed the integration of functions in Sobolev space $H^s(\mathbb{S}^d)$ with $s > d/2$. And the so-called QMC designs represent a kind of sequence with its worst-case error converges to zero with its number of points $N \to \infty$ with a certain order.

Definition 1.13. [19] **(QMC designs)** *Given $s > \frac{d}{2}$, a sequence (X_N) of N-point configurations on $\mathbb{S}^d$ with $N \to \infty$ is said to be a sequence of QMC designs for $\mathbb{H}^s(\mathbb{S}^d)$ if there exists a positive number $c(s,d) > 0$, independent of N, such that*

$$\sup_{\substack{f \in \mathbb{H}^s \\ \|f\|_s \leqslant 1}} \Big|\frac{4\pi}{N}\sum_{j=1}^{N} f(\mathbf{x}_i) - \int_{\mathbb{S}^d} f(\mathbf{x}) d\omega_d(\mathbf{x})\Big| \leqslant \frac{c(s,d)}{N^{s/d}}. \tag{1.37}$$

For brevity of notations, denote the worst-case error of a quadrature rule $Q[X_N, w]$ on $\mathbb{H}^s(\mathbb{S}^d)$ by

$$E_{s,d}(Q[X_N, w]) \quad = \quad \sup_{f \in H^s, \|f\|_s \leqslant 1} |Q[X_N, w](f) - I(f)|\,. \tag{1.38}$$

For sequences of positive weight cubature rules there have been some results about its fast convergence property in Sobolev spaces, as shown in the following theorem. This theorem was first proved for the case $s = 3/2$ and $d = 2$ in [44], then extended to all $s > 1$ for $d = 2$ in [45], and finally extended to all $s > d/2$ and all $d \geqslant 2$ in [18].

Theorem 1.14. [18] *Given $s > d/2$, there exists a positive number $c(s,d)$ depending on the $\mathbb{H}^s(\mathbb{S}^d)$-norm such that for every N-point spherical t-design X_N on $\mathbb{S}^d$ there holds*

$$E_{s,d}(Q[X_N]) \leqslant c(s,d) N^{-\frac{s}{d}}. \tag{1.39}$$

In the following of this subsection, we will discuss the worst-case error of spherical t_ϵ-design on $\mathbb{H}^s(\mathbb{S}^2)$. Again for brevity of notations we denote $E_s(Q[X_N]) := E_{s,2}(Q[X_N])$ in the following. We will use the reproducing kernel theory to analyze the worst-case

error. The Riesz representation theorem and the additional theorem assures the existence of a reproducing kernel of

$$\begin{aligned} K_s(\mathbf{x},\mathbf{y}) &= \sum_{\ell=0}^{\infty}(2\ell+1)\alpha_\ell^{(s)}P_\ell(\mathbf{x}\cdot\mathbf{y}) \\ &= \sum_{\ell=0}^{\infty}\sum_{k=1}^{2\ell+1}\alpha_\ell^{(s)}Y_{\ell,k}(\mathbf{x})Y_{\ell,k}(\mathbf{y}), \end{aligned} \tag{1.40}$$

where P_ℓ denotes the Legendre Polynomial with degree ℓ.

Proposition 1.15. [18] *For $s > 1$, let $\mathbb{H}^s(\mathbb{S}^2)$ be the Hilbert space with norm (1.32), where the sequence $\alpha_\ell^{(s)}$ satisfies (1.33), and let K_s be given by (1.40). Then, for a equal weight quadrature rule $Q[X_N]$ with node set $X_N = \{\mathbf{x}_1,\ldots,\mathbf{x}_N\} \subset \mathbb{S}^2$,*

$$E_s(Q[X_N]) = \frac{1}{N}\left(\sum_{\ell=1}^{\infty}\sum_{k=1}^{2\ell+1}\alpha_\ell^{(s)}\left(\sum_{i=1}^{N}Y_{\ell,k}(\mathbf{x}_i)\right)^2\right)^{\frac{1}{2}}. \tag{1.41}$$

In what follows, we will firstly introduce some theoretical results about the equal weight case. The following theorem, obtained by appealing to results of Brandolini et al. [17], asserts that if (X_N) is a sequence of QMC designs for $H^s(\mathbb{S}^2)$, then it is also so for all coarser Sobolev spaces $H^{s'}(\mathbb{S}^2)$ with $1 < s' < s$.

Theorem 1.16. [17] *Given $s> 1$, let (X_N) be a sequence of QMC designs for $\mathbb{H}^s(\mathbb{S}^2)$. Then (X_N) is a sequence of QMC designs for $\mathbb{H}^{s'}(\mathbb{S}^2)$, for all s satisfying $1 < s' \leqslant s$.*

According to this theorem, for every sequence of QMC designs (X_N), there exists a number s^* such that (X_N) is a sequence of QMC design for all s satisfying $1 < s < s^*$, and is not a QMC design for $s > s^*$, that is

$$s^* := s^*[(X_N)] := \sup\left\{s : (X_N)\ is\ a\ sequence\ of\ QMC\ designs\ for\ \mathbb{H}^s(\mathbb{S}^2)\right\}. \tag{1.42}$$

When $s^* = +\infty$, we call the sequence (X_N) "generic" QMC design.

Proposition 1.17. *Given $s > 1$, a sequence of QMC design for $\mathbb{H}^s(\mathbb{S}^2)$ is asymptotically uniformly distributed on $\mathbb{S}^2$.*

Reproducing kernels for $\mathbb{H}^s(\mathbb{S}^2)$ for $s > 1$ can be constructed utilizing powers of distances, provided the power $2s-2$ is not an even integer. Indeed, it is known (cf., e.g., [11, 18]) that the signed power of the distance, with sign $(-1)^{L+1}$ with $L := L(s) := \lfloor s-1 \rfloor$, has the following Laplace-Fourier expansion:

$$(-1)^{L+1}|\mathbf{x}-\mathbf{y}|^{2s-2} = (-1)^{L+1}V_{2-2s}(\mathbb{S}^2) + \sum_{\ell=1}^{\infty} a_\ell^{(s)}(2\ell+1)P_\ell(\mathbf{x}\cdot\mathbf{y}), \tag{1.43}$$

where

$$V_{2-2s}(\mathbb{S}^2) := \int_{\mathbb{S}^2}\int_{\mathbb{S}^2} |\mathbf{x}-\mathbf{y}|^{2s-2} d\omega(\mathbf{x}) d\omega(\mathbf{y}) = 2^{2s-1}\frac{\Gamma(3/2)\Gamma(s)}{\sqrt{\pi}\Gamma(1+s)}, \tag{1.44}$$

and

$$a_\ell^{(s)} := V_{2-2s}(\mathbb{S}^2)\frac{(-1)^{L+1}(1-s)_\ell}{(1+s)_\ell},\ \ell \geqslant 1. \tag{1.45}$$

Here

$$\frac{(1-s)_\ell}{(1+s)_\ell} := \frac{\Gamma(1+s)}{\Gamma(1-s)}\frac{\Gamma(\ell+1-s)}{\Gamma(\ell+1+s)} \sim \frac{\Gamma(1-s)}{\Gamma(1+s)}\ell^{-2s} \sim \ell^{-2s}.$$

By Proposition 1.15 the worst-case error on $\mathbb{H}^s(\mathbb{S}^2)$ could be obtained as [18]

1. for $1 < s \leqslant 2$,

$$E_s(Q[X_N]) = \left(V_{2-2s}(\mathbb{S}^2) - \frac{1}{N^2}\sum_{i=1}^N\sum_{j=1}^N |\mathbf{x}_i-\mathbf{x}_j|^{2s-2}\right)^{\frac{1}{2}}, \tag{1.46}$$

2. for $s > 2$,

$$E_s(Q[X_N]) = \left(\frac{1}{N^2}\sum_{i=1}^N\sum_{j=1}^N \left[\mathcal{Q}_L(\mathbf{x}_i\cdot\mathbf{x}_j) + (-1)^{L+1}|\mathbf{x}_i-\mathbf{x}_j|^{2s-2}\right] - (-1)^{L+1}V_{2-2s}(\mathbb{S}^2)\right)^{\frac{1}{2}}, \tag{1.47}$$

where

$$\mathcal{Q}_L(\mathbf{x}\cdot\mathbf{y}) := \sum_{\ell=1}^{L}((-1)^{L+1-\ell}-1)a_\ell^{(s)}(2\ell+1)P_\ell(\mathbf{x}\cdot\mathbf{y}), \quad \mathbf{x},\mathbf{y}\in\mathbb{S}^2.$$

1.3 Numerical approximation on the sphere

Much attention are given to the numerical approximation problem on the sphere in recent decades, which could be applied to solve physical problems arising in plenty of science landscapes such as geophysics, astrophysics, and surface reconstruction. In this section we review the two regularized approaches for numerical approximation on the sphere.

1.3.1 Regularized least squares problem on the sphere

Numerical approximation for continuous functions on the unit sphere is widely studied in recent decades. Among the methods and models for this problem, polynomial approximation is a basic approach and has long been paid much attention. A regularized discrete least squares form polynomial approximations on the unit sphere is usually considered: $\mathbb{S}^2 = \{\mathbf{x} = (x, y, z)^T \in \mathbb{R}^3 \ : \ x^2 + y^2 + z^2 = 1\}$ arising as minimizers

$$\min_{p \in \mathbb{P}_L} \sum_{j=1}^{N} (p(\mathbf{x}_j) - f(\mathbf{x}_j))^2 + \lambda \sum_{j=1}^{N} (\mathcal{R}_L p(\mathbf{x}_j))^2 \tag{1.48}$$

where f is a given continuous function with values (possibly noisy) given at N points X_N. The regularizer, $\mathcal{R}_L : \mathbb{P}_L \to \mathbb{P}_L$, is a linear operator which can be chosen in different ways, and $\lambda > 0$ is a parameter. Usually we assume always that the problem is well posed, which requires the number N to be at least $\dim(\mathbb{P}_L) = (L+1)^2$.

All approximations of the form (1.48) are special cases of the penalized least squares method, studied in a general context by [71].

It is easy to see that $\{Y_{\ell,k},\ \ell = 0, \ldots, L,\ k = 1, \ldots, 2\ell + 1\}$ is a basis of $\mathbb{P}_L$ with $\mathbb{L}_2(\mathbb{S}^d)$ norm. Then for arbitrary $p \in \mathbb{P}_L$, there is a unique vector $\boldsymbol{\alpha} = (\alpha_{\ell k}) \in \mathbb{R}^{(L+1)^2}$ such that

$$p(\mathbf{x}) = \sum_{\ell=0}^{L} \sum_{k=1}^{2\ell+1} \alpha_{\ell k} Y_{\ell,k}(\mathbf{x}), \quad \mathbf{x} \in \mathbb{S}^2. \tag{1.49}$$

We can define the regularizing operator $\mathcal{R}_L$ in its most general rotationally invariant

form by its action on $p \in \mathbb{P}_L$:

$$\mathcal{R}_L p(\mathbf{x}) = \sum_{\ell=0}^{L} \beta_\ell \sum_{k=1}^{2\ell+1} Y_{\ell,k}(\mathbf{x})(Y_{\ell,k},\, p)_{\mathbb{L}_2} \tag{1.50}$$

$$= \sum_{\ell=0}^{L} \beta_\ell \int_{\mathbb{S}^2} \frac{(2\ell+1)}{4\pi} P_\ell(\mathbf{x}\cdot\mathbf{y}) p(\mathbf{y}) d\omega(\mathbf{y}), \tag{1.51}$$

where $\beta_0, \beta_1, \ldots, \beta_L$ are at this point arbitrary non-negative numbers, which may depend on L.

Given a continuous function f defined on $\mathbb{S}^2$, let $\mathbf{f} := \mathbf{f}(X_N)$ be the column vector

$$\mathbf{f} = [f(\mathbf{x}_1), \ldots, f(\mathbf{x}_N)]^T \in \mathbb{R}^N,$$

and let $\mathbf{Y}_L := \mathbf{Y}_L(X_N) \in \mathbb{R}^{N\times(L+1)^2}$ be a matrix of spherical harmonics evaluated at the points of X_N, with elements

$$(\mathbf{Y}_L)_{i,\ell^2+k}(X_N) = Y_{\ell,k}(\mathbf{x}_i), \quad i = 1,\ldots,N,\ k = 1,\ldots,2\ell+1,\ \ell = 0,\ldots,L.$$

Substituting of (1.49) into (1.48), the problem (1.48) reduces to the following discrete regularized least squares problem

$$\min_{\boldsymbol{\alpha}\in\mathbb{R}^{(L+1)^2}} \|\mathbf{Y}_L\boldsymbol{\alpha} - \mathbf{f}\|_2^2 + \lambda\|\mathbf{R}_L^T\boldsymbol{\alpha}\|_2^2, \quad \lambda > 0, \tag{1.52}$$

where $\mathbf{R}_L := \mathbf{R}_L(X_N) = \mathbf{B}\mathbf{Y}_L^T \in \mathbb{R}^{(L+1)^2\times N}$, with $\mathbf{B}$ a positive semi-definite diagonal matrix defined by

$$\mathbf{B} := \operatorname{diag}(\beta_0,\ \underbrace{\beta_1,\ \beta_1, \beta_1}_{3},\ \ldots,\ \underbrace{\beta_L, \ldots, \beta_L}_{2L+1}) \in \mathbb{R}^{(L+1)^2\times(L+1)^2}. \tag{1.53}$$

Thus the matrix $\mathbf{R}_L$ is determined by the elements of the diagonal matrix $\mathbf{B}$ and the choice of the points X_N. The problem (1.52) is a convex unconstrained optimization problem. Its solution set coincides with the solution set of the system of linear equations

$$\mathbf{T}_L\boldsymbol{\alpha} = \mathbf{Y}_L^T\mathbf{f}, \tag{1.54}$$

where $\mathbf{T}_L := \mathbf{T}_L(X_N)$ is given by

$$\mathbf{T}_L = (\mathbf{H}_L + \lambda\mathbf{B}\mathbf{H}_L\mathbf{B}) \in \mathbb{R}^{(L+1)^2\times(L+1)^2}, \tag{1.55}$$

$$\mathbf{H}_L := \mathbf{H}_L(X_N) = \mathbf{Y}_L^T \mathbf{Y}_L \in \mathbb{R}^{(L+1)^2 \times (L+1)^2}. \tag{1.56}$$

To guarantee that (1.48) always has a unique solution even when $\lambda = 0$, we always impose conditions on X_N that ensure that the matrix $\mathbf{H}_L$ is non-singular. We denote that solution by $\alpha := \alpha(L, X_N, \mathbf{B}) \in \mathbb{R}^{(L+1)^2}$, and the corresponding polynomial approximation by

$$p_{L,N} = \sum_{\ell=0}^{L} \sum_{k=1}^{2\ell+1} \alpha_{\ell,k} Y_{\ell,k}. \tag{1.57}$$

As stated before, we assume that X_N is a spherical t-design for some $t \geqslant L$. It is useful to consider separately the cases $L \leqslant t < 2L$ and $t \geqslant 2L$, because in the first case important issues arise from the conditioning of the least squares problem (1.52), while in the second case, An, Chen, Sloan, Womersley [3] prove that the matrix becomes diagonal and hence the linear algebra becomes trivial.

Theorem 1.18. [3] *Assume $f \in C(\mathbb{S}^2)$. Let $L \geqslant 0$ be given, and let $X_N = \{\mathbf{x}_1, \ldots, \mathbf{x}_N\}$ be a spherical t-design on $\mathbb{S}^2$ with $t \geqslant 2L$. Then*

$$\mathbf{H}_L = \mathbf{Y}_L^T \mathbf{Y}_L = \frac{N}{4\pi} \mathbf{I}_{(L+1)^2} \in \mathbb{R}^{(L+1)^2 \times (L+1)^2}, \tag{1.58}$$

while (1.54) *has a unique solution*

$$\alpha_{\ell k} = \frac{4\pi}{N(1+\lambda\beta_\ell^2)} \sum_{j=1}^{N} Y_{\ell,k}(\mathbf{x}_j) f(\mathbf{x}_j), \tag{1.59}$$

and the unique minimizer of (1.48) *is given by*

$$\begin{aligned} p_{L,N}(\mathbf{x}) =& \frac{4\pi}{N} \sum_{\ell=0}^{L} \sum_{k=1}^{2\ell+1} \frac{Y_{\ell,k}(\mathbf{x})}{1+\lambda\beta_\ell^2} \sum_{j=1}^{N} Y_{\ell,k}(\mathbf{x}_j) f(\mathbf{x}_j) \\ =& \sum_{\ell=0}^{L} \frac{2\ell+1}{(1+\lambda\beta_\ell^2)N} \sum_{j=1}^{N} P_\ell(\mathbf{x} \cdot \mathbf{x}_j) f(\mathbf{x}_j). \end{aligned} \tag{1.60}$$

The choice of the regularized operator $\mathcal{R}_L$ is multiple. In [3] several interesting choices of the regularizing matrix $\mathbf{B}$ are discussed:

1 The choice $\mathbf{B} = \mathbf{0}$, gives the unregularized problem. This choice includes (depending on N, L and t) the classical interpolation problem (when $N = (L+1)^2$), quasi-interpolation (when $N > (L+1)^2$), hyperinterpolation [22] (when $t \geqslant 2L$), and orthogonal projection in the limit $t \to \infty$ with fixed L.

2 Choices of $\mathbf{B}$ related to "filtered" polynomial approximation [65], in which the diagonal elements β_ℓ of $\mathbf{B}$ are chosen so that

$$\frac{1}{1+\lambda\beta_\ell^2} = h\left(\frac{\ell}{L}\right), \quad \ell = 0, \ldots, L-1, \tag{1.61}$$

where $h(x)$ is a prescribed "filter" function on $\mathbb{R}^+$, vanishing for $x > 1$. The motivation is that, as we shall see, for $t \geqslant 2L$ such approximations can have excellent approximation properties in the uniform norm if h is well chosen. We shall see that they may also therefore be good candidates when $t < 2L$.

3 Choices related to the Laplace-Beltrami operator Δ^*. (Laplace-Beltrami regularizers). The Laplace-Beltrami regularizer has proved to be effective in recovering functions form contaminated data.

1.3.2 Hybrid approximation using radial basis functions and spherical polynomials

Another important approach of numerical approximation on the sphere is the hybrid approximation scheme, which is widely applied to deal with approximation to continuous functions on the sphere [39, 62, 72]. It employs both the radial basis functions and spherical harmonic polynomials as the basis of approximation by adding an orthogonal condition to guarantee the efficiency. Usually, the radial basis functions could approximate rapidly varying data over short distance effectively, whereas the spherical harmonic polynomials are more suitable for slowly varying data on a global scale.

In this subsection we will discuss approximating a continuous function $f \in C(\mathbb{S}^2)$ using both radial basis functions (RBF) and spherical harmonic polynomials, where $C(\mathbb{S}^2)$

denotes all continuous functions defined on $\mathbb{S}^2$. We assume that the values of f are given at a distinct data point set $X_N = \{\mathbf{x}_1, \ldots, \mathbf{x}_N,\ N \in \mathbb{N}\}$.

To construct the radial basis functions, we choose all points in X_N as the center points and employs a (strictly) positive definite kernel ϕ [58, 72, 73] which satisfies

$$\sum_{i=1}^{N}\sum_{j=1}^{N} \alpha_i \phi(\mathbf{x}_i, \mathbf{x}_j)\alpha_j \geqslant 0, \tag{1.62}$$

for any point set of $X_N \subset \mathbb{S}^2$ and for all $N \in \mathbb{N}$, with equality for distinct points $\mathbf{x}_j$ only if $\alpha_1 = \alpha_2 = \ldots = \alpha_N = 0$. Then the RBFs are defined as $\phi(\cdot, \mathbf{x}_j)$ with $j = 1, \ldots, N$. Additionally, we assume that ϕ is zonal, which means

$$\phi(\mathbf{x}_i, \mathbf{x}_j) = \phi(\mathbf{x}_i \cdot \mathbf{x}_j),$$

for arbitrary $i, j = 1, \ldots, N$, where $\mathbf{x}_i \cdot \mathbf{x}_j$ denotes the Euclidean inner product in $\mathbb{R}^3$. According to the addition theorem, a zonal radial basis function has an expansion of the form

$$\phi(\cdot, \mathbf{x}) = \sum_{\ell=0}^{\infty} \hat{\phi}_\ell P_\ell(\cdot, \mathbf{x}) = \sum_{\ell=0}^{\infty} \frac{\hat{\phi}_\ell}{2\ell+1} \sum_{k=1}^{2\ell+1} Y_{\ell,k}(\cdot) Y_{\ell,k}(\mathbf{x}), \tag{1.63}$$

where $\hat{\phi}_\ell > 0,\ \ell = 0, \ldots, \infty$ when ϕ is a strictly positive kernel.

We define the RBF approximation space as

$$\mathcal{X}_{N,\phi} = \mathcal{X}_N = \operatorname{span}\{\phi(\cdot, \mathbf{x}_j) :\ \mathbf{x}_j \in X_N\}.$$

Furthermore, denote by

$$\mathcal{F}_\phi = \operatorname{span}\{\phi(\cdot, \mathbf{x}_j) :\ \mathbf{x}_j \in \mathbb{S}^2, j \in 1, \ldots, N,\ N \in \mathbb{N}\},$$

which is a reproducing kernel pre-Hilbert space [72] under the inner product

$$\left\langle \sum_{i=1}^{N} \alpha_i \phi(\cdot, \mathbf{x}_i), \sum_{j=1}^{N} \alpha'_j \phi(\cdot, \mathbf{x}_j) \right\rangle_\phi = \sum_{i=1}^{N}\sum_{j=1}^{N} \alpha_i \alpha'_j \phi(\mathbf{x}_i, \mathbf{x}_j), \tag{1.64}$$

and the norm

$$\left\| \sum_{i=1}^{N} \alpha_i \phi(\cdot, \mathbf{x}_i) \right\|_\phi = \sum_{i=1}^{N}\sum_{j=1}^{N} \alpha_i \alpha_j \phi(\mathbf{x}_i, \mathbf{x}_j), \tag{1.65}$$

with $\alpha_j \in \mathbb{R}$, $j = 1, \cdots, N$. Let $\mathcal{N}_\phi$ be the completion of $\mathcal{F}_\phi$ and then we can obtain that $\mathcal{N}_\phi$ is a reproducing kernel Hilbert space (RKHS).

Now let $X_N \subset \mathbb{S}^2$ be fixed. Then the approximation of $f \in C(\mathbb{S}^2)$ with both RBFs and spherical harmonics can be defined as

$$\Lambda_{X,L} f = \sum_{j=1}^{N} \alpha_j \phi(\cdot, \mathbf{x}_j) + \sum_{\ell=0}^{L} \sum_{k=1}^{2\ell+1} \beta_{\ell,k} Y_{\ell,k}, \tag{1.66}$$

with the orthogonal condition

$$\sum_{j=1}^{N} \alpha_j v(\mathbf{x}_j) = 0, \quad \forall v \in \mathbb{P}_L, \tag{1.67}$$

where $\alpha_j,\ j = 1, \ldots, N,\ \beta_{\ell,k},\ \ell = 0, \ldots, L,\ k = 1, \ldots, 2\ell + 1$, are the coefficients of the RBFs and spherical harmonics, and L denotes the maximal degree of the spherical harmonics applied in the approximation. The values of f are given at the N-point set $X_N = \{\mathbf{x}_1, \ldots, \mathbf{x}_N\} \subset \mathbb{S}^2$, and we insist that X_N is a fundamental system of degree L, see [2, 29, 62]. Thus the approximation $\Lambda_{X,L} f$ is to find an element $u \in \mathcal{X}_N$ and a $v \in \mathbb{P}_L$ as

$$u = \sum_{j=1}^{N} \alpha_j \phi(\cdot, \mathbf{x}_j),$$

$$v = \sum_{\ell=0}^{L} \sum_{k=1}^{2l+1} \beta_{\ell,k} Y_{\ell,k},$$

satisfying condition (1.66) and (1.67). To obtain the approximation, we can directly force $\Lambda_{X,L} f(\mathbf{x}_i) = f(\mathbf{x}_i), i = 1, \ldots, N$. Then let $\mathbf{f} := \mathbf{f}(X_N)$ be the column vector with

$$\mathbf{f} := [f(\mathbf{x}_1), \ldots, f(\mathbf{x}_N)]^T \in \mathbb{R}^N,$$

$A := A(X_N) \in \mathbb{R}^{N \times N}$ and $Q := Q(X_N) \in \mathbb{R}^{N \times (L+1)^2}$ with their entries as

$$A_{i,j} := \phi(\mathbf{x}_i, \mathbf{x}_j), \qquad i, j = 1, \ldots, N, \tag{1.68}$$

and

$$Q_{i,\ell k} := Y_{\ell,k}(\mathbf{x}_i), \quad i = 1, \ldots, N,\ \ell = 0, \ldots, L,\ k = 1, \ldots, 2\ell + 1, \tag{1.69}$$

and substitute (1.68), (1.69) to (1.66), (1.67), we could obtain a saddle point linear system as

$$\begin{bmatrix} A & Q \\ Q^T & 0 \end{bmatrix} \begin{bmatrix} \alpha \\ \beta \end{bmatrix} = \begin{bmatrix} \mathbf{f} \\ 0 \end{bmatrix}. \tag{1.70}$$

Since the kernel we choose for constructing the RBFs is strictly positive definite, the matrix A here is positive definite. Moreover, the fact that X_N is a fundamental system implies that Q is of full column rank. Under these two conditions, equation (1.70) is well-posed and has a unique solution.

Condition (1.67) is added to guarantee the polynomial accuracy and the efficiency of the approximation (1.66). Under the assumption that Q is of full column rank, the approximation form (1.66) with condition (1.67) has an algebraic accuracy with degree L. That means, when the function f is a spherical polynomial with its order no greater than L, the condition will guarantee that $\Lambda_{X,L} f \equiv f$ no matter how the point set X_N is chosen.

To keep the efficiency of the approximation with both RBFs and spherical harmonics, the obtained linear combination of RBFs u is expected to be ϕ–orthogonal or L_2–orthogonal to the spherical harmonic space $\mathbb{P}_L$. In this sense we can have that $\langle u, v \rangle_\phi = 0$ or $\langle u, v \rangle_{L_2} = 0$ for arbitrary element $v \in \mathbb{P}_L$. Since $Y_{\ell,k},\ \ell = 1, \ldots, L,\ k = 1, \ldots, 2\ell + 1$ is a basis of $\mathbb{P}_L$, the orthogonal condition could be presented as

$$\langle u, Y_{\ell,k} \rangle_\phi = 0 \quad \text{for } \ell = 0, \ldots, L,\ k = 1, \ldots, 2\ell + 1, \tag{1.71}$$

or

$$\langle u, Y_{\ell,k} \rangle_{\mathbb{L}_2} = 0 \quad \text{for } \ell = 0, \ldots, L,\ k = 1, \ldots, 2\ell + 1. \tag{1.72}$$

From the definition of the two different inner products and $\hat{\phi}_\ell > 0,\ \ell = 0, \ldots, \infty$ in (1.63)

we can obtain that

$$\begin{aligned}
\langle u, Y_{\ell,k}\rangle_\phi &= \left\langle \sum_{j=1}^{N} \alpha_j \phi(\cdot, \mathbf{x}_j), Y_{\ell,k} \right\rangle_\phi \\
&= \sum_{j=1}^{N} \alpha_j \langle \phi(\cdot, \mathbf{x}_j), Y_{\ell,k}\rangle_\phi \\
&= \sum_{j=1}^{N} \alpha_j Y_{\ell,k}(\mathbf{x}_j) = 0, \quad \text{for } \ell = 1, ..., L,\ k = 1, ...2\ell + 1,
\end{aligned}$$

and

$$\begin{aligned}
\langle u, Y_{\ell,k}\rangle_{\mathbb{L}_2} &= \langle \sum_{j=1}^{N} \alpha_j \phi(\cdot, \mathbf{x}_j), Y_{\ell,k}\rangle_{\mathbb{L}_2} \\
&= \sum_{j=1}^{N} \alpha_j \int_{\mathbb{S}^2} \phi(\mathbf{x}, \mathbf{x}_j) Y_{\ell,k}(\mathbf{x}) \mathrm{d}\omega(\mathbf{x}) \\
&= \sum_{j=1}^{N} \alpha_j \int_{\mathbb{S}^2} \sum_{\ell'=0}^{\infty} \frac{\hat{\phi}_\ell}{2\ell+1} \sum_{k'=1}^{2\ell+1} Y_{\ell',k'}(\mathbf{x}) Y_{\ell',k'} Y_{\ell,k}(\mathbf{x}) \mathrm{d}\omega(\mathbf{x}) \\
&= \sum_{j=1}^{N} \alpha_j \frac{\hat{\phi}_\ell}{2\ell+1} Y_{\ell,k}(\mathbf{x}_j) = 0, \quad \text{for } \ell = 1, ..., L,\ k = 1, ...2\ell + 1,
\end{aligned}$$

which are both equivalent to the equation

$$Q^T \alpha = 0. \tag{1.73}$$

Le Gia, Watson, Sloan in [48] indicated that problem (1.70) can also be explained as a constrained optimization problem as

$$\min_{u \in \mathcal{X}_N} \frac{1}{2} \|u - f\|_\phi^2 \tag{1.74}$$

$$\text{s.t.} \quad \langle u,\ Y_{\ell,k}\rangle_\phi = 0,\ \ell = 0, \ldots, L,\ k = 1, \ldots, 2\ell + 1,$$

where the $\|\cdot\|_\phi$ is defined as in (1.65). The problem can be reformulated as

$$\begin{aligned}
&\min_\alpha \alpha^T A \alpha - \alpha^T \mathbf{f} \\
&\text{s.t.} \quad Q^T \alpha = 0.
\end{aligned} \tag{1.75}$$

By introducing the vector β as the Lagrangian multiplier and deriving the KKT condition of this problem we can also obtain system (1.70).

Chapter 2

Spherical t_ϵ-Designs

In this chapter we will introduce a new class of point sets on the unit sphere $\mathbb{S}^2$ which is called spherical t_ϵ-design on the unit sphere $\mathbb{S}^2$. Spherical t_ϵ-design is a generalization of the spherical t-design.

A spherical t-design provides an equal weight cubature rule with its algebraic accuracy as degree t for numerical integration on the whole sphere, which, further, also performs well for numerical integration of spherical functions belonging to Sobolev spaces. Different from spherical designs, spherical t_ϵ-design relaxes the weights to be chosen in a small interval around $\frac{4\pi}{N}$ with respect to a positive parameter ϵ. With this kind of positive weights we can get numerical integration with polynomial precision using fewer points than spherical t-designs.

This chapter is organized as following. In Section 2.1 we mainly introduce the definition of spherical t_ϵ-designs and discuss its relationship with these points in the interval enclosures of spherical t-design calculated in [25]. In Section 2.2 we generalize some results in [64] about the variational characterization of spherical t-designs to spherical t_ϵ-designs. In Section 2.3 we analyze the worse-case error for spherical t_ϵ-design when applied to numerical integration on the unit sphere $\mathbb{S}^2$.

In this chapter, we assume that all the point sets located on the unit sphere are distinct, which means that each point in the set is different from others.

2.1 Spherical t_ϵ-design: a generalization of spherical t-design

The definition of spherical t_ϵ-design is presented as following:

Definition 2.1. (Spherical t_ϵ-deisgn) *A spherical t_ϵ-design with $0 \leqslant \epsilon < 1$ on $\mathbb{S}^2$ is a set of points $X_N^\epsilon := \{\mathbf{x}_1^\epsilon, \ldots, \mathbf{x}_N^\epsilon\} \subset \mathbb{S}^2$ such that the cubature rule with weights $w = (w_1, \ldots, w_N)^T$ satisfying*

$$\frac{4\pi}{N}(1-\epsilon) \leqslant w_i \leqslant \frac{4\pi}{N}(1-\epsilon)^{-1}, \quad i = 1, \ldots, N, \tag{2.1}$$

is exact for all spherical polynomials of degree at most t, that is,

$$\sum_{i=1}^{N} w_i p(\mathbf{x}_i^\epsilon) = \int_{\mathbb{S}^2} p(\mathbf{x}) d\omega(\mathbf{x}) \quad \forall p \in \mathbb{P}_t. \tag{2.2}$$

From Definition 2.1 we can see that the spherical t_ϵ-design is a kind of positive weight cubature rule and ϵ restricts the differences among each weights $w_i,\ i = 1, \ldots, N$ round the mean value at $\frac{4\pi}{N}$. Especially, when $\epsilon = 0$, spherical t_ϵ-design reduces to the spherical t-design that is an equally weighted ($w_i = \frac{4\pi}{N}$) cubature rule [28, 2]. Since the existence of spherical t-designs has been proved for arbitrary t and they are special spherical t_ϵ-designs with $\epsilon = 0$, we have the existence of spherical t_ϵ-designs. In this section we will study the relationship between spherical t_ϵ-design and spherical t-design when they have the same number of points.

Let $w = (w_1, \ldots, w_N)^T$ and define $\mathbf{Y}(X_N^\epsilon) \in \mathbb{R}^{N \times d_t}$ with elements

$$\mathbf{Y}_{i,\ell^2+k}(X_N^\epsilon) = Y_{\ell,k}(\mathbf{x}_i^\epsilon), \quad i = 1, \ldots, N,\ k = 1, \ldots, 2\ell+1,\ \ell = 0, \ldots, t.$$

Let $a = \frac{4\pi(1-\epsilon)}{N} e$ and $b = \frac{4\pi(1-\epsilon)^{-1}}{N} e$ where $e = (1, \ldots, 1)^T \in \mathbb{R}^N$. Then we could obtain the following proposition.

Proposition 2.2. *The set $X_N^\epsilon := \{\mathbf{x}_1^\epsilon, \ldots, \mathbf{x}_N^\epsilon\} \subset \mathbb{S}^2$ is a spherical t_ϵ-design if and only if*

$$\mathbf{Y}(X_N^\epsilon)^T w - \sqrt{4\pi} e_1 = 0 \quad \text{and} \quad w - \text{mid}(a, w, b) = 0, \tag{2.3}$$

where

$$(\mathrm{mid}(a,w,b))_i = \mathrm{mid}(a_i,w_i,b_i) = \begin{cases} a_i, & w_i < a_i \\ w_i, & a_i \leqslant w_i \leqslant b_i \\ b_i, & w_i > b_i \end{cases} \quad i = 1,\ldots,N.$$

Proof. It is easy to see that $w - \mathrm{mid}(a,w,b) = 0$ if and only if $a \leqslant w \leqslant b$. Hence,we only need to prove the equivalence between (2.2) and the first equality in (2.3).

Assume (2.2) holds. Since $Y_{0,1}(\mathbf{x})$ is a spherical harmonic of degree 0 with

$$\int_{\mathbb{S}^2} Y_{0,1}(\mathbf{x})^T Y_{0,1}(\mathbf{x}) d\omega(\mathbf{x}) = 1$$

and the fact that

$$\int_{\mathbb{S}^2} d\omega(\mathbf{x}) = 4\pi,$$

we have $Y_{0,1}(\mathbf{x}) \equiv 1/\sqrt{4\pi}$ and

$$\sum_{i=1}^{N} w_i Y_{0,1}(\mathbf{x}_i^\epsilon) = \int_{\mathbb{S}^2} Y_{0,1}(\mathbf{x}) d\omega(\mathbf{x}) = Y_{0,1}(\mathbf{x}) \int_{\mathbb{S}^2} d\omega(\mathbf{x}) = \sqrt{4\pi}.$$

Moreover, from that $\{Y_{\ell,k}, k = 1,\ldots,2\ell+1, \ell = 0,\ldots,t\}$ is a set of L_2-orthonormal basis functions of $\mathbb{P}_t$, we obtain

$$\sum_{i=1}^{N} w_i Y_{\ell,k}(\mathbf{x}_i^\epsilon) = \int_{\mathbb{S}^2} Y_{\ell,k}(\mathbf{x}) d\omega(\mathbf{x}) = \sqrt{4\pi} \int_{\mathbb{S}^2} Y_{\ell,k}(\mathbf{x}) Y_{0,1}(\mathbf{x}) d\omega(\mathbf{x}) = 0$$

for $k = 1,\ldots,2\ell+1$, and $1 \leqslant \ell \leqslant t$. This implies the first equality in (2.3).

Now we assume that the first equality in (2.3) holds. Then we obtain that

$$\sum_{i=1}^{N} w_i Y_{0,1}(\mathbf{x}_i^\epsilon) = \sqrt{4\pi} = \int_{\mathbb{S}^2} Y_{0,1}(\mathbf{x}) d\omega(\mathbf{x}),$$

and

$$\sum_{i=1}^{N} w_i Y_{\ell,k}(\mathbf{x}_i^\epsilon) = 0 = \int_{\mathbb{S}^2} Y_{\ell,k}(\mathbf{x}) d\omega(\mathbf{x}), \text{ for } \ell = 1,\ldots,t,\ k = 1,\ldots,2\ell+1.$$

Moreover, for any $p \in \mathbb{P}_t$, there exists a unique group of numbers $p_{\ell,k}$ satisfying

$$p = \sum_{\ell=0}^{t} \sum_{k=1}^{2l+1} p_{\ell,k} Y_{\ell,k}.$$

Hence (2.2) is derived as the following

$$\begin{aligned} \int_{\mathbb{S}^2} p(\mathbf{x}) d\omega(\mathbf{x}) &= \sum_{\ell=0}^{t} \sum_{k=1}^{2\ell+1} p_{\ell,k} \int_{\mathbb{S}^2} Y_{\ell,k}(\mathbf{x}) d\omega(\mathbf{x}) \\ &= \sum_{\ell=0}^{t} \sum_{k=1}^{2\ell+1} p_{\ell,k} \sum_{i=1}^{N} w_i Y_{\ell,k}(\mathbf{x}_i^{\epsilon}) \\ &= \sum_{i=1}^{N} w_i \sum_{\ell=0}^{t} \sum_{k=1}^{2\ell+1} p_{\ell,k} Y_{\ell,k}(\mathbf{x}_i^{\epsilon}) = \sum_{i=1}^{N} w_i p(\mathbf{x}_i^{\epsilon}). \end{aligned}$$

□

Let $X_N^0 = \{\mathbf{x}_1^0, \ldots, \mathbf{x}_N^0\} \subset \mathbb{S}^2$ be a spherical t-design system and corresponding matrix $\mathbf{Y}_0 \in \mathbb{R}^{N \times d_t}$ is defined as

$$(\mathbf{Y}_0)_{i,\ell k} = Y_{\ell,k}(\mathbf{x}_i^0), \quad i = 1, \ldots, N;\ k = 1, \ldots, 2\ell + 1,\ \ell = 0, \ldots, t.$$

For two points $\mathbf{x}_i, \mathbf{x}_j$ on the sphere $\mathbb{S}^2$, as is well known, the geodesic distance between them is defined as

$$\operatorname{dist}(\mathbf{x}_i, \mathbf{x}_j) = \cos^{-1}(\mathbf{x}_i \cdot \mathbf{x}_j),$$

and for a point set $X_N = \{\mathbf{x}_1, \cdots, \mathbf{x}_N\} \subset \mathbb{S}^2$, the separate distance of X_N is defined as

$$\rho(X_N) = \min_{i \neq j} \cos^{-1}(\mathbf{x}_i \cdot \mathbf{x}_j),$$

which represents the minimal geodesic distance between two different points in X_N.

In addition, we define the distance from the point $\mathbf{x} \in \mathbb{S}^2$ to the set X_N by

$$\operatorname{dist}(\mathbf{x}, X_N) = \min_{1 \leqslant i \leqslant N} \operatorname{dist}(\mathbf{x}, \mathbf{x}_i) = \min_{1 \leqslant i \leqslant N} \cos^{-1}(\mathbf{x} \cdot \mathbf{x}_i),$$

which can also be seen as the geodesic distance from $\mathbf{x}$ to its projection on X_N. And based on this definition, we denote the *Hausdorff distance* between two point sets X_N

and X'_N as

$$\begin{aligned}\sigma(X_N, X'_N) &= \max\{\max_{1\leqslant i\leqslant N} \mathrm{dist}(\mathbf{x}'_i, X_N),\ \max_{1\leqslant i\leqslant N} \mathrm{dist}(\mathbf{x}_i, X'_N)\} \\ &= \max\{\max_i \min_j \cos^{-1}(\mathbf{x}'_i \cdot \mathbf{x}_j), \max_j \min_i \cos^{-1}(\mathbf{x}'_i \cdot \mathbf{x}_j)\}. \qquad (2.4)\end{aligned}$$

Note that $\sigma(X_N, X'_N) = \sigma(X'_N, X_N)$ and $\sigma(X_N, X'_N) = 0$ if and only if $X_N = X'_N$.

Remark 2.3. *For two point sets X_N and X'_N, if $\sigma(X_N, X'_N) < \frac{1}{2}\rho(X_N)$, then for each $\mathbf{x}_i \in X_N$ there exists a unique $\mathbf{x}'_j \in X'_N$ satisfying $\mathbf{x}'_j \in \mathcal{C}(\mathbf{x}_i, \frac{1}{2}\rho(X_N))$, where*

$$\mathcal{C}(\mathbf{x}_i, \frac{1}{2}\rho(X_N)) = \{\mathbf{x} \in \mathbb{S}^2 \mid \cos^{-1}(\mathbf{x} \cdot \mathbf{x}_i) \leqslant \frac{1}{2}\rho(X_N)\}.$$

From the remark we know that, for two point sets $X'_N, X_N \subset \mathbb{S}^2$, if the Hausdorff distance between them is smaller than separate distance of X'_N, then every cap region $\mathcal{C}(\mathbf{x}_i, \frac{1}{2}\rho(X_N))$ includes a unique point in X'_N. Based on this uniqueness property, in what follows we will let $\mathbf{x}'_i$ be the point in $\mathcal{C}(\mathbf{x}_i, \frac{1}{2}\rho(X_N))$ for simplicity if we assume $\sigma(X_N, X'_N) < \frac{1}{2}\rho(X_N)$.

In the following part we will investigate the relationship between spherical t-designs and spherical t_ϵ-designs when they are all fundamental systems with $N = (t+1)^2$. Let the point set $X_N = \{\mathbf{x}_1, \ldots \mathbf{x}_N\} \subset \mathbb{S}^2$ be a fundamental system with order t and $N = (t+1)^2$. We denote $\mathbf{Y} = \mathbf{Y}(X_N) \in \mathbb{R}^{N\times(t+1)^2}$ by

$$\mathbf{Y}_{i,\ell^2+k} = Y_{\ell,k}(\mathbf{x}_i) \text{ for } i = 1, \ldots, N, \ell = 1, \ldots, t, k = 1, \ldots, 2\ell+1,$$

which is nonsigular and thus there exists a unique vector $w \in \mathbb{R}^N$ such that

$$\mathbf{Y}^T \cdot w = \sqrt{4\pi} e_1. \qquad (2.5)$$

Correspondingly, for a spherical t-design point set X_N^0 we have known that [64]

$$\mathbf{Y}_0^T \cdot \frac{4\pi}{N} e = \sqrt{4\pi} e_1. \qquad (2.6)$$

Then together with these two equalities and Theorem 2.1 in [37], if $\|(\mathbf{Y}_0^T)^\dagger((\mathbf{Y}_0 - \mathbf{Y})^T)\| < 1$ we can obtain that

$$\frac{\|w-\frac{4\pi}{N}e\|}{\|\frac{4\pi}{N}e\|} \leqslant \frac{\|(\mathbf{Y}_0^T)^\dagger\| \cdot \|(\mathbf{Y}_0-\mathbf{Y})^T\|}{1-\|(\mathbf{Y}_0^T)^\dagger(\mathbf{Y}_0-\mathbf{Y})^T\|}, \tag{2.7}$$

where $(\mathbf{Y}_0^T)^\dagger$ is the generalized inverse of $\mathbf{Y}_0^T$. Since X_N^0 is a fundamental system with order t and $N=(t+1)^2$, $\mathbf{Y}_0$ is also nonsingular and we have

$$\frac{\|w-\frac{4\pi}{N}e\|}{\|\frac{4\pi}{N}e\|} \leqslant \frac{\|(\mathbf{Y}_0^T)^{-1}\| \cdot \|(\mathbf{Y}_0-\mathbf{Y})^T\|}{1-\|(\mathbf{Y}_0^T)^{-1}(\mathbf{Y}_0-\mathbf{Y})^T\|}. \tag{2.8}$$

By the definition of matrix $(\mathbf{Y}_0-\mathbf{Y})^T$ we have

$$\big((\mathbf{Y}_0-\mathbf{Y})^T\big)_{\ell^2+k,i} = Y_{\ell,k}(\mathbf{x}_i^0) - Y_{\ell,k}(\mathbf{x}_i).$$

Let $Q_{\ell,k}$ be the restriction of $Y_{\ell,k}$ on the great circle through $\mathbf{x}_i^0$ and $\mathbf{x}_i$, see [64]. Then $Q_{\ell,k}$ is a trigonometric function and by Bernstein's inequality (1.19) we can obtain

$$\begin{aligned} |Y_{\ell,k}(\mathbf{x}_i^0) - Y_{\ell,k}(\mathbf{x}_i)| &= |Q_{\ell,k}(\mathbf{x}_i^0) - Q_{\ell,k}(\mathbf{x}_i)| \\ &\leqslant \cos^{-1}(\mathbf{x}_i^0\cdot\mathbf{x}_i)\sup|Q'_{\ell,k}| \\ &\leqslant \cos^{-1}(\mathbf{x}_i^0\cdot\mathbf{x}_i)(t+1)\sup|Q_{\ell,k}| \\ &\leqslant \cos^{-1}(\mathbf{x}_i^0\cdot\mathbf{x}_i)(t+1)\sup_{\mathbf{x}\in\mathbb{S}^2}|Y_{\ell,k}(\mathbf{x})|. \end{aligned} \tag{2.9}$$

For a point set $X_N^0\subset\mathbb{S}^2$, given a positive number σ^*, denote the neighborhood with respect to σ^* of X_N by

$$\mathcal{C}(X_N^0,\sigma^*) = \big\{X_N\subset\mathbb{S}^2 : \sigma(X_N,X_N^0)<\sigma^*\big\}.$$

The following theorem shows that for any fundamental spherical t-design under certain conditions, such that for any point set contained in this neighborhood is a spherical t_ϵ-design.

Lemma 2.4. *Assume that the spherical t-design X_N^0 is a fundamental system with order t and $N=(t+1)^2$. Then there exists a positive number $\sigma^*<\frac{1}{2}\rho(X_N^0)$ such that any point set X_N satisfying $0\leqslant\sigma(X_N,X_N^0)<\sigma^*$ is a fundamental spherical t_ϵ-design.*

Proof. For all $Y_{\ell,k}(\mathbf{x})$ with $\ell \leqslant t$ denote their upper bound by

$$M_t = \max_{0\leqslant\ell\leqslant t,\ 1\leqslant k\leqslant 2\ell+1} \sup_{\mathbf{x}\in\mathbb{S}^2} |Y_{\ell,k}(\mathbf{x})| = \sqrt{\frac{2t+1}{4\pi}}. \tag{2.10}$$

Then for a point set $X_N \in \mathcal{C}(X_N^0, \frac{1}{2}\rho(X_N^0))$, with inequality (2.9) we have

$$|Y_{\ell,k}(\mathbf{x}_i^0) - Y_{\ell,k}(\mathbf{x}_i)| \leqslant M_t(t+1)\sigma(X_N, X_N^0),$$

for $i = 1, \ldots, N,\ \ell = 0, \ldots, t,\ k = 1, \ldots, 2\ell+1$. Then it is easy to obtain that

$$\|(\mathbf{Y}_0 - \mathbf{Y})^T\|_\infty \leqslant N(t+1)M_t\sigma(X_N, X_N^0) = (t+1)^3 M_t\sigma(X_N, X_N^0), \tag{2.11}$$

by the definition of matrix norm $\|\cdot\|_\infty$. For fixed t it is obvious that we can let

$$\sigma_1 = \frac{1}{(t+1)^3 M_t \|(\mathbf{Y}_0^T)^{-1}\|_\infty},$$

so that for any set X_N satisfying $\sigma(X_N, X_N^0) < \sigma_1$ the condition $\|(\mathbf{Y}_0^T)^{-1}\| \cdot \|(\mathbf{Y}_0 - \mathbf{Y})^T\|_\infty < 1$ is satisfied. Then together by the fact

$$\|\mathbf{I} - (\mathbf{Y}_0^T)^{-1}\mathbf{Y}\|_\infty \leqslant \|(\mathbf{Y}_0^T)^{-1}\|_\infty \|\mathbf{Y}_0^T - \mathbf{Y}^T\|_\infty < 1,$$

It can be concluded that $\mathbf{Y}$ is always nonsigular for point set X_N satisfying $\sigma(X_N, X_N^0) < \sigma_1$, which implies that X_N is a fundamental system.

Now let

$$\sigma^* = \frac{1}{2}\sigma_1 = \frac{1}{2\|(\mathbf{Y}_0^T)^{-1}\|_\infty M_t (t+1)^3}.$$

Together with inequality (2.8) we have

$$\begin{aligned}
\|w - \frac{4\pi}{N}e\|_\infty &= \frac{4\pi}{N}\frac{\|w - \frac{4\pi}{N}e\|_\infty}{\|\frac{4\pi}{N}e\|_\infty} \\
&\leqslant \frac{4\pi}{N}\frac{\|(\mathbf{Y}_0^T)^{-1}\|_\infty \|(\mathbf{Y}_0 - \mathbf{Y})^T\|_\infty}{1 - \|(\mathbf{Y}_0^T)^{-1}(\mathbf{Y}_0 - \mathbf{Y})^T\|_\infty} \\
&< \frac{4\pi}{N}\frac{\|(\mathbf{Y}_0^T)^{-1}\|_\infty M_t (t+1)^3 \sigma^*}{1 - \|(\mathbf{Y}_0^T)^{-1}\|_\infty M_t (t+1)^3 \sigma^*} \leqslant \frac{4\pi}{N},
\end{aligned}$$

which implies that w is a positive vector. Then σ^* is the positive number which satisfies the lemma. □

Corollary 2.5. *Let X_N^0 be a fundamental spherical t-design with order t and $N = (t+1)^2$. Then X_N is a fundamental spherical t_ϵ-design if*

$$\sigma < \frac{1}{2}\rho(X_N^0) \text{ and } \sigma \leqslant \frac{\epsilon}{\|(\mathbf{Y}_0^T)^{-1}\|_\infty M_t(t+1)^3}.$$

Proof. By the fact that $\sigma(X_N, X_N^\epsilon) < \sigma_1$, we can have

$$\begin{aligned} \|w - \frac{4\pi}{N}e\|_\infty &\leqslant \frac{4\pi}{N}\frac{\|(\mathbf{Y}_0^T)^{-1}\|_\infty M_t(t+1)^3\sigma}{1 - \|(\mathbf{Y}_0^T)^{-1}\|_\infty M_t(t+1)^3\sigma} \\ &\leqslant \frac{4\pi}{N}\frac{\epsilon}{1-\epsilon}. \end{aligned}$$

Then we have

$$w \geqslant (1 - \frac{\epsilon}{1-\epsilon})\frac{4\pi}{N}e > \frac{4\pi(1-\epsilon)}{N}e,$$

and

$$w \leqslant (1 + \frac{\epsilon}{1-\epsilon})\frac{4\pi}{N}e = \frac{4\pi(1-\epsilon)^{-1}}{N}e.$$

We complete the proof. □

In the above theorem and corollary we have both assumed that there exists a fundamental spherical t-design for $N = (t+1)^2$. Until now, there have been a lot of ways about how to calculate the spherical t-designs in 2-dimensional case, such as [2, 43, 64]. But as is well known, there is no theoretical result which proves the existence of a spherical t-design with $(t+1)^2$ nodes or less. However, Chen, Frommer and Lang in [25] proposed computer-assisted proof of spherical t-designs with $N = (t+1)^2$ for $t \leqslant 100$. In this paper, they propose a computational algorithm based on interval arithmetic which, for given $t \leqslant 100$, upon successful completion has proved the existence of a spherical t-design with $(t+1)^2$ nodes on $\mathbb{S}^2 \subset \mathbb{R}^3$ and computed narrow interval enclosures which are known to contain a well-conditioned fundamental spherical t-design. From Corollary 2.5 we can know that, if the range of of interval enclosure is small enough, we can definitely say that any point set selected from these interval enclosures is a fundamental spherical t_ϵ-design.

In the following part, we will emphasize on the relationship between spherical t_ϵ-design and the interval enclosures proposed in [25].

Now let

$$\mathbb{X}_N = \{[\mathbf{x}]_i = \mathcal{C}(\mathbf{x}_{c,i}, \gamma_i) \subset \mathbb{S}^2,\ i = 1, \ldots, N\} \tag{2.12}$$

be a set of spherical caps, with $\mathbf{x}_{c,i}$ as the center and γ_i as the radius of each cap. We say that $\mathbb{X}_N$ is an interval enclosure of a point set X_N if $\mathbf{x}_i \in [\mathbf{x}]_i$ for $i = 1, \ldots, N$. Denote the radius of $\mathbb{X}_N$ by

$$\mathrm{rad}(\mathbb{X}_N) = \max_{1 \leqslant i \leqslant N} \gamma_i,$$

and the separate distance of $\mathbb{X}_N$ by

$$\rho(\mathbb{X}_N) = \min_{\substack{i \neq j \\ \mathbf{x}_i \in [\mathbf{x}]_i, \mathbf{x}_j \in [\mathbf{x}]_j,}} \cos^{-1}(\mathbf{x}_i \cdot \mathbf{x}_j).$$

In [25], the points $\mathbf{x}_i,\ i = 1, \ldots, N$, on the sphere are presented by spherical coordinates with θ_i and φ_i as stated in Chapter 1, and then they seek intervals $[\theta]_i$, $[\varphi]_i$ such that there is a well-conditioned spherical t-design in the interval set $\mathbb{Z}_N = \{[\mathbf{z}]_1, \ldots, [\mathbf{z}]_N\}$, in which the interval for each point is defined by

$$[\mathbf{z}]_i = \begin{pmatrix} \sin([\theta]_i)\cos([\varphi]_i) \\ \sin([\theta]_i)\sin([\varphi]_i) \\ \cos([\theta]_i) \end{pmatrix}, \quad i = 1, \ldots, N. \tag{2.13}$$

In this sense, different from the interval enclosure defined in this section, each interval enclosure calculated in [25] is a rectangle as $[\theta]_i \times [\varphi]_i$, whereas in our section we deal with a spherical cap. To deal with this difference, we need to construct a series of spherical caps which include the spherical rectangles in [25]. For the spherical rectangle $[\theta]_i \times [\varphi]_i =$

$[\underline{\theta}_i, \bar{\theta}_i] \times [\underline{\varphi}_i, \bar{\varphi}_i]$, we denote a pair of its four vertice as

$$\mathbf{x}_{i,1} = \begin{pmatrix} \sin(\underline{\theta}_i)\cos(\underline{\varphi}_i) \\ \sin(\underline{\theta}_i)\sin(\underline{\varphi}_i) \\ \cos(\underline{\theta}_i) \end{pmatrix}, \quad \mathbf{x}_{i,2} = \begin{pmatrix} \sin(\underline{\theta}_i)\cos(\bar{\varphi}_i) \\ \sin(\underline{\theta}_i)\sin(\bar{\varphi}_i) \\ \cos(\underline{\theta}_i) \end{pmatrix},$$

$$\mathbf{x}_{i,3} = \begin{pmatrix} \sin(\bar{\theta}_i)\cos(\bar{\varphi}_i) \\ \sin(\bar{\theta}_i)\sin(\bar{\varphi}_i) \\ \cos(\bar{\theta}_i) \end{pmatrix}, \quad \mathbf{x}_{i,4} = \begin{pmatrix} \sin(\bar{\theta}_i)\cos(\underline{\varphi}_i) \\ \sin(\bar{\theta}_i)\sin(\underline{\varphi}_i) \\ \cos(\bar{\theta}_i) \end{pmatrix}.$$

By the symmetric property of of the spherical rectangle $[\theta]_i \times [\varphi]_i$, we can know that there exists a point $\mathbf{x}_{c,i} \in [\theta]_i \times [\varphi]_i$ with its spherical coordinate as $(\theta_i^c, \frac{1}{2}(\underline{\varphi}_i + \bar{\varphi}_i))$ satisfying

$$\mathrm{dist}(\mathbf{x}_{c,i}, \mathbf{x}_{i,j}) = \mathrm{dist}(\mathbf{x}_{c,i}, \mathbf{x}_{i,k}) \quad \text{for } j,k = 1,2,3,4. \tag{2.14}$$

Also note that all the points with whose geodesic distance to $\mathbf{x}_i^1$ and $\mathbf{x}_i^4$ are located on a great circle

$$\begin{cases} x^2 + y^2 + z^2 = 1 \\ ax + by + cz = 0 \end{cases}, \tag{2.15}$$

with $a, b, c \in \mathbb{R}$, which crosses $(\frac{1}{2}(\underline{\theta}_i + \bar{\theta}_i), \underline{\varphi}_i)$, the geodesic middle point of $\mathbf{x}_i^1$ and $\mathbf{x}_i^4$, is orthogonal to the line segment through these two points. Therefore, the center point $\mathbf{x}_c^i$ will also located on this great circle. By the fact that $(\frac{\pi}{2}, \underline{\varphi}_i + \frac{\pi}{2})$ is also on this great circle, we can then uniquely obtain the proportion of $a,\ b,\ c$. Then the center point $\mathbf{x}_{c,i}$ can be obtained by substituting its azimuthal angle $\frac{1}{2}(\underline{\varphi}_i + \bar{\varphi}_i)$ to the form of the great circle. After that, let

$$\gamma_i = \mathrm{dist}(\mathbf{x}_{c,i}, \mathbf{x}_i^1), \tag{2.16}$$

and then the cap region $\mathcal{C}(\mathbf{x}_c^i, \gamma_i)$ is a spherical cap and we can have that

$$[\mathbf{z}]_i \subseteq \mathcal{C}(\mathbf{x}_{c,i}, \gamma_i).$$

By this strategy, we can obtain the center point $\mathbf{x}_{c,i}$ with its distance to the four vertice equal to each other, and the generated spherical cap has a minimal possible radius. However, in this process, for each interval $[\mathbf{z}]_i$, we need first obtain the close form of the great circle including $\mathbf{x}_{c,i}$ by substituting two points into (2.15). Then, we substitute the azimuthal angles of $\mathbf{x}_{c,i}$ to the great circle and obtain the polar angle of $\mathbf{x}_{c,i}$ and then calculate the radius. This approach is time-consuming and will import more round-off errors. Since the measure of intervals $[\theta]_i \times [\varphi]_i$ are usually very small, this approach is not recommended to use. Instead, we will create another strategy which is coarser but more suitable for our problem.

For the interval enclosure set $[\mathbf{z}]_i$, by $\tilde{\mathbf{x}}_i$ we denote the point with its spherical coordinate as $(\frac{1}{2}(\underline{\theta}_i + \bar{\theta}_i), \frac{1}{2}(\underline{\varphi}_i + \bar{\varphi}_i))$, with its cartesian coordinate as

$$\tilde{\mathbf{x}}_i = \begin{pmatrix} \sin(\frac{1}{2}(\bar{\theta}_i + \underline{\theta}_i)) \cos(\frac{1}{2}(\bar{\varphi}_i + \underline{\varphi}_i)) \\ \sin(\frac{1}{2}(\bar{\theta}_i + \underline{\theta}_i)) \sin(\frac{1}{2}(\bar{\varphi}_i + \underline{\varphi}_i)) \\ \cos(\frac{1}{2}(\bar{\theta}_i + \underline{\theta}_i)) \end{pmatrix}. \tag{2.17}$$

Note that its spherical coordinate is the center point of the interval $[\theta]_i \times [\varphi]_i$ but $\tilde{\mathbf{x}}_i$ itself is not necessary to be the center point of $[\mathbf{z}]_i$. Still, we have that

$$\mathrm{dist}(\tilde{\mathbf{x}}_i, \mathbf{x}_i^1) = \mathrm{dist}(\tilde{\mathbf{x}}_i, \mathbf{x}_i^1), \quad \mathrm{dist}(\tilde{\mathbf{x}}_i, \mathbf{x}_i^3) = \mathrm{dist}(\tilde{\mathbf{x}}_i, \mathbf{x}_i^4). \tag{2.18}$$

And we know that the distance between $\tilde{\mathbf{x}}_i$ and any point in $[\mathbf{z}]_i$ does not exceed the maximum of the four in (2.18) when the measures of $[\theta]_i$ and $[\varphi]_i$ are sufficiently small. Therefore, if we let

$$\gamma_i = \max\{\mathrm{dist}(\tilde{\mathbf{x}}_i, \mathbf{x}_i^1) \ , \ \mathrm{dist}(\tilde{\mathbf{x}}_i, \mathbf{x}_i^3)\}, \tag{2.19}$$

then we can have

$$[\mathbf{z}]_i \subseteq \mathcal{C}(\tilde{\mathbf{x}}_i, \gamma_i). \tag{2.20}$$

Similarly, we define the radius of $\mathbb{Z}_N$ by

$$\mathrm{rad}(\mathbb{Z}_N) = \max_{1 \leqslant i \leqslant N} \big\{ \max\{\mathrm{dist}(\tilde{\mathbf{x}}_i, \mathbf{x}_i^1) \ , \ \mathrm{dist}(\tilde{\mathbf{x}}_i, \mathbf{x}_i^3)\}\big\}, \tag{2.21}$$

and the separate distance by

$$\rho(\mathbb{Z}_N) = \min_{\substack{i \neq j \\ 1 \leqslant i,j \leqslant N}} \{\mathrm{dist}(\tilde{\mathbf{x}}_i, \tilde{\mathbf{x}}_j) - \gamma_i - \gamma_j\}. \tag{2.22}$$

Then we can have the following theorem.

Theorem 2.6. *Let $\mathbb{X}_N$ defined by (2.12) and $\mathbb{Z}_N$ defined by (2.13) be two interval enclosure sets containing a fundamental spherical t-design X_N^0 and assume that* $\mathrm{rad}(\mathbb{X}_N) < \rho(\mathbb{X}_N)$, $\mathrm{rad}(\mathbb{Z}_N) < \rho(\mathbb{Z}_N)$. *Then all the point sets X_N with $\mathbf{x}_i \in [\mathbf{x}]_i,\ i = 1, \ldots N$, are fundamental spherical t_ϵ-designs with*

$$\epsilon = C_{t,1}(t+1)^3, \tag{2.23}$$

where

$$C_{t,1} = 2\mathrm{rad}(\mathbb{X}_N) M_t \max_{X_N \in \mathbb{X}_N} \|(\mathbf{Y}^T)^{-1}\|_\infty.$$

And all the point sets X_N with $\mathbf{x}_i \in [\mathbf{z}]_i,\ i = 1, \ldots N$, are fundamental spherical t_ϵ-designs with

$$\epsilon = C_{t,2}(t+1)^3, \tag{2.24}$$

where

$$C_{t,2} = 2\mathrm{rad}(\mathbb{Z}_N) M_t \max_{X_N \in \mathbb{Z}_N} \|(\mathbf{Y}^T)^{-1}\|_\infty.$$

Proof. First we prove the formula (2.23). Since for X_N^0 we have $\mathbf{x}_i \in [\mathbf{x}]_i$ for $i = 1, \ldots, N$, we can have

$$\rho(X_N^0) \leqslant \rho(\mathbb{X}_N).$$

And for arbitrary X_N with $\mathbf{x}_i \in [\mathbf{x}^0]_i,\ i = 1, \ldots N$, we also have

$$\sigma = \sigma(X_N, X_N^0) \leqslant \max_{1 \leqslant i \leqslant N} \cos^{-1}(\underline{\mathbf{x}}_i \cdot \bar{\mathbf{x}}_i) = 2\mathrm{rad}(\mathbb{X}_N).$$

Thus together by the assumption $\mathrm{rad}(\mathbb{X}_N) < \rho(\mathbb{X}_N)$ we have $\sigma < \frac{1}{2}\rho(X_N^0)$. And together

with the fact

$$\begin{aligned}\sigma &\leqslant 2\mathrm{rad}(\mathbb{X}_N)\\ &= \frac{\epsilon}{M_t \max_{X_N\in\mathbb{X}_N}\|(\mathbf{Y}^T)^{-1}\|_\infty}\\ &\leqslant \frac{\epsilon}{\|(\mathbf{Y}_0^T)^{-1}\|_\infty M_t(t+1)^3},\end{aligned}$$

we can obtain (2.23) according to Corollary 2.5.

For the interval enclosure $\mathbb{Z}_N$, we define a new set of spherical caps on the sphere as

$$\tilde{\mathbb{X}}_N = \{\mathcal{C}(\tilde{\mathbf{x}}_i, \gamma_i),\ i = 1, \ldots, N\},$$

with $\tilde{\mathbf{x}}_i$, γ_i defined by (2.17) and (2.19). Then by (2.21) and (2.22) we have $\mathrm{rad}(\tilde{\mathbb{X}}_N) = \mathrm{rad}(\mathbb{Z}_N)$ and $\rho(\tilde{\mathbb{X}}_N) = \rho(\mathbb{Z}_N)$. With similar process of proving (2.23), we can obtain (2.24) and complete the proof. □

The next problem we need to solve is that how to calculate the value or an upper bound of $\max_{X_N\in\mathbb{X}_N}\|(\mathbf{Y}^T)^{-1}\|_\infty$, and then we can give the upper bound of ϵ, denoted by $\bar{\epsilon}$, for the interval enclosure provided in [25].

Denote $\mathbf{x}_{c,i}$ by the center of the interval closure $[\mathbf{x}]_i$. Let $X_{c,N} = \{\mathbf{x}_{c,1}, \ldots, \mathbf{x}_{c,N}\} \subset \mathbb{S}^2$, and for simplicity we denote $\mathbf{Y}_c = \mathbf{Y}(X_{c,N})$. By Corollary 2.7 in [66] we conclude that for arbitrary X_N with $\mathbf{x}_i \in [\mathbf{x}]_i,\ i = 1, \ldots, N$, we have

$$\|(\mathbf{Y}^T)^{-1}\|_\infty \leqslant \frac{\|(\mathbf{Y}_c^T)^{-1}\|_\infty}{1 - \kappa(\mathbf{Y}_c^T)\dfrac{\|\mathbf{Y}_c^T - \mathbf{Y}^T\|_\infty}{\|\mathbf{Y}_c^T\|_\infty}}.$$

Additionally, since each $\mathbf{x}_{c,i}$ is the center of $[\mathbf{x}]_i$, which implies that $\sigma(X_N, X_{c,N}) \leqslant \mathrm{rad}(\mathbb{X}_N)$, then together with inequality (2.11) we can obtain

$$\|(\mathbf{Y}_c - \mathbf{Y})^T\|_\infty \leqslant (t+1)^3 M_t \mathrm{rad}(\mathbb{X}_N).$$

Finally we can conclude that if $\mathrm{rad}(\mathbb{X}_N) < \dfrac{\|\mathbf{Y}_c^T\|_\infty}{M_t(t+1)^3\kappa(\mathbf{Y}_c^T)}$, the upper bound of infinity norm of $(\mathbf{Y}^T)^{-1}$ can be estimated as

$$\max_{X_N \in \mathbb{X}_N} \|(\mathbf{Y}^T)^{-1}\|_\infty \leqslant \frac{\|(\mathbf{Y}_c^T)^{-1}\|_\infty}{1 - \kappa(\mathbf{Y}_c^T)\dfrac{(t+1)^3 M_t \mathrm{rad}(\mathbb{X}_N)}{\|\mathbf{Y}_c^T\|_\infty}}. \tag{2.25}$$

Now we prepare to calculate the upper bound of ϵ for the interval inclosures proposed in [25], which we denote by $\bar{\epsilon}$ here. Based on this relationship, now we can calculate the $\bar{\epsilon}$ for the interval enclosures proposed in [25]. Then according to Theorem 2.6 we can say that arbitrary point set chosen from the interval enclosure set X_N satisfying $\mathbf{x}_i \in [\mathbf{x}]_i$ for $i = 1, \ldots, N$ is a fundamental spherical t_ϵ-design. The data containing the enclosures for the parameterization of the spherical t-designs and the programs can be downloaded from the web site http://www-ai.math.uni-wuppertal.de/SciComp/SphericalTDesigns.

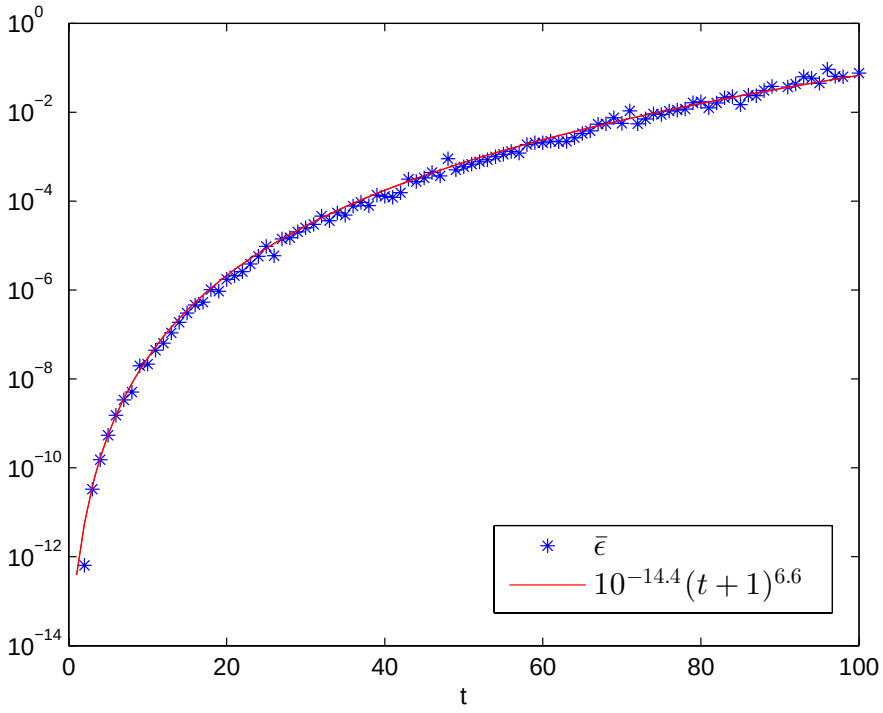

Figure 2.1: $\bar{\epsilon}$ for $t = 2, \ldots, 100$

In Fig. 2.1 we report the upper bound of ϵ for interval enclosures computed in [25] for $t = 2, \ldots, 100$ (for $t = 1$ we have known an exact form of spherical t-design so that we would not consider this case here), based on formula (2.23) and (2.25). In this figure we

also plot a function

$$y = 10^{-14.4}(t+1)^{6.6}, \tag{2.26}$$

to approximately discribe the track of $\bar{\epsilon}$ with respect to t. From the figure we can conclude that the upper bound of ϵ grows with the increase of t. Additionally, from (2.25) we know that the condition number of $\mathbf{Y}_c^T$ is also of great importance in this process. Since the interval enclosures provided by [25] seek to include a well-conditioned spherical t-design, the growth of upper bound of ϵ keeps stable for all the t considered here.

Table 2.1: Information for interval enclosures $\mathbb{Z}_N$ for selected t

t	$\text{rad}(\mathbb{Z}_N)$	$\rho(\mathbb{Z}_N)$	$\bar{\epsilon}$	ϵ for $X_{c,N}$
10	1.843454e-12	3.396362e-01	2.148389e-08	6.694645e-14
20	1.515848e-11	1.805783e-01	1.744486e-06	1.783018e-13
30	5.588085e-11	1.249714e-01	2.510650e-05	2.480238e-13
40	1.044163e-10	9.203055e-02	1.285961e-04	5.339063e-13
50	2.199182e-10	7.638945e-02	5.906459e-04	5.057066e-13
60	4.006638e-10	6.302748e-02	2.043721e-03	6.747935e-13
70	6.143914e-10	5.421869e-02	5.594428e-03	8.820722e-13
80	1.220430e-09	4.771142e-02	1.722072e-02	1.151368e-12
90	2.089473e-09	4.264961e-02	4.686558e-02	1.228462e-12
100	2.273791e-09	3.846343e-02	7.549403e-02	1.880540e-12

We also report some information of the interval enclosures and their theoretical upper bound of ϵ for some selected t in Table 2.1. The radius and separate distance for $\mathbb{X}_N$ are shown in the table as the second and the third column. We can see that the radius of each interval enclosures is far smaller than their separate distance, which means that the assumption in the above lemmas and theorems are satisfied. For a fixed t, with all the interval $([\theta]_i, [\phi]_i) \in \mathbb{Z}_N$, $i = 1, \cdots, N$, we choose their middle points and build a new point set $\tilde{X}_N = \{\tilde{\mathbf{x}}_1 \cdots, \tilde{\mathbf{x}}_N\}$, with $\tilde{\mathbf{x}}_i$ defined by (2.17). For each new point set $\tilde{X}_N$ we compute its ϵ so that it forms an spherical t_ϵ-design. As shown in the table, the ϵ's for each $\tilde{X}_N$ are all very close to zero but they still do not equal to, and they are growing

with the increase of t. This means that $\tilde{X}_N$ which is selected properly from the interval enclosures is still not a spherical t-design, but a spherical t_ϵ-design.

2.2 Variational characterization of spherical t_ϵ-designs

In this section we focus on investigating the variational characterization of spherical t_ϵ-designs on $\mathbb{S}^2$. In [64] Sloan and Womersley proposed some variational characterizations for spherical t-designs. In this section, we will generalize their results to spherical t_ϵ-designs case. Different from spherical t-design case, in spherical t_ϵ-design case the weights is allowed to be chosen in an interval, instead of restricting them to be equal to each other. Therefore, other than only the set of points, the weights are also variables in the study of spherical t_ϵ-designs. Now we denote by the matrix $\mathbf{Y}_1 = \mathbf{Y}_1(X_N^\epsilon) \in \mathbb{R}^{N\times(d_t-1)}$ with

$$(\mathbf{Y}_1)_{i,\ell^2+k}(X_N^\epsilon) = Y_{\ell,k}(\mathbf{x}_i), \quad i = 1,\dots,N;\ k = 1,\dots,2\ell+1,\ \ell = 1,\dots,t.$$

Let $Q[X_N^\epsilon, w]$ be the integration rule with node set X_N^ϵ and weights w approximating the integral $I(f)$, which are defined by

$$Q[X_N^\epsilon, w](f) = \sum_{i=1}^{N} w_i f(\mathbf{x}_i), \tag{2.27}$$

and

$$I(f) = \int_{\mathbb{S}^2} f(\mathbf{x}) d\omega(\mathbf{x}). \tag{2.28}$$

where $\omega(\mathbf{x})$ is the surface measure. For the cubature rule $Q[X_N^\epsilon, w]$ we define a quantity function as

$$A_t(X_N^\epsilon, w) = \frac{1}{2}\|\mathbf{Y}_1^T(X_N^\epsilon)w\|_2^2 = \frac{1}{2}w^T\mathbf{Y}_1(X_N^\epsilon)\mathbf{Y}_1^T(X_N^\epsilon)w. \tag{2.29}$$

Obviously, by the definition of $\mathbf{Y}_1(X_N^\epsilon)$, this non-negative function $A_t(X_N^\epsilon, w) : \mathbb{S}^2 \times \mathbb{R} \to \mathbb{R}$ can also represented as

$$A_t(X_N^\epsilon, w) = \frac{1}{2}\sum_{i=1}^{N}\sum_{j=1}^{N} w_i w_j \Psi(\mathbf{x}_i, \mathbf{x}_j), \tag{2.30}$$

where

$$\Psi(\mathbf{x}_i, \mathbf{x}_j) = \sum_{\ell=1}^{t}\sum_{k=1}^{2\ell+1} Y_{\ell,k}(\mathbf{x}_i)Y_{\ell,k}(\mathbf{x}_j).$$

According to the new notation (2.29), we can reformulate proposition (2.2) as the following.

Remark 2.7. *$X_N^\epsilon := \{\mathbf{x}_1, \ldots, \mathbf{x}_N\} \subset \mathbb{S}^2$ is a spherical t_ϵ-design if and only if there exists a vector w satisfying*

$$\begin{pmatrix} e^T w \\ w - \mathrm{mid}(a, w, b) \end{pmatrix} = \begin{pmatrix} 4\pi \\ 0 \end{pmatrix}, \tag{2.31}$$

where $e = (1, \ldots, 1)^T \in \mathbb{R}^N$, such that

$$A_t(X_N^\epsilon, w) = 0.$$

Note that equality (2.2) implies

$$\frac{1}{\sqrt{4\pi}} e^T w = \sum_{i=1} w_i Y_{0,1} = \sqrt{4\pi},$$

and

$$\mathbf{Y}_1^T(X_N^\epsilon) w = 0.$$

Remark 2.8. *The quantity function $A_t(X_N^\epsilon, w)$ is rotationally invariant, i.e., let $SX_N^\epsilon = \{S\mathbf{x}_1^\epsilon, \ldots, S\mathbf{x}_N^\epsilon\} \subset \mathbb{S}^2$ with $S \in \mathfrak{U}^3$, then there always holds*

$$A_t(SX_N^\epsilon, w) = A_t(X_N^\epsilon, w). \tag{2.32}$$

Proof. By the addition theorem 1.4 we can have

$$\Psi(\mathbf{x}_i^\epsilon, \mathbf{x}_j^\epsilon) = \sum_{\ell=1}^{t} \frac{2\ell + 1}{4\pi} P_\ell(\mathbf{x}_i^\epsilon \cdot \mathbf{x}_j^\epsilon), \quad \forall \mathbf{x}_i^\epsilon, \mathbf{x}_j^\epsilon \in \mathbb{S}^2.$$

Then

$$\begin{aligned} A_t(SX_N^\epsilon, w) &= \frac{1}{2}\sum_{i=1}^{N}\sum_{j=1}^{N} w_i w_j \Psi(S\mathbf{x}_i^\epsilon, S\mathbf{x}_j^\epsilon) \\ &= \frac{1}{2}\sum_{i=1}^{N}\sum_{j=1}^{N} w_i w_j \sum_{\ell=1}^{t} \frac{2\ell+1}{4\pi} P_\ell((S\mathbf{x}_i^\epsilon)\cdot(S\mathbf{x}_j^\epsilon)) \\ &= \frac{1}{2}\sum_{i=1}^{N}\sum_{j=1}^{N} w_i w_j \sum_{\ell=1}^{t} \frac{2\ell+1}{4\pi} P_\ell((\mathbf{x}_i^\epsilon)^T S^T S\mathbf{x}_j^\epsilon) \\ &= \frac{1}{2}\sum_{i=1}^{N}\sum_{j=1}^{N} w_i w_j \Psi(\mathbf{x}_i^\epsilon, \mathbf{x}_j^\epsilon) \\ &= A_t(X_N^\epsilon, w). \end{aligned}$$

We complete the proof. □

The remark illustrates that, like spherical t-designs on the sphere, spherical t_ϵ-designs can be mapped upon each other via a rotation on the sphere and regarded to be equivalent with respect to the quantity function A_t, even when they have different weights.

The second result discusses the bound of the quantity function for arbitrary point set on the sphere $\mathbb{S}^2$.

Lemma 2.9. *Let $t \geqslant 1$. If w satisfies (2.31), then*

$$0 \leqslant A_t(X_N^\epsilon, w) \leqslant \pi(t^2+2t). \tag{2.33}$$

Proof. Recall the notation (2.30) and by Addtion Theorem 1.4 we can obtain that

$$\begin{aligned} A_t(X_N^\epsilon, w) &= \frac{1}{2}\sum_{i=1}^{N}\sum_{j=1}^{N} w_i w_j \Psi(\mathbf{x}_i^\epsilon, \mathbf{x}_j^\epsilon) \\ &= \frac{1}{2}\sum_{i=1}^{N}\sum_{j=1}^{N} w_i w_j \sum_{\ell=1}^{t} \frac{2\ell+1}{4\pi} P_\ell(\mathbf{x}_i^\epsilon \cdot \mathbf{x}_j^\epsilon) \\ &\leqslant \frac{1}{8\pi}\sum_{i=1}^{N}\sum_{j=1}^{N} w_i w_j \sum_{\ell=1}^{t} 2\ell+1 \\ &\leqslant \frac{t^2+2t}{8\pi}\cdot\frac{1}{2}(\sum_{i=1}^{N} w_i)^2 \\ &= \frac{1}{2}\cdot\frac{t^2+2t}{8\pi}(4\pi)^2 \\ &= \pi(t^2+2t). \end{aligned}$$

The proof is completed. □

In the following part we need a notion of stationary points and stationary quadratures. Usually, a point $\mathbf{x} \in \mathbb{S}^2$ is called a stationary point of $f \in C^1(\mathbb{S}^2)$ if $(\nabla^*)f(\mathbf{x}) = 0$, where ∇^* denotes the surface gradient [39] of f. Similarly, we say that (X_N^ϵ, w) with $X_N^\epsilon \subset \mathbb{S}^2$, $w \in \mathbb{R}^N$ is a stationary point of $A_t(X_N^\epsilon, w)$ when $\nabla^*_{\mathbf{x_i}} A_t(X_N^\epsilon, w) = 0$ for $i = 1, \ldots, N$ and $\nabla_w A_t(X_N^\epsilon, w) = 0$. If we have $\nabla^*_{\mathbf{x_i}^\epsilon} A_t(X_N^\epsilon, w) = 0$ for $i = 1, \ldots, N$, we say that $\nabla^* A_t(X_N^\epsilon, w) = 0$.

Lemma 2.10. *Assume that $t \geqslant 1$ and for X_N^ϵ there exists a w which satisfies (2.31) and $\nabla^* A_t(X_N^\epsilon, w) = 0$. Then either X_N^ϵ is an spherical t_ϵ-design, or there exists a nonconstant polynomial $p_{X_N^\epsilon} \in \mathbb{P}_t$ with each $\mathbf{x}_i^\epsilon \in X_N^\epsilon$, $i = 1, \ldots, N$, as its stationary point.*

Proof. First we denote that $\alpha_{\ell,k}(X_N^\epsilon, w) = \sum_{i=1}^{N} w_i Y_{\ell,k}(\mathbf{x}_i)$. Then we have that

$$A_t(X_N^\epsilon, w) = \frac{1}{2}\sum_{l=1}^{t}\sum_{k=1}^{2l+1} \alpha_{\ell,k}(X_N^\epsilon, w)^2$$

and for $i = 1, \ldots, N$,

$$\nabla^*_{\mathbf{x}_i} A_t(X_N^\epsilon, w) = \sum_{\ell=1}^{t} \sum_{k=1}^{2l+1} \alpha_{\ell,k}(X_N^\epsilon, w)(\nabla^*_{\mathbf{x}_i^\epsilon} \alpha_{\ell,k})(X_N^\epsilon, w).$$

From the equality

$$(\nabla^*_{\mathbf{x}_i^\epsilon} \alpha_{\ell,k})(X_N^\epsilon, w) = w_i(\nabla^* Y_{\ell,k})(\mathbf{x}_i),\ \ell = 1, \ldots, t,\ k = 1, \ldots, 2\ell + 1$$

we could have that

$$\begin{aligned} \nabla^*_{\mathbf{x}_i} A_t(X_N^\epsilon, w) &= \sum_{l=1}^{t} \sum_{k=1}^{2l+1} w_i \alpha_{\ell,k}(X_N^\epsilon, w)(\nabla^* Y_{\ell,k})(\mathbf{x}_i^\epsilon) \\ &= (\nabla^* p_{X_N^\epsilon})(\mathbf{x}_i^\epsilon), \end{aligned} \tag{2.34}$$

where

$$p_{X_N^\epsilon} = \sum_{l=1}^{t} \sum_{k=1}^{2l+1} w_i \alpha_{\ell,k}(X_N, w) Y_{\ell,k} \tag{2.35}$$

From (2.34) and (2.35) we see that if $\nabla^*_{\mathbf{x}_i^\epsilon} A_t(X_N^\epsilon, w) = 0$ for $i = 1, \ldots, N$, then either $\alpha_{\ell,k}(X_N^\epsilon, w) = 0$, $\ell = 1, \ldots, t,\ k = 1, \ldots, 2\ell + 1$, in which case X_N is an spherical t_ϵ-design, or $p_{X_N^\epsilon}$ is a non-constant polynomial in $\mathbb{P}_t$ which has a stationary point at each $\mathbf{x}_i^\epsilon \in X_N$. □

Based on the above lemma we can conclude another result for the characterization of spherical t_ϵ-design.

Theorem 2.11. *Let $t \geqslant 1$ and w satisfy (2.31). Suppose that we have $\nabla^* A_t(X_N^\epsilon, w) = 0$, and the mesh norm of X_N^ϵ satisfies $h_{X_N^\epsilon} < 1/(t+1)$. Then X_N^ϵ is a spherical t_ϵ-design.*

Proof. We assume that X_N^ϵ is not a spherical t_ϵ-design and seek a contradiction.

Since X_N^ϵ is a stationary point of A_t which is not a spherical t_ϵ-design, from Lemma 2.10 we conclude that there exists a nonconstant polynomial $p = p_{X_N^\epsilon} \in \mathbb{P}_t$ with each $\mathbf{x}_i^\epsilon \in X_N^\epsilon$ as its stationary point. Define

$$q_j = e_j \cdot \nabla^* p, \quad j = 1, 2, 3,$$

where $e_j, j = 1, 2, 3$ are the unit vectors in the direction of the coordinate $x_j, j = 1, 2, 3$, and the dot indicates the inner product in $\mathbb{R}^3$. By the stationary property of p, each q_j for $j = 1, 2, 3$ satisfies

$$q_j(\mathbf{x}_i^\epsilon) = 0 \quad \text{for } i = 1, \ldots, N. \tag{2.36}$$

Since p is a nonconstant polynomial, we have that at least one $q_j, j = 1, 2, 3$ is not identically zero. We assume this q is q_j. According (1.15) and (1.16) we obtain that $q \in \mathbb{P}_{t+1}$. Let $\mathbf{x}_0 \in \mathbb{S}^d$ be a point at which $\|q\|$ attains its maximum value $\|q\|_\infty$. By the definition of the mesh norm $h_{X_N^\epsilon}$ and the assumption of the theorem, there exists an $\mathbf{x}_i^\epsilon \in X_N^\epsilon$ such that

$$\cos^{-1}(\mathbf{x}_i^\epsilon \cdot \mathbf{x}_0) \leqslant h_{X_N^\epsilon} < \frac{1}{t+1}.$$

Now let Q be the restriction of q to the great circle through $\mathbf{x}_i^\epsilon$ and $\mathbf{x}_0$, parameterised by arc length, and let q' denote its derivative. Since Q is a trigonometric polynomial of degree $\leqslant t + 1$,it follows from the Bernstein's inequlity (1.5) that

$$\sup |Q'| \leqslant (t+1)\|Q\|_\infty.$$

Thus

$$\begin{aligned} |q(\mathbf{x}_0) - q(\mathbf{x}_i)| &\leqslant \sup |Q'| \cos^{-1}(\mathbf{x}_0 \cdot \mathbf{x}_i^\epsilon) \\ &\leqslant (t+1)\cos^{-1}(\mathbf{x}_0 \cdot \mathbf{x}_i^\epsilon)\|Q\|_\infty \\ &< \|Q\|_\infty, \end{aligned}$$

and in consequence

$$\begin{aligned} |q(\mathbf{x}_i^\epsilon)| &\geqslant |q(\mathbf{x}_0)| - |q(\mathbf{x}_0) - q(\mathbf{x}_i^\epsilon)| \\ &> |q(\mathbf{x}_0)| - \|Q\|_\infty = 0, \end{aligned}$$

which is a contradiction with (2.36). We complete the proof. □

In [64] Sloan and Womersley discussed the mean value of the quantity function A_t for spherical t-designs which here can be defined as

$$\bar{A}_t := (4\pi)^{-N} \int_{\mathbb{S}^2} \cdots \int_{\mathbb{S}^2} A_t(X_N, w) d\omega(\mathbf{x}_1^\epsilon) \cdots d\omega(\mathbf{x}_N^\epsilon). \tag{2.37}$$

We can also generate this result to spherical t_ϵ-design case as the following.

Theorem 2.12. *The mean value defined by (2.37) has the value*

$$\bar{A}_t = \frac{t^2+2t}{8\pi}\sum_{i=1}^{N} w_i.$$

Proof. By the definition of $\bar{A}_t$ and separating the diagonal and the off-diagonal terms of the double sum in (2.30), we can obtain that

$$\begin{aligned}
\bar{A}_t &= (4\pi)^{-N}\int_{\mathbb{S}^2}\cdots\int_{\mathbb{S}^2} A_t(X_N,w)d\omega(\mathbf{x}_1^\epsilon)\cdots d\omega(\mathbf{x}_N^\epsilon) \\
&= (4\pi)^{-N}\int_{\mathbb{S}^2}\cdots\int_{\mathbb{S}^2}\frac{1}{2}\sum_{i=1}^{N}\sum_{j=1}^{N} w_i w_j \Psi(\mathbf{x}_i^\epsilon,\mathbf{x}_j^\epsilon)d\omega(\mathbf{x}_1^\epsilon)\cdots d\omega(\mathbf{x}_N^\epsilon) \\
&= \frac{1}{2}\Bigg[(4\pi)^{-1}\sum_{i=1}^{N} w_i^2\int_{\mathbb{S}^2}\Psi(\mathbf{x}_i^\epsilon,\mathbf{x}_i^\epsilon)d\omega(\mathbf{x}_i^\epsilon) \\
&\quad +(4\pi)^{-2}\sum_{i=1}^{N}\sum_{j=1,j\neq i}^{N} w_i w_j\int_{\mathbb{S}^2}\int_{\mathbb{S}^2}\Psi(\mathbf{x}_i^\epsilon,\mathbf{x}_j^\epsilon)d\omega(\mathbf{x}_i^\epsilon)d\omega(\mathbf{x}_j^\epsilon)\Bigg].
\end{aligned}$$

By the fact

$$\begin{aligned}
\int_{\mathbb{S}^2}\Psi(\mathbf{x}_i^\epsilon,\mathbf{x}_i^\epsilon)d\omega(\mathbf{x}_i^\epsilon) &= \sum_{\ell=1}^{t}\sum_{k=1}^{2\ell+1}\int_{\mathbb{S}^2} Y_{\ell,k}^2(\mathbf{x}_i^\epsilon)d\omega(\mathbf{x}_i^\epsilon) \\
&= \sum_{\ell=1}^{t}\sum_{k=1}^{2\ell+1} 1 = t^2+2t,
\end{aligned}$$

and

$$\int_{\mathbb{S}^2}\Psi(\mathbf{x}_i^\epsilon,\mathbf{x}_j^\epsilon)d\omega(\mathbf{x}_i^\epsilon)d\omega(\mathbf{x}_j^\epsilon) = \sum_{\ell=1}^{t}\sum_{k=1}^{2\ell+1}\int_{\mathbb{S}^2} Y_{\ell,k}(\mathbf{x}_i^\epsilon)Y_{\ell,k}(\mathbf{x}_j^\epsilon)d\omega(\mathbf{x}_i^\epsilon)d\omega(\mathbf{x}_i^\epsilon) = 0,$$

we can obtain

$$\bar{A}_t = \frac{t^2+2t}{8\pi}\sum_{i=1}^{N} w_i.$$

□

2.3 Worst-case error of spherical t_ϵ-designs

In this section we will investigate the worse-case error for numerical integration on the Sobolev spaces defined on the sphere using spherical t_ϵ-designs. Until now, there are a lot of remarkable work about the constructive theory of functions including interpolation and cubature on the sphere. In some of the early work, the main tool of analyzing multivariate functions is to trace back them to univariate problems by product argument[31, 59]. In the recent development, the reproducing kernel theory is applied to analyze these problems[18, 19, 44, 45, 72]. In this section, since the Sobolev spaces are finite-dimensional rotationally invariant subspaces of $C(\mathbb{S}^2)$, the bizonal reproducing kernel will naturally be used in the analysis.

Similar with what is defined in Section 1.2, we define

$$Q[X_N, w](f) := \sum_{j=1}^{N} \frac{w_i}{4\pi} f(\mathbf{x}_j), \quad I(f) := \int_{\mathbb{S}^d} f(\mathbf{x}) d\omega_d(\mathbf{x}), \tag{2.38}$$

and

$$E_{s,d}(Q[X_N, w]) := \sup \big\{ |Q[X_N, w](f) - I(f)| : f \in \mathbb{H}^s(\mathbb{S}^d), \|f\|_{\mathbb{H}^s} \leqslant 1 \big\}. \tag{2.39}$$

And for simplicity we denote $E_s(Q[X_N, w]) = E_{s,2}(Q[X_N, w])$. Together with the property of reproducing kernel $K_s(\cdot, \cdot)$ defined in (1.40) and the addition theorem, we can

have

$$\begin{aligned}
\big(E_s(Q[X_N,w])\big)^2 &= \left[\sup_{\substack{f\in H^s\\ \|f\|_s\leqslant 1}} |Q[X_N,w](f)-I(f)|\right]^2\\
&= \left[\sup_{\substack{f\in H^s\\ \|f\|_s\leqslant 1}} \left|\left\langle f,\sum_{i=1}^N \frac{w_i}{4\pi}K_s(\cdot,\mathbf{x})\right\rangle_s - \int_{\mathbb{S}^2} f(\mathbf{x})d\omega(\mathbf{x})\right|\right]^2\\
&= \left[\sup_{\substack{f\in H^s\\ \|f\|_s\leqslant 1}} \left|\left\langle f,\sum_{i=1}^N \frac{w_i}{4\pi}K_s(\cdot,\mathbf{x})\right\rangle_s - \int_{\mathbb{S}^2} \langle f,K_s(\cdot,\mathbf{x})\rangle_s d\omega(\mathbf{x})\right|\right]^2\\
&= \left[\sup_{\substack{f\in H^s\\ \|f\|_s\leqslant 1}} \left|\left\langle f,\sum_{i=1}^N \frac{w_i}{4\pi}K_s(\cdot,\mathbf{x})\right\rangle_s - \left\langle f,\int_{\mathbb{S}^2} K_s(\cdot,\mathbf{x})d\omega(\mathbf{x})\right\rangle_s\right|\right]^2\\
&= \left[\sup_{\substack{f\in H^s\\ \|f\|_s\leqslant 1}} \left|\left\langle f,\sum_{i=1}^N \frac{w_i}{4\pi}K_s(\cdot,\mathbf{x}) - \int_{\mathbb{S}^2} K_s(\cdot,\mathbf{x})d\omega(\mathbf{x})\right\rangle_s\right|\right]^2\\
&= \left\|\sum_{i=1}^N \frac{w_i}{4\pi}K_s(\cdot,\mathbf{x}) - \int_{\mathbb{S}^2} K_s(\cdot,\mathbf{x})d\omega(\mathbf{x})\right\|_s^2.
\end{aligned}$$

Then with the fact that

$$\int_{\mathbb{S}^2} K_s(\mathbf{x},\cdot)d\omega(\mathbf{x}) = \alpha_0^{(s)},$$

the worst-case error could be represented as

$$\begin{aligned}
(E_s(Q[X_N,w]))^2 &= \left[\sum_{\ell=1}^{\infty}\sum_{k=1}^{2\ell+1}\alpha_\ell^{(s)}\left(\sum_{i=1}^N \frac{w_i}{4\pi}Y_{\ell,k}(\mathbf{x}_i)\right)^2\right]\\
&= \sum_{\ell=1}^{\infty}\sum_{k=1}^{2\ell+1}\alpha_\ell^{(s)}\sum_{i=1}^N\sum_{j=1}^N \frac{w_iw_j}{16\pi^2}Y_{\ell,k}(\mathbf{x}_i)Y_{\ell,k}(\mathbf{x}_j)\\
&= \sum_{i=1}^N\sum_{j=1}^N \frac{w_iw_j}{16\pi^2}\sum_{\ell=1}^{\infty}\sum_{k=1}^{2\ell+1}\alpha_\ell^{(s)}Y_{\ell,k}(\mathbf{x}_i)Y_{\ell,k}(\mathbf{x}_j). \qquad (2.40)
\end{aligned}$$

Now we recall formula (1.43), which describes the the Laplace-Fourier transformation

of the signed distances between two points on $\mathbb{S}^2$:

$$(-1)^{L+1}|\mathbf{x}-\mathbf{y}|^{2s-2} = (-1)^{L+1}V_{2-2s}(\mathbb{S}^2) + \sum_{\ell=1}^{\infty} a_\ell^{(s)}(2\ell+1)P_\ell(\mathbf{x}\cdot\mathbf{y}),$$

where

$$V_{2-2s}(\mathbb{S}^2) := \int_{\mathbb{S}^2}\int_{\mathbb{S}^2} |\mathbf{x}-\mathbf{y}|^{2s-2} d\omega(\mathbf{x}) d\omega(\mathbf{y}) = 2^{2s-1}\frac{\Gamma(3/2)\Gamma(s)}{\sqrt{\pi}\Gamma(1+s)},$$

and

$$a_\ell^{(s)} := V_{2-2s}(\mathbb{S}^2)\frac{(-1)^{L+1}(1-s)_\ell}{(1+s)_\ell},\ \ell \geqslant 1.$$

Thus we have

$$\begin{aligned}(-1)^{L+2}(V_{2-2s}(\mathbb{S}^2) - |\mathbf{x}-\mathbf{y}|^{2s-2}) &= \sum_{\ell=1}^{\infty} a_\ell^{(s)}(2\ell+1)P_\ell(\mathbf{x}\cdot\mathbf{y}) \qquad (2.41)\\ &= \sum_{\ell=1}^{\infty} a_\ell^{(s)} \sum_{k=1}^{2\ell+1} Y_{\ell,k}(\mathbf{x})Y_{\ell,k}(\mathbf{y}). \qquad (2.42)\end{aligned}$$

Note that for $a_\ell^{(s)}$ we have

$$a_\ell^{(s)} \sim 2^{2s-1}\frac{\Gamma(\frac{d+1}{2})\Gamma(s)}{\sqrt{\pi}(-1)^{L+1}\Gamma(\frac{d}{2}+s)}\ell^{-2s} \quad \text{as } \ell\to\infty, \qquad (2.43)$$

and when $1 < s \leqslant 2$, which means $L = L(s) = \lfloor s - d/2 \rfloor = 0$, we have $a_\ell^{(s)} > 0$ for all $\ell = 1, \ldots, \infty$. Therefore, we regard the left hand side of (2.41) as the reproducing kernel of $\mathbb{H}^s(\mathbb{S}^2)$, which is

$$K_s(\mathbf{x},\mathbf{y}) = V_{2-2s}(\mathbb{S}^2) - |\mathbf{x}-\mathbf{y}|^{2s-2},$$

and then we obtain

$$(E_s(Q[X_N,w]))^2 = \sum_{i=1}^{N}\sum_{j=1}^{N}\frac{w_i w_j}{16\pi^2}(V_{2-2s}(\mathbb{S}^2) - |\mathbf{x}_i-\mathbf{x}_j|^{2s-2}). \qquad (2.44)$$

For the case $s > 2$, we know that $a_\ell^{(s)} > 0$ does not hold for all $\ell = 1, \ldots, \infty$. In this situation, similar with (1.47) in Section 1.2, we let

$$K_s(\mathbf{x},\mathbf{y}) = (1-(-1)^{L+1})V_{2-2s}(\mathbb{S}^2) + \mathcal{Q}_L(\mathbf{x}\cdot\mathbf{y}) + (-1)^{L+1}|\mathbf{x}-\mathbf{y}|^{2s-2},$$

with

$$\mathcal{Q}_L(\mathbf{x}\cdot\mathbf{y}) := \sum_{\ell}^{L}((-1)^{L+1-\ell}-1)a_\ell^{(s)}(2\ell+1)P_\ell(\mathbf{x}\cdot\mathbf{y}), \quad \mathbf{x},\mathbf{y}\in\mathbb{S}^2,$$

which changes the signs if the negative coefficients $a_\ell^{(s)}$ in (1.43). Then we can obtain that the worst-case error on $\mathbb{H}^s(\mathbb{S}^2)$ with $s>2$ can be represented as

$$(E_s(Q[X_N,w]))^2 = \sum_{i=1}^{N}\sum_{j=1}^{N}\frac{w_iw_j}{16\pi^2}\left(\mathcal{Q}_L(\mathbf{x}_i\cdot\mathbf{x}_j)+(-1)^{L+1}|\mathbf{x}_i-\mathbf{x}_j|^{2s-2}-(-1)^{L+1}V_{2-2s}(\mathbb{S}^2)\right). \tag{2.45}$$

Chapter 3

Filter Algorithm for Finding Spherical t_ϵ-Designs

In this chapter we develop an efficient algorithm to find spherical t_ϵ-designs on $\mathbb{S}^2$. By the result shown in Section 2, Chapter 2, we reformulate the problem for finding spherical t_ϵ-design as a system of polynomial equations with box constrains. Using the projection operator, the system can be written as a nonsmooth nonconvex least squares problem (3.2) with zero residual.

Throughout this chapter, $\|\cdot\|$ represents the Euclidean norm and $\mathbb{R}_{++} = \{\alpha \in \mathbb{R} | \alpha > 0\}$.

3.1 Nonlinear least squares reformulation for finding spherical t_ϵ-designs

We represent the points $\mathbf{x}_i \in \mathbb{S}^2$ using spherical coordinates with angles θ_i, φ_i. Since (2.3) is rotationally invariant with respect to X_N^ϵ, we fix $\mathbf{x}_1$ at the north pole and $\mathbf{x}_2$ on the zero meridian as [28]

$$\mathbf{x}_1 = \begin{pmatrix} 0 \\ 0 \\ 1 \end{pmatrix}, \ \mathbf{x}_2 = \begin{pmatrix} \sin(\theta_2) \\ 0 \\ \cos(\theta_2) \end{pmatrix}, \ \mathbf{x}_i = \begin{pmatrix} \sin(\theta_i)\cos(\varphi_i) \\ \sin(\theta_i)\sin(\varphi_i) \\ \cos(\theta_i) \end{pmatrix}, \ i = 3, \ldots, N.$$

Let $x_\theta = (\theta_2, \ldots, \theta_N)^T, x_\varphi = (\varphi_3, \ldots, \varphi_N)^T, x = (x_\theta^T, x_\varphi^T, w^T)^T \in \mathbb{R}^{3N-3}$ and

$$r(x) = \begin{pmatrix} r_{I_1}(x) \\ r_{I_2}(w) \end{pmatrix} = \begin{pmatrix} \mathbf{Y}^T(x_\theta, x_\varphi)w - \sqrt{4\pi}\mathbf{e}_0 \\ w - \mathrm{mid}(a, w, b) \end{pmatrix}, \tag{3.1}$$

where $r(x) : \mathbb{R}^{3N-3} \to \mathbb{R}^{(t+1)^3}$ is a locally continuous but not differentiable function. A solution of the nonsmooth equation $r(x) = 0$ defines a spherical t_ϵ-design. It is difficult to solve (3.1) directly and we consider its least squares form as

$$\min_{x \in \mathbb{R}} f(x) = \frac{1}{2}\|r(x)\|^2. \tag{3.2}$$

Then a global minimizer of (3.2) is a solution of (3.1), which also forms a spherical t_ϵ-design.

In general, $f : \mathbb{R}^n \to \mathbb{R}$ in (3.2) is nonconvex and nonsmooth. In the presence of nonsmoothness and noncovexity, most optimization methods only guarantee convergence to a Clarke stationary point of the objective function f [23, 24, 32, 40].

In this chapter, we propose a smoothing trust region filter (STRF) algorithm to find a global minimizer of f. This algorithm combines smoothing approximations [20, 24, 26], trust region methods [34, 52] and filter algorithms [38, 41]. Using a smoothing function of f, we can construct a good quadratic approximation of f in a certain region at each iteration. The smoothing trust region method [26] can reduce the objective values and guarantee convergence to a Clarke stationary point, but has no convergence results to a global minimizer. The filter method [38, 41] is a technique for finding a global minimizer

of a twice continuously differentiable function under certain conditions, but application to a nonsmooth nonconvex minimization problem has not been investigated. The proposed STRF algorithm is a novel combination of these optimization techniques for nonsmooth and nonconvex least squares problems.

3.2 Smoothing trust region filter (STRF) algorithm

We use the ideas in [41] to construct the filter, which partition $r(x)$ into p sets $\{r_i(x)\}_{i\in I_j}, j = 1, \cdots, p$, with $\{1, \cdots, m\} = I_1 \bigcup \cdots \bigcup I_p$. For readability and simplicity, we explain how to construct the filter with a disjoint partition. Let

$$r(x) = \begin{pmatrix} r_{I_1}(x) \\ \vdots \\ r_{I_p}(x) \end{pmatrix}, \quad \Theta_j(x) = \|r_{I_j}(x)\|, \quad j = 1, \ldots, p, \quad \Theta(x) = \begin{pmatrix} \Theta_1(x) \\ \vdots \\ \Theta_p(x) \end{pmatrix},$$

where $r_{I_j} : \mathbb{R}^n \to \mathbb{R}^{m_j}$ and $\sum_{j=1}^{p} m_j = m$.

Obviously, a vector x is a solution of (3.2) with $f(x) = 0$ if and only if $\Theta(x) = 0$.

We say that a vector x_1 dominates a vector x_2 whenever $\Theta(x_1) \leqslant \Theta(x_2)$. If x_1 dominates x_2, we do not need to consider x_2 anymore.

At the kth iteration, the filter $\mathcal{F}$ is a subset of $\{\Theta(x_0), \Theta(x_1), \ldots, \Theta(x_k)\}$. A new trial point x_k^+ is acceptable for the filter $\mathcal{F}$ if and only if there is $j \in \{1, \ldots, p\}$ such that

$$\Theta_j(x_k^+) < \Theta_j(x_\ell) - \gamma \min\{\|\Theta(x_k^+)\|, \|\Theta(x_\ell)\|\}, \quad \forall\, \Theta(x_\ell) \in \mathcal{F}, \tag{3.3}$$

where $\gamma \in (0, 1/\sqrt{p})$ is a positive constant.

We remove $\Theta(x_\ell)$ from the filter $\mathcal{F}$ if

$$\exists \quad \Theta(x_j) \in \mathcal{F}, \quad \text{such that } \Theta(x_\ell) - \gamma\|\Theta(x_\ell)\|e \geqslant \Theta(x_j), \tag{3.4}$$

where $e = (1, \ldots, 1)^T$. The inequality in (3.4) implies that x_j dominates x_ℓ.

To overcome the nonsmoothness of r, we use a smoothing function $\tilde{r}(\cdot, \mu)$ of r.

Definition 3.1. (Smoothing function) *Let $r : \mathbb{R}^n \to \mathbb{R}^m$ be a locally Lipschitz continuous function. We call $\tilde{r} : \mathbb{R}^n \times \mathbb{R}_{++} \to \mathbb{R}^m$ a smoothing function of r, if for any fixed $\mu \in \mathbb{R}_{++}$, $\tilde{r}(\cdot, \mu)$ is continuously differentiable in $\mathbb{R}^n$ and for any fixed $\hat{x} \in \mathbb{R}^n$,*

$$\lim_{x \to \hat{x}, \mu \downarrow 0} \tilde{r}(x, \mu) = r(\hat{x}).$$

A smoothing function $\tilde{r}$ defines a smoothing function $\tilde{f}$ of f and a smoothing least squares problem of (3.2) as the following

$$\min_{x\in\mathbb{R}^n} \tilde{f}(x,\mu) := \frac{1}{2}\|\tilde{r}(x,\mu)\|^2. \tag{3.5}$$

By Definition 3.1, for any fixed $\mu > 0$, $\tilde{f}(\cdot,\mu)$ is continuously differentiable in $\mathbb{R}^n$ and for any fixed $\hat{x} \in \mathbb{R}^n$

$$\lim_{x\to\hat{x},\mu\downarrow 0} \tilde{f}(x,\mu) = f(\hat{x}).$$

In this paper, we assume that the smoothing function $\tilde{r}$ satisfies the following condition

$$|\tilde{r}_i(x,\mu) - r_i(x)| \leqslant \kappa(\mu), \quad i = 1,\ldots,m, \tag{3.6}$$

where $\kappa : \mathbb{R}_{++} \to \mathbb{R}_+$ satisfies $\kappa(\mu_1) \leqslant \kappa(\mu_2)$ for $\mu_1 \leqslant \mu_2$, and $\kappa(\mu) \to 0$ as $\mu \to 0$.

Denote $J(x,\mu) = \nabla_x \tilde{r}(x,\mu)$ and $g(x,\mu) = \nabla_x \tilde{f}(x,\mu) = J(x,\mu)^T \tilde{r}(x,\mu)$.

The smoothing trust region method computes a trial point $x_k^+ = x_k + d_k$ for some step d_k by a quadratic approximation function $q_k(d)$ of $\tilde{f}(x,\mu)$ in a trust region $\{x_k + d \mid \|d\| \leqslant \Delta_k\}$, where Δ_k is the radius of the trust region. Namely, d_k is the unique solution of the following quadratic program

$$\min_{\|d\|\leqslant\Delta_k} q_k(d) := \tilde{f}(x_k,\mu_k) + g(x_k,\mu_k)^T d + \frac{1}{2} d^T B_k d \tag{3.7}$$

where $B_k = J(x_k,\mu_k)^T J(x_k,\mu_k) + \sqrt{\mu_k} I$.

The term $\sqrt{\mu} I$ in B_k plays a regularization role and ensures the nonsingularity of B_k. When both smoothing and regularization techniques are used in an algorithm, it is recommended to let the smoothing parameter go to zero faster than the regularization parameter for good numerical performance [27].

Smoothing Trust Region Filter (STRF) Algorithm

Step 0: Initialization. Given constants $0 < \bar{\Delta} < \infty$, $0 < \eta_1 < \eta_2 < 1$, $0 < \gamma_1 < 1 < \gamma_2$, $0 < \sigma < 1$, $0 < \gamma < 1/\sqrt{p}$, $0 < \beta < \infty$, an initial vector $x_0 \in \mathbb{R}^n$, the radius of a trust region $\Delta_0 \in (0, \bar{\Delta})$, the smoothing parameter $\mu_0 > 0$, and filter $\mathcal{F} = \{\Theta(x_0)\}$.

Step 1: Define a trial point. Compute d_k by (3.7) and set $x_k^+ = x_k + d_k$.

Step 2: Evaluate the reduction at the trial step. If $d_k = 0$, set $x_{k+1} = x_k$, $\Delta_{k+1} = \Delta_k$, and go to Step 5. Otherwise, compute

$$\rho_k = \frac{\tilde{f}(x_k, \mu_k) - \tilde{f}(x_k^+, \mu_k)}{q_k(0) - q_k(d_k)}.$$

Step 3: Update the trust-region radius. Set

$$\Delta_{k+1} = \begin{cases} \min\{\gamma_2 \Delta_k, \bar{\Delta}\} & \text{if } \rho_k \geqslant \eta_2, \|d_k\| = \Delta_k, \\ \gamma_1 \Delta_k & \text{if } \rho_k \leqslant \eta_1, \\ \Delta_k & \text{otherwise,} \end{cases}$$

Step 4: Test to accept the trial step.

- x_k^+ is acceptable for the current filter by (3.3): Set $x_{k+1} = x_k^+$ and add $\Theta(x_k^+)$ to the filter if $\rho_k < \eta_1$. Update $\mathcal{F}$ by (3.4).
- x_k^+ is not acceptable for the current filter: If $\rho_k \geqslant \eta_1$, set $x_{k+1} = x_k^+$. Otherwise, set $x_{k+1} = x_k$.

Step 5. Update the smoothing parameter. If $\min\{f(x_k), \|\nabla_x \tilde{f}(x_k, \mu_k)\|\} \leqslant \beta \mu_k$, set $\mu_{k+1} = \sigma \mu_k$. Otherwise, set $\mu_{k+1} = \mu_k$. Go to **Step 1**.

3.3 Convergence analysis

Now we investigate the convergence of the STRF algorithm. We first consider the case that infinitely many values are added to the filter in the STRF algorithm.

Theorem 3.2. *Assume that $\tilde{r}$ satisfies condition (3.6). If infinitely many values of $\Theta(x_k)$ are added to the filter by the STRF algorithm, then*

$$\lim_{k\to\infty} \|\Theta(x_k)\| = \lim_{k\to\infty} f(x_k) = 0.$$

Proof. Let $\Theta_k = \Theta(x_k)$, $\Theta_k^+ = \Theta(x_k^+)$ and $\Theta_{j,k} = \Theta_j(x_k), j = 1, \ldots, p$.

Let $\{k_i\}$ index the subsequence of iterations at which $\Theta_{k_i} = \Theta_{k_i-1}^+$ is added to the filter. Assume by contradiction that there exists a subsequence $\{k_\nu\} \subseteq \{k_i\}$ such that $\|\Theta_{k_\nu}\| \geqslant \epsilon$ for some $\epsilon > 0$. Since $\{\Theta_{k_\nu}\}$ is bounded, there exists a further subsequence $\{k_\ell\} \subseteq \{k_\nu\}$ such that

$$\lim_{\ell\to\infty} \Theta_{k_\ell} = \bar{\Theta}. \tag{3.8}$$

Since $\{k_\ell\} \subseteq \{k_\nu\} \subseteq \{k_i\}$ and $\|\Theta_{k_\nu}\| \geqslant \epsilon$ for all ν, we know that for all ℓ, $\min\{\|\Theta_{k_{\ell-1}}\|, \|\Theta_{k_\ell}\|\} \geqslant \epsilon$ and Θ_{k_ℓ} is acceptable for the filter. Hence for each ℓ, there exists a $j \in \{1, \cdots, p\}$ such that

$$\Theta_{j,k_\ell} - \Theta_{j,k_{\ell-1}} < -\gamma \min\{\|\Theta_{k_{\ell-1}}\|, \|\Theta_{k_\ell}\|\} \leqslant -\gamma\epsilon. \tag{3.9}$$

However, by (3.8), we get $\Theta_{j,k_\ell} - \Theta_{j,k_{\ell-1}} \to 0$, as $\ell \to \infty$. This is a contradiction. Hence, we obtain

$$\lim_{i\to\infty} \|\Theta_{k_i}\| = 0. \tag{3.10}$$

Now, we consider any $\ell \notin \{k_i\}$ and let $k_{i(\ell)}$ be the last iteration before ℓ such that $\Theta_{k_{i(\ell)}}$ was added to the filter. By the definition of $\{k_{i(\ell)}\}$ and (3.10), we have

$$\lim_{\ell\to\infty} f(x_{k_{i(\ell)}}) = 0. \tag{3.11}$$

Moreover, we have $\mu_{k_{i(\ell)}} \to 0$ as $\ell \to \infty$ by Step 5 of the STRF algorithm. Hence, using $\mu_{k+1} \leqslant \mu_k$, we obtain $\mu_k \to 0$ as $k \to \infty$.

From the condition on the smoothing function (3.6), we derive

$$\begin{aligned}
|\tilde{f}(x_{k_{i(\ell)}}, \mu_{k_{i(\ell)}}) - f(x_{k_{i(\ell)}})| &= \frac{1}{2}|\|\tilde{r}(x_{k_{i(\ell)}}, \mu_{k_{i(\ell)}})\|^2 - \|r(x_{k_{i(\ell)}})\|^2| \\
&= \frac{1}{2}|\sum_{j=1}^{m}(\tilde{r}_j^2(x_{k_{i(\ell)}}, \mu_{k_{i(\ell)}}) - r_j^2(x_{k_{i(\ell)}}))| \\
&\leqslant \frac{1}{2}\sum_{j=1}^{m}|\tilde{r}_j(x_{k_{i(\ell)}}, \mu_{k_{i(\ell)}}) - r_j(x_{k_{i(\ell)}})| \cdot |\tilde{r}_j(x_{k_{i(\ell)}}, \mu_{k_{i(\ell)}}) + r_j(x_{k_{i(\ell)}})| \\
&\leqslant \frac{1}{2}\sum_{j=1}^{m}\kappa(\mu_{k_{i(\ell)}})|\tilde{r}_j(x_{k_{i(\ell)}}, \mu_{k_{i(\ell)}}) + r_j(x_{k_{i(\ell)}})| \\
&\leqslant \frac{1}{2}\sum_{j=1}^{m}\kappa(\mu_{k_{i(\ell)}})(\kappa(\mu_{k_{i(\ell)}}) + 2|r_j(x_{k_{i(\ell)}})|) \\
&\leqslant \frac{m}{2}\kappa^2(\mu_{k_{i(\ell)}}) + \kappa(\mu_{k_{i(\ell)}})\|r(x_{k_{i(\ell)}})\|_1 \\
&\leqslant \frac{m}{2}\kappa^2(\mu_{k_{i(\ell)}}) + \kappa(\mu_{k_{i(\ell)}})\sqrt{m}\|r(x_{k_{i(\ell)}})\|_2 \\
&\leqslant \frac{m}{2}\kappa^2(\mu_{k_{i(\ell)}}) + \kappa(\mu_{k_{i(\ell)}})\sqrt{2mf(x_{k_{i(\ell)}})}. \qquad (3.12)
\end{aligned}$$

Hence from (3.11) and $\mu_k \to 0$, we obtain

$$\lim_{\ell\to\infty}\tilde{f}(x_{k_{i(\ell)}}, \mu_{k_{i(\ell)}}) = 0. \qquad (3.13)$$

By Step 2 and Step 4 of the STRF algorithm, if $\Theta(x_{k_{i(\ell)}+1})$ is not included in the filter, then we have

$$\tilde{f}(x_{k_{i(\ell)}}, \mu_{k_{i(\ell)}}) - \tilde{f}(x_{k_{i(\ell)}+1}, \mu_{k_{i(\ell)}}) \geqslant 0,$$

which, together with (3.13), implies

$$\lim_{l\to\infty}\tilde{f}(x_{k_{i(\ell)}+1}, \mu_{k_{i(\ell)}}) = 0. \qquad (3.14)$$

Using the similar argument in (3.12), we can show

$$|\tilde{f}(x_{k_{i(\ell)}+1}, \mu_{k_{i(\ell)}}) - f(x_{k_{i(\ell)}+1})| \leqslant \frac{m}{2}\kappa^2(\mu_{k_{i(\ell)}}) + \kappa(\mu_{k_{i(\ell)}})\sqrt{2m\tilde{f}(x_{k_{i(\ell)}+1}, \mu_{k_{i(\ell)}})} \qquad (3.15)$$

which, together with (3.14) and

$$\lim_{\ell\to\infty} |\tilde{f}(x_{k_{i(\ell)}+1}, \mu_{k_{i(\ell)}}) - f(x_{k_{i(\ell)}+1})| \leqslant \lim_{\ell\to\infty} (\frac{m}{2}\kappa^2(\mu_{k_{i(\ell)}}) + \kappa(\mu_{k_{i(\ell)}})\sqrt{2m\tilde{f}(x_{k_{i(\ell)}+1}, \mu_{k_{i(\ell)}})}) = 0,$$

we obtain

$$\lim_{\ell\to\infty} f(x_{k_{i(\ell)}+1}) = 0.$$

By recurrence relations, we get

$$\lim_{k\to\infty} f(x_k) = 0 \quad \text{and} \quad \lim_{k\to\infty} \|\Theta(x_k)\| = 0. \tag{3.16}$$

We complete the proof. □

Now, we study the convergence of the STRF algorithm without assuming that infinitely many values of $\Theta(x_k)$ are added to the filter.

We say that f has bounded level sets, if for any $\alpha \geqslant 0$, the level set $\{x \,|\, f(x) \leqslant \alpha\}$ is bounded.

If f has bounded level sets and condition (3.6) holds, then the smoothing function $\tilde{f}$ has bounded level sets for any fixed $\mu > 0$. In fact, using the argument in (3.12) and (3.15) with condition (3.6) and $\mu \leqslant \mu_0$, for any $\alpha > 0$, the following holds

$$\begin{array}{rcl} \{x \,|\, \tilde{f}(x,\mu) \leqslant \alpha\} & \subseteq & \{x \,|\, f(x) \leqslant \alpha + \frac{m}{2}\kappa^2(\mu) + \kappa(\mu)\sqrt{2m\alpha}\} \\ & \subseteq & \{x \,|\, f(x) \leqslant \alpha + \frac{m}{2}\kappa^2(\mu_0) + \kappa(\mu_0)\sqrt{2m\alpha}\}. \end{array} \tag{3.17}$$

Lemma 3.3. *Suppose that f has bounded level sets and $\nabla\tilde{f}(\cdot,\mu)$ is Lipschitz continuous for any fixed $\mu > 0$, then*

$$\lim_{k\to\infty} \mu_k = 0. \tag{3.18}$$

Proof. Let K contain all iterations at which $\mu_{k+1} = \sigma\mu_k$, namely,

$$K = \{\, k \,|\, \min\{f(x_k), \|\nabla_x \tilde{f}(x_k, \mu_k)\|\} \leqslant \beta\mu_k\}. \tag{3.19}$$

If K is an infinite set, then $\lim_{k\to\infty} \mu_k = 0$. Moreover, from Theorem 3.2, if infinitely many values of Θ_k are added to the filter, then $\lim_{k\to\infty} \mu_k = 0$. Hence, in the following,

we will prove that K is an infinite set in the case when only finitely many values of Θ_k are added to the filter.

Assume by contradiction that K is finite and only finitely values of Θ_k are added to the filter. Then there exists a nonnegative integer $\hat{k}$, such that for all nonnegative integers j, $\Theta(x^+_{\hat{k}+j})$ are not added to the filter and $\mu_{\hat{k}+j} = \mu_{\hat{k}}$. This means

$$\tilde{f}(x_{\hat{k}+j}, \mu_{\hat{k}}) - \tilde{f}(x_{\hat{k}+j+1}, \mu_{\hat{k}}) \geqslant 0, \quad \text{for} \quad j \geqslant 0 \tag{3.20}$$

and

$$\min\{f(x_{\hat{k}+j}),\ \|\nabla_x \tilde{f}(x_{\hat{k}+j}, \mu_{\hat{k}})\|\} > \beta\mu_{\hat{k}}, \quad \text{for } j \geqslant 0. \tag{3.21}$$

By (3.17) and the assumption that f has bounded level sets, we know that $\tilde{f}(\cdot, \mu_{\hat{k}})$ has bounded level sets. Hence, in such case, the STRF Algorithm reduces to Algorithm 4.1 for solving the smooth optimization problem with the objective $\tilde{f}(\cdot, \mu_{\hat{k}})$ in [52]. From the assumption of this Lemma, $\nabla\tilde{f}(\cdot, \mu_{\hat{k}})$ is Lipschitz continuous, and thus B_k is bounded. Note that d_k is the exact solution of (3.7). All conditions of Theorem 4.6 in [52] hold. Similar to the proof of Theorem 4.6 in [52], we can show

$$\lim_{j\to\infty} \|\nabla_x \tilde{f}(x_{\hat{k}+j}, \mu_{\hat{k}})\| = 0. \tag{3.22}$$

This contradicts to (3.21). Hence (3.18) holds. □

Since r is locally Lipschitz continuous, f is locally Lipschitz continuous and almost everywhere differentiable. The Clarke subdifferential of f at $x \in \mathbb{R}^n$ can be defined by

$$\partial f(x) = \text{con}\{v \,|\, \nabla f(z) \to v,\ f \text{ is differentiable at } z,\ z \to x\},$$

where "con" denotes the convex hull. A vector x is called a Clarke stationary point of f if $0 \in \partial f(x)$. To show that any accumulation point of $\{x_k\}$ generated by the STRF algorithm is a Clarke stationary point of f, we need functions r_i, $i = 1, \ldots, m$ to be regular and their smoothing functions $\tilde{r}_i$ to satisfy the gradient consistency.

Definition 3.4. [32] *A function $h : \mathbb{R}^n \to \mathbb{R}$ is said to be regular at $x \in \mathbb{R}^n$ if for all $v \in \mathbb{R}^n$, the directional derivative exists and*

$$h(x; v) = \lim_{t\downarrow 0} \frac{h(x+tv) - h(x)}{t} = \limsup_{y\to x, t\downarrow 0} \frac{h(y+tv) - h(y)}{t}.$$

Definition 3.5. (Gradient consistency)[24] *A smoothing function $\tilde{h}$ of $h : \mathbb{R}^n \to \mathbb{R}$ is said to satisfy the gradient consistency if*

$$\mathrm{con}\{v \mid \nabla_x \tilde{h}(x^k, \mu_k) \to v, \text{ for } x^k \to x,\ \mu_k \downarrow 0\} = \partial h(x).$$

Theorem 3.6. *Assume that $\tilde{r}_i$ satisfies condition (3.6) and the gradient consistency, for $i = 1, \ldots, m$, f has bounded level sets and $\nabla \tilde{f}(\cdot, \mu)$ is Lipschitz continuous for any fixed $\mu > 0$. Then the sequences $\{x_k\}$ and $\{\mu_k\}$ generated by the STRF algorithm satisfy*

$$\liminf_{k\to\infty} \|\nabla_x \tilde{f}(x_k, \mu_k)\| = 0. \tag{3.23}$$

In addition, if r_i is regular $i = 1, \ldots, m$, then any accumulation point of $\{x_k\}$ is a Clarke stationary point of f.

Proof. We consider two cases. Case I. $\liminf_{k\to\infty} f(x_k) = 0$.

In this case, we have

$$\liminf_{k\to\infty} \|r(x_k)\|^2 = \liminf_{k\to\infty} \sum_{j=1}^{m} r_j^2(x_k) = 0.$$

From condition (3.6) and Lemma 3.3, we get $\mu_k \to 0$, and

$$0 \leqslant \liminf_{k\to\infty} |\tilde{r}_j(x_k, \mu_k)| \leqslant \liminf_{k\to\infty} (|r_j(x_k)| + \kappa(\mu_k)) = 0, \quad \text{for} \quad j = 1, \ldots, m.$$

Since r_i is Lipschitz continuous, the Clarke subdifferential ∂r_i is bounded. Hence from the gradient consistency of r_i, we can get $\|\nabla_x \tilde{r}_i(x_k, \mu_k)\|$ is bounded and

$$\liminf_{k\to\infty} \|\nabla_x \tilde{f}(x_k, \mu_k)\| \quad = \quad \liminf_{k\to\infty} \|\nabla_x \tilde{r}(x_k, \mu_k)^T \tilde{r}(x_k, \mu_k)\| = 0.$$

Case II. $\liminf_{k\to\infty} f(x_k) > 0$.

In this case, there exist $\bar{k}$ and $\epsilon > 0$, such that for $k > \bar{k}$, $f(x_k) \geqslant \epsilon$. By Lemma 3.3, $\mu_k \to 0$. Thus from $\min\{f(x_k), \|\nabla_x \tilde{f}(x_k, \mu_k)\|\} \leqslant \beta\mu_k$, we have

$$\liminf_{k\to\infty} \|\nabla_x \tilde{f}(x_k, \mu_k)\| = 0.$$

Hence we complete the proof for (3.23).

If r_i is regular and $\tilde{r}_i$ satisfies the gradient consistency, then by Proposition 2.1 in [12], $\tilde{r}_i^2$ is a smoothing function of r_i^2 and satisfies the gradient consistency. Since $f(x) = \frac{1}{2}\sum_{i=1}^m r_i^2(x)$ is a convex composite function of $r_i^2(x)$, $\tilde{f}(x,\mu) = \frac{1}{2}\sum_{i=1}^m \tilde{r}_i^2(x,\mu)$ is a smoothing function of f and satisfies the gradient consistency, which means

$$\mathrm{con}\{v|\nabla f(z) \to v, f \text{ is differentiable at } z, z \to x\} = \mathrm{con}\{v|\nabla \tilde{f}(z,\mu) \to v,\ z \to x, \mu \downarrow 0\}.$$

Hence, from (3.23), any accumulation point of $\{x_k\}$ is a Clarke stationary point of f. □

Example 3.7. *To explain the smoothing approximation and gradient consistency, we consider the following example. Let*

$$r(x) = Mx + \max(0,x) + q, \text{ where } M = \begin{pmatrix} 1 & 1 \\ 1 & 1 \end{pmatrix} \text{ and } q = \begin{pmatrix} 1 \\ -1 \end{pmatrix}.$$

At $\bar{x} = (0,0)^T$, $r(x)$ and $f(x)$ are not differentiable. Since r_1 and r_2 are convex, by Proposition 2.3.6 in [32], they are regular. By Corollary 3 in [32], the Clarke gradient of $f(x)$ at $\bar{x}$ is

$$\begin{aligned} \partial f(\bar{x}) &= \frac{1}{2}(\partial r_1^2(x) + \partial r_2^2(x)) \\ &= \mathrm{con}\{v \mid \nabla r_1(x) r_1(x) + \nabla r_2(x) r_2(x) \to v, x_1 \neq 0, x_2 \neq 0, x \to \bar{x}\} \\ &= \{\begin{pmatrix} \alpha_1 & 1 \\ 1 & \alpha_2 \end{pmatrix}\begin{pmatrix} 1 \\ -1 \end{pmatrix},\ \alpha_1, \alpha_2 \in [1,2]\}. \end{aligned}$$

Since $0 \in \partial f(\bar{x})$, $\bar{x}$ is a stationary point.

We use the smoothing function

$$\varphi(t,\mu) = \begin{cases} \max(0,t) & \text{if } |t| > \frac{\mu}{2} \\ \frac{t^2}{2\mu} + \frac{t}{2} + \frac{\mu}{8} & \text{otherwise} \end{cases}$$

for $\max(0,t)$, *and*

$$\tilde{r}(x) = Mx + \Phi(x,\mu) + q$$

for $r(x)$ where $\Phi(x,\mu) = (\varphi(x_1,\mu), \varphi(x_2,\mu))^T$. It is easy to see that $0 \leqslant \varphi'(t,\mu) \leqslant 1$. In particular, $\varphi'(-\frac{\mu}{2},\mu) = 0$ and $\varphi'(\frac{\mu}{2},\mu) = 1$. Hence, we find that f satisfies the gradient consistency, that is,

$$\mathrm{con}\{v|\nabla \tilde{f}(x,\mu) = \nabla \tilde{r}(x,\mu)^T \tilde{r}(x,\mu) \to v,\ x \to \bar{x}, \mu \downarrow 0\} = \partial f(\bar{x}).$$

More examples and results on the smoothing approximation, regularity and gradient consistency can be found in [20, 21, 24].

3.4 Numerical results

All numerical experiments in this thesis are implemented in MATLAB 2012b on a Lenovo Thinkcenter PC equipped with Intel Core i7-3770 3.4G Hz CPU, 8 GB RAM running Windows 7.

In this section we report numerical results of the STRF algorithm for solving non-smooth nonconvex least squares problems (3.2) arising from spherical t_ϵ-designs. The problem is highly nonlinear and have many stationary points at which the residual is not zero. Numerical results show that the STRF algorithm is efficient and robust for finding global minimizers of the problem.

The values of parameters in the STRF algorithm are chosen as follows: $\Delta_0 = 10^{-1}$, $\overline{\Delta} = 10^{12}$, $\eta_1 = 0.2$, $\eta_2 = 0.8$, $\gamma_1 = 0.8$, $\gamma_2 = 1.25$, $\sigma = 0.95$, $\mu_0 = 0.5$, $\gamma = 0.01, \beta = 10$.

To use the STRF algorithm, we need a smoothing function $\tilde{r}$ of r and the Jacobian of $\tilde{r}$. Since $r_{I_1} : \mathbb{R}^{3N-3} \to \mathbb{R}^{(t+1)^3}$ is differentiable, we only define a smoothing function of $r_{I_2} : \mathbb{R}^N \to \mathbb{R}^N$ as follows:

$$(\tilde{r}_{I_2}(w,\mu))_i = \begin{cases} w_i - a_i & w_i < a_i - \mu, \\ w_i - \frac{1}{4\mu}(w_i - a_i)^2 - \frac{1}{2}(w_i - a_i) - \mu/4 - a_i & a_i - \mu < w_i < a_i + \mu, \\ 0 & a_i + \mu \leqslant w_i \leqslant b_i - \mu, \\ w_i + \frac{1}{4\mu}(w_i - b_i)^2 - \frac{1}{2}(w_i - b_i) + \mu/4 - b_i & b_i - \mu < w_i < b_i + \mu, \\ w_i - b_i & w_i > b_i + \mu. \end{cases}$$

The function r_{I_2} is Lipschitz continuous and regular. The smoothing function $\tilde{r}_{I_2}$ satisfies the gradient consistency. Moreover, $f(x) = \frac{1}{2}\|r(x)\|^2 = \frac{1}{2}r(x)^T r(x)$ is continuously differentiable and has bounded level sets. Hence all conditions on r and f in the last section hold.

The function f is nonconvex with many stationary points. It is hard to find a global minimizer of f by using most existing methods. We use this example to test the STRF algorithm and compare it with smoothing trust region (STR) algorithm and `fmincon, lsqnonlin, fsolve` codes in Matlab. To guarantee the fairness of the comparison, we use same parameters in STR and STRF algorithms, and same initial points for all algorithms and codes.

First we generate N points distributed evenly on the whole sphere. The points are generated by "The Recursive Zonal Equal Area Sphere Partitioning (EAP) Toolbox" proposed by P. Leopardi, which could be downloaded from http://sourceforge.net/projects/eqsp/. Next, we add a small random perturbation on the points to create more initial point sets with the same cardinalities. All the perturbation obeys a uniform distribution with expectation as 0.1. We choose initial weights $w_i^0 = \frac{4\pi}{N},\ i = 1, \ldots, N$.

In Table 3.1 we show numerical results for finding spherical $t_{0.1}$-designs with different t and N points on the sphere. The final value of the residual $\|r(x)\|$ and the CPU time (CPUtime) are reported in the table. Compared with other methods, the STRF algorithm can find a good numerical global minimizer efficiently.

Table 3.1: Values of $r(x)$(CPUtime) for spherical t_ϵ-design with $\epsilon = 0.1$

$t,\ N$	fmincon	lsqnonlin	fsolve	STR	STRF
4, 12	1.41e-07(1.39)	1.91e-05(0.281)	3.28e-15(0.185)	2.64e-03(1.94)	7.78e-11(0.038)
9, 45	8.54e-07(10.1)	2.00e-04(2.29)	3.96e-06(1.89)	6.81e-03(6.26)	9.39e-11(0.35)
12, 80	1.16e-06(52.5)	3.19e-04(13.8)	3.95e-06(15.8)	1.01e-2(12.1)	7.12e-11(0.888)
14, 105	1.61e-06(107)	4.99e-03(66.1)	3.68e-06(46.8)	1.06e-3(22.3)	9.68e-11(2.07)
19, 190	7.66e-06(492)	1.1e-02(189)	2.78e-07(207)	3.06e-04(70.5)	9.79e-11(12.1)
21, 235	1.91e-06(856)	1.18e-04(193)	3.98e-08(310)	1.89e-03(115)	9.35e-11(98)
24, 305	2.30e-05(2064)	6.13e-04(382)	8.66e-07(689)	1.56e-03(220)	9.05e-11(36)

Note that there is no theoretical result which proves the existence of a spherical t-design with $N \leqslant (t+1)^3$ points for arbitrary t. In [25], using a computational algorithm based on interval arithmetic, Chen-Frommer-Lang proved the existence of a spherical t-design with $N = (t+1)^3$ points on the unit sphere $\mathbb{S}^2 \subset \mathbb{R}^3$ for $t = 1, 2, \ldots, 100$. In [64], Sloan and Womersley, conjectured the existence of a spherical t-design with $N = \lceil (t+1)^3/2 \rceil + 1$ points on the unit sphere $\mathbb{S}^2 \subset \mathbb{R}^3$ for some small t, where $\lceil \cdot \rceil$ denotes rounding up to

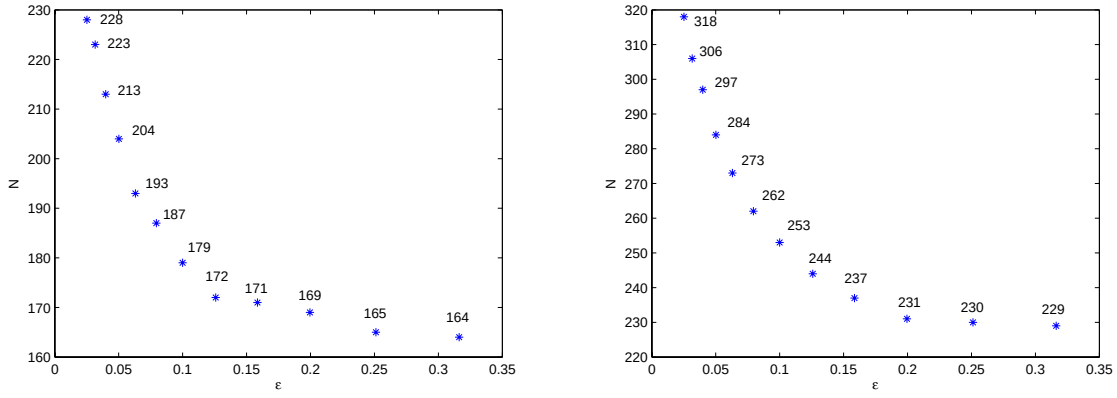

(a) $t = 21$ (b) $t = 25$

Figure 3.1: Possible minimal number N of points for spherical t_ϵ-designs

next integer. We believe that with the flexibility of choice for the weights, the number of points for a spherical t_ϵ-design can be less than $\lceil (t+1)^2/2 \rceil + 1$. To see the minimum number of points for a spherical t_ϵ-design, we solve the least squares problem with $r(x)$ defined in (3.1) for $\lceil (t+1)^3/3 \rceil \leqslant N \leqslant \lceil (t+2)^2/2 \rceil + 1$ with different ϵ and t. Figure 3.4 shows the minimal values N such that $\|r(x)\| \leqslant 10^{-10}$ with $t = 21, 25$ and $\epsilon = 10^{-\alpha}$, $\alpha = 0.5 + i \times 0.1,\ i = 0, 1, \ldots, 11$. From Figure 3.1, we see that the bigger value of ϵ we choose, the smaller number of points for a spherical t_ϵ-design we need.

Since we have develop a way for finding spherical t_ϵ-designs by the STRF algorithm proposed in this chapter, now it is possible for us to implement the worst-case error of spherical t_ϵ designs on $\mathbb{H}^s(\mathbb{S}^2)$ obtained in Section 2.3. In what follows we will calculate the worst-case errors of the spherical t_ϵ-designs found in the previous part of this section. In this experiment we choose $\epsilon = 0.1$ for spherical t_ϵ-designs. For comparison, the worst-case errors for spherical t-designs on $\mathbb{H}^s(\mathbb{S}^2)$ will also be implemented.

The worst-case errors in $\mathbb{H}^s(\mathbb{S}^2)$ for $s = 1.5$ ($s < d/2 + 1$) are illustrated in Figure 3.2. For all spherical $t_{0.1}$-designs, the worst-case error with $s = 1.5$ is calculated using (2.44) and the distance kernel, and for spherical t-designs the worst-case error are calculated by (1.46). From the figure we can see that in this case, the computed worst-case errors of spherical t-designs and spherical $t_{0.1}$-designs essentially lie on the same curve, which is similar to the numerical results shown in [19, Fig.1]. Based on Fig. 3.2 and [19, Fig.1], we

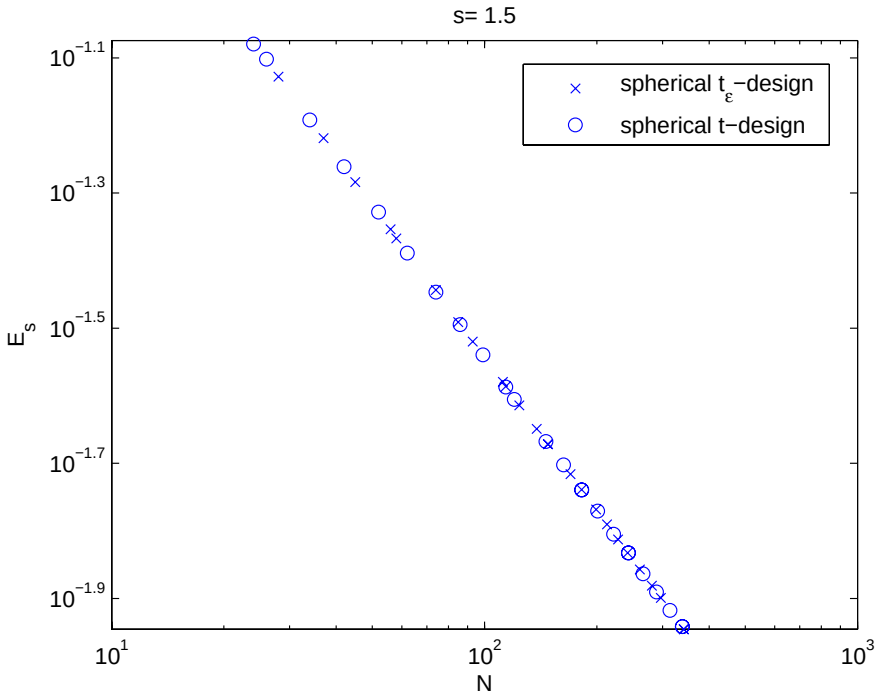

Figure 3.2: Worst-case error for $\mathbb{H}^s(\mathbb{S}^2)$ and $s = 1.5$

can conjecture that the worst-case errors of both QMC designs which include spherical t-designs and spherical t_ϵ-designs decay in the same speed with respect to the number of points in the case $s < d/2 + 1$.

Figure 3.3 plots the worst-case errors for $s = 5.5$ of both spherical t-designs and spherical $t_{0.1}$-designs. For spherical t-designs the worst-case errors with $s = 5.5$ are calculated using the generalized distance kernel and (1.47) (for which $L = 4$), and for spherical t_ϵ-designs the worst-case errors are calculated using (2.45). From the figure we can see that the worst-case errors of spherical t_ϵ-designs decay faster than the ones of spherical t-design with respect to the number of points.

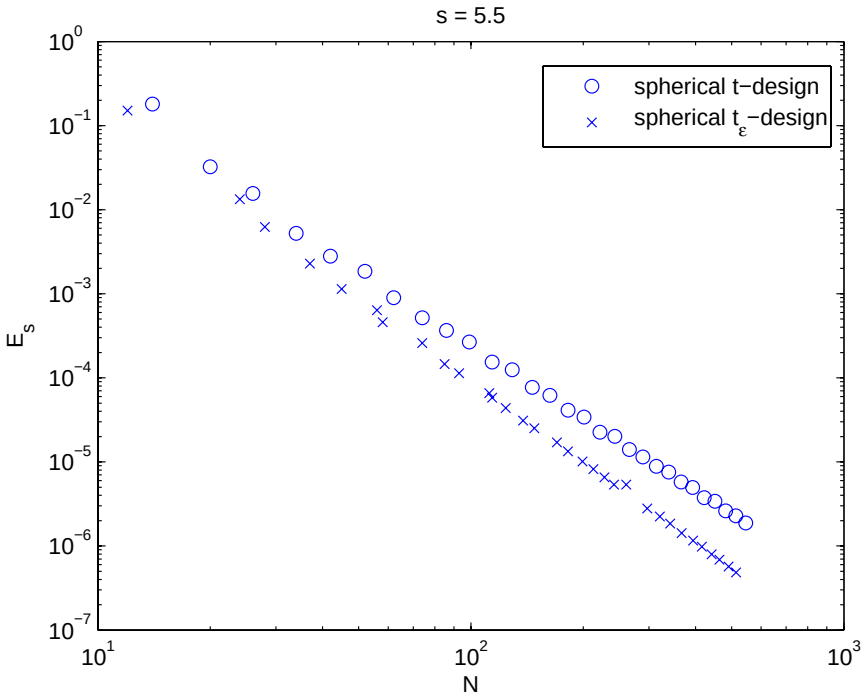

Figure 3.3: Worst-case error for $\mathbb{H}^s(\mathbb{S}^2)$ and $s = 5.5$

Chapter 4

Regularized Least Squares Problem on the Sphere

In this chapter we investigate two regularized problems for numerical approximation of continuous functions on $\mathbb{S}^2$ using spherical t_ϵ-designs.

In the first section we consider a regularized weighted least squares problem only using spherical polynomials. In the second section we consider a generalized regularized least squares problem of hybrid approximation using both radial basis functions and spherical polynomials. Numerical results are presented in the last section.

4.1 Regularized weighted approximation using spherical t_ϵ-designs

In this section we consider the polynomial approximation of continuous functions on the unit sphere $\mathbb{S}^2$ arising as minimizers of the regularized weighted discrete least squares form

$$\min_{p\in\mathbb{P}_L} \sum_{j=1}^{N} w_j (p(\mathbf{x}_j) - f(\mathbf{x}_j))^2 + \lambda \sum_{j=1}^{2} (\mathcal{R}_L p(\mathbf{x}_j))^2 \tag{4.1}$$

where $w_j > 0$, $j = 1, \ldots, N$ are the weights for each term of the least squares, $f \in C(\mathbb{S}^2)$ has its values given at N points $X_N = \{\mathbf{x}_1, \ldots, \mathbf{x}_N\} \subset \mathbb{S}^2$, $\lambda > 0$ is the regularization parameter, and $\mathcal{R}_L$ is the regularization parameter which is linear and can be chosen in different ways. Note that $\{Y_{\ell,k},\ k = 1, \ldots, 2\ell + 1,\ \ell = 0, \ldots, L\}$ is a basis of $\mathbb{P}_L$, so we can represent $p(\mathbf{x})$ as a linear combination of the basis as

$$p = \sum_{\ell=0}^{L} \sum_{k=1}^{2\ell+1} \alpha_{\ell,k} Y_{\ell,k}.$$

Let the entries of matrix $\mathbf{Y}_L \in \mathbb{R}^{N\times(L+1)^2}$ be

$$(\mathbf{Y}_L)_{\ell^2+k,i} = Y_{\ell,k}(\mathbf{x}_i), \quad \ell = 0, \ldots, L,\ k = 1, \ldots, 2\ell + 1,\ i = 1, \ldots, N,$$

and $\mathbf{f} = (f(\mathbf{x}_1), \ldots, f(\mathbf{x}_N))^T$. We could reformulate the problem as

$$\min_{\alpha\in\mathbb{R}^{(N+1)^2}} \|\mathrm{diag}(\sqrt{w})(\mathbf{Y}_L\alpha - \mathbf{f})\|_2^2 + \lambda\|\mathbf{R}_L\alpha\|_2^2, \tag{4.2}$$

where

$$\mathrm{diag}(\sqrt{w}) = \begin{bmatrix} \sqrt{w_1} & & \\ & \ddots & \\ & & \sqrt{w_N} \end{bmatrix},$$

and $\mathbf{R}_L = \mathbf{R}_L(X_N) = \mathbf{B}_L\mathbf{Y}_L^T \in \mathbb{R}^{(L+1)^2\times N}$ with $\mathbf{B}_L$ defined as in (1.53).

Problem (4.2) is a quadratic convex programming and it is easy to verify that (4.2) has a unique optimal solution. Deriving the first and second order optimality condition, the minimizer of (4.2) satisfies the following linear system

$$\left(\mathbf{H}_L + \lambda\mathbf{R}_L^T\mathbf{R}_L\right)\alpha = \mathbf{Y}_L^T\mathrm{diag}(w)\mathbf{f}, \tag{4.3}$$

where

$$\mathbf{H}_L = \left(\mathrm{diag}(\sqrt{w})\mathbf{Y}_L\right)^T \mathrm{diag}(\sqrt{w})\mathbf{Y}_L = \mathbf{Y}_L^T \mathrm{diag}(w)\mathbf{Y}_L \in \mathbb{R}^{(L+1)^2\times(L+1)^2}.$$

Theorem 4.1. *Assume $f \in C(\mathbb{S}^2)$. Let $L \geqslant 0$ be given , and let $X_N = \{\mathbf{x}_1, \ldots, \mathbf{x}_N\} \subset \mathbb{S}^2$ be a spherical t_ϵ-design on $\mathbb{S}^2$ with respect to w with $t \geqslant 2L$ .Then*

$$\mathbf{H}_L = \mathbf{Y}_L^T \mathrm{diag}(w)\mathbf{Y}_L = \mathbf{I}_{(L+1)^2}, \tag{4.4}$$

while (4.2) has the unique solution

$$\alpha_{\ell,k} = \frac{1}{1+\beta_\ell^2} \sum_{j=1}^{N} w_j Y_{\ell,k}(\mathbf{x}_j) f(\mathbf{x}_j), \tag{4.5}$$

and the unique minimizer of (4.1) is given by

$$\begin{aligned} p_{L,N}(\mathbf{x}) &= \sum_{\ell=0}^{L}\sum_{k=1}^{2\ell+1} \frac{Y_{\ell,k}(\mathbf{x})}{1+\beta_\ell^2} \sum_{j=1}^{N} w_j Y_{\ell,k}(\mathbf{x}_j) f(\mathbf{x}_j) \\ &= \sum_{\ell=0}^{L} \frac{2\ell+1}{4\pi(1+\beta_\ell^2)} \sum_{j=1}^{N} w_j P_\ell(\mathbf{x}\cdot\mathbf{x}_j) f(\mathbf{x}_j) \end{aligned} \tag{4.6}$$

Proof. Note that when X_N is a spherical t_ϵ-design,

$$\begin{aligned} (\mathbf{H}_L)_{\ell^2+k,(\ell')^2+k'} &= \sum_{i=1}^{N} w_i Y_{\ell,k}(\mathbf{x}_i) Y_{\ell',k'}(\mathbf{x}_i) \\ &= \int_{\mathbb{S}^2} Y_{\ell,k} Y_{\ell',k'} d\omega(\mathbf{x}) \\ &= \delta_{\ell\ell'}\delta_{kk'}, \end{aligned}$$

with the third equal sign established by the orthonormality of spherical harmonics. Substitute $\mathbf{H}_L = \mathbf{I}_{(L+1)^2}$ to system (4.3) and we can obtain the equality (4.5) and (4.6). □

It is interesting to note that when $w_j = \frac{4\pi}{N}$ for all $j = 1, \ldots, N$, Theorem 4.1 achieves the same result with Theorem 2.1 in [3]. That is to say, problem (4.1) is indeed a generalized form of problem (1.48) by adding the weights w_i to each element of the least squares part. Therefore, we can also generalize some other conclusions in (4.1) to our

problem. The following theorem tells the convergence of model (4.1) that polynomial approximation (1.48) using spherical t_ϵ will converges to a continuous form.

Theorem 4.2. *Let $f \in C(\mathbb{S}^2)$, and let $L \geqslant 0$ be given. Assume that the sets $X_{N_t}^\epsilon = \{\mathbf{x}_{1,t}^\epsilon, \ldots, \mathbf{x}_{N_t,t}^\epsilon\}$ for $t = 1, 2, \ldots$ form a sequence of spherical t_ϵ-designs with $w_t = [w_{1,t}, \ldots, w_{N_t,t}]^T$ and $t \geqslant 2L$. Then the unique minimizer $p_{L,N_t} \in \mathbb{P}_L$ of (1.48) has the uniform limit p_L as $t \to \infty$, that is*

$$\lim_{t\to\infty} \|p_{L,N_t} - p_L\|_{C(\mathbb{S}^2)} = 0, \tag{4.7}$$

where $p_L \in \mathbb{P}_L$ denotes the unique minimizer of the continuous regularized least squares problem

$$\min_{p\in\mathbb{P}_L} \left\{ \|f - p\|_{\mathbb{L}_2}^2 + \lambda \| \mathcal{R}_L p\|_{\mathbb{L}_2}^2 \right\}, \quad \lambda > 0. \tag{4.8}$$

Proof. We have seen already that p_{L,N_t} is uniquely determined when $t \geqslant 2L$, and that in this case p_{L,N_t} is given explicitly by (4.6). It is easy to see that the minimizer of problem (4.8) is in a similar way given by

$$p_L(\mathbf{x}) = \sum_{\ell=0}^{L} \frac{2\ell + 1}{(1 + \lambda\beta_\ell^2)4\pi} \int P_\ell(\mathbf{x} \cdot \mathbf{y}) f(\mathbf{y}) d\omega(\mathbf{y}). \tag{4.9}$$

Since the sums over ℓ in (1.60) and (4.9) are finite, to prove the theorem it is sufficient to prove that for $0 \leqslant \ell \leqslant L$

$$\lim_{t\to\infty} \sum_{j=1}^{N_t} w_{j,t} P_\ell(\mathbf{x} \cdot \mathbf{x}_{j,t}) f(\mathbf{x}_{j,t}) = \int P_\ell(\mathbf{x} \cdot \mathbf{y}) f(\mathbf{y}) d\omega(\mathbf{y}). \tag{4.10}$$

Noting that $P_\ell(\mathbf{x} \cdot \mathbf{y}) f(\mathbf{y})$ is a continuous function of $\mathbf{y}$ for each fixed $\mathbf{x} \in \mathbb{S}^2$, the result now follows from the well known result that, for a positive weight quadrature rule with polynomial degree of accuracy L, the quadrature rule applied to a continuous function g converges to the integral of g as $L \to \infty$. For an explicit proof for the case of the sphere (and indeed for an error estimate) see [45, Therorm 10] combined with Jackson's theorem [53, Theorem 3.3]. □

Based on the numerical results in Section 3.4, we know that due to the flexibility of choice for the weights, the number of points for constructing a spherical t_ϵ-design can be less than constructing a spherical t-design. In another way, using same number of points we may construct a spherical t_ϵ-design but may not be able to construct a spherical t-design. That is to say, a spherical t_ϵ-design can have higher algebraic accuracy than the spherical designs constructed using same number of points. As is shown in the numerical results in Section 3.4, spherical t_ϵ-designs have a smaller worst-case error than spherical t-designs.

4.2 Regularized hybrid approximation using radial basis function plus polynomials

In this section we will investigate the hybrid approximation scheme using both radial basis functions (RBFs) and spherical polynomials. As is shown in Subsection 1.3.2, approximating a function $f \in C(\mathbb{S}^2)$ using formula (1.66) and (1.67) leads to solving a "saddle point" linear system (1.70).

It is well known that (1.70) is an effective model for approximation problem in many cases. Now we consider a gerneralized least squares formula for hybrid approximation. Firstly, instead of using the data point set X_N as the center point set of RBFs, we use a different point set $X_{N_*} = \{\mathbf{x}_1^*, \mathbf{x}_2^*, \ldots, \mathbf{x}_{N_*}^*\}$ as the center point set to construct the RBFs. As we declared in the last section, in the original saddle point model (1.70) the data point set is directly chosen as the center point set when we creating RBFs. However, no theoretical result has been established to insist this choice as far as we know. Naturally, we have some new notations about this new center point set as matrix $A \in \mathbb{R}^{N \times N_\star}$ and $Q_* \in \mathbb{R}^{N \times (L+1)^2}$ defined by

$$A_{i,j} := \phi(\mathbf{x}_i, \mathbf{x}_j^*), \qquad i = 1, \ldots, N,\ j = 1, \ldots, N_*, \tag{4.11}$$

and

$$(Q_*)_{i,\ell^2+k} := Y_{\ell,k}(\mathbf{x}_i^*), \quad i = 1, \ldots, N_*,\ k = 1, \ldots, 2\ell+1,\ \ell = 0, \ldots, L. \tag{4.12}$$

Then the orthogonal condition (1.67) is equivalent to

$$Q_*^T \alpha = 0. \tag{4.13}$$

In this case, we still always assume that X_{N_*} to be a fundamental system, which implies that Q_* is of full column rank. Now we consider the new linear system

$$\begin{bmatrix} A & Q \\ Q_* & 0 \end{bmatrix} \begin{bmatrix} \alpha \\ \beta \end{bmatrix} = \begin{bmatrix} \mathbf{f} \\ 0 \end{bmatrix}. \tag{4.14}$$

If we here assume that $N > N_*$ and A is of full column rank, this system will be over determined and has no solution. In this case, instead of equation (4.14), we consider its

least squares form as

$$\min_{\alpha,\beta} \frac{1}{2}\|A\alpha + Q\beta - \mathbf{f}\|_2^2 \tag{4.15}$$

$$\text{s.t.} \quad Q_*^T\alpha = 0,$$

or

$$\min_{\alpha,\beta} \frac{1}{2}\alpha Q_* Q_*^T\alpha \tag{4.16}$$

$$\text{s.t.} \quad A\alpha + Q\beta - \mathbf{f} = 0.$$

The solution of problem (4.15) satisfies the condition (1.67) strictly whereas the solution of problem (4.16) interpolates the data $\mathbf{f}$ exactly. To meet a balance of this two aspects, we consider its penalized form as a more general case. we plus the two objective functions in the two models with a penalized parameter multiplied on one of them, and then can obtain its $l_2 - l_2$ penalized form as

$$\min_{\alpha,\beta} \frac{1}{2}\|A\alpha + Q\beta - \mathbf{f}\|_2^2 + \lambda\|Q_*^T\alpha\|_2, \tag{4.17}$$

where λ is the regularized or penalized parameter to balance the approximation and the orthogonal condition. This problem is a smooth convex unconstrained programming. By deriving its first order necessary condition, we can obtain a linear system which is easy to solve.

Moreover, we usually want the orthogonal condition to hold for as many ℓ and k, $\ell = 0, \ldots, L,\ k = 1, \ldots, 2\ell + 1$, as possible. That is to say, we want the vector $Q_*^T\alpha$ as sparse as possible. Based on this point of view, the $l_2 - l_0$ is more advisable to consider:

$$\min_{\alpha,\beta} \frac{1}{2}\|A\alpha + Q\beta - \mathbf{f}\|_2^2 + \lambda\|Q_*^T\alpha\|_0. \tag{4.18}$$

This problem is non-lipschitz nonconvex and can have multiple local minimizers. However, we should note that problem (4.18) is non-convex and NP hard [30, 49, 51]. Hence we

should consider an approximation of this model instead. A good approximation is that replacing the ℓ_0 norm by ℓ_p norm, with the form as

$$\min_{\alpha,\beta} \frac{1}{2}\|A\alpha + Q\beta - \mathbf{f}\|_2^2 + \lambda\|Q_*^T\alpha\|_p, \tag{4.19}$$

where $0 < p < 1$, which is named low order penalty problem. However, the problem is nonsmooth and nonconvex. For the convenience of computing, a convex approximation form is expected to make this problem easier to solve. As the closest convex form of model (4.18), we take the ℓ_1 regularization replacing the ℓ_0 one. Thus problem (4.15) becomes non-smooth but convex programming as

$$\min_{\alpha,\beta} \frac{1}{2}\|A\alpha + Q\beta - \mathbf{f}\|_2^2 + \lambda\|Q_*^T\alpha\|_1. \tag{4.20}$$

Remark 4.3. *The solution of the saddle point system (1.70), if exists, is also an optimal solution of optimization problem (4.15), (4.18),(4.19) and (4.20) when choosing* $X_{N_*} = \{\mathbf{x}_1^*, \mathbf{x}_2^*, \ldots, \mathbf{x}_{N_*}^*\} = X_N$.

The existence of solution for system (1.70) guarantees that the optimal values of all objective functions in (4.20), (4.15), (4.19) and (4.18) equals to 0.

Remark 4.4. *Systems (4.20), (4.15), (4.19) and (4.18) all guarantee the exactness for polynomials of degree* $\leqslant L$. *That is, for* $\forall f \in \mathbb{P}_L$, (α^*, β^*) *is the optimal solution for all the four problems, in which* $\alpha^* = 0$ *and* β^* *satisfies*

$$f = \sum_{l=0}^{L}\sum_{k=1}^{2\ell+1} \beta_{\ell,k}^* Y_{\ell,k},$$

where $\beta^* = (\beta_{\ell,k}^*),\ \ell = 0, \ldots, L,\ k = 1, \ldots, 2\ell + 1$. *In this situation,* β^* *is unique and all the objective functions equal to 0.*

The $\|\cdot\|_1$ regularizer in (4.20) is to guarantee condition (1.73) which forces u, the linear combination of RBFs, separated from the spherical harmonic polynomial space $\mathbb{P}_L$ and λ is the regularization parameter to balance the two parts. This leads to (4.20) as a non-smooth and convex optimization problem. The problem also requires that both X_N

and X_{N_*} are fundamental systems [2] which guarantee that both Q and Q_* are of full column rank.

Now we consider using the alternating direction method (ADM) to solve the problem (4.20). The motivation of this method is to solve a separable programming by separating it into two or more easier subproblems. Since the method requires that the objective function is separable, first we introduce an auxiliary variable vector $\mathbf{y} = Q_*^T\alpha \in \mathbb{R}^{(L+1)^2}$ and (4.26) can be reformulated into a constrained optimization problem as

$$\min_{\alpha,\beta} \frac{1}{2}\|A\alpha + Q\beta - \mathbf{f}\|_2^2 + \lambda\|\mathbf{y}\|_1 \tag{4.21}$$

$$\text{s.t.} \quad Q_*^T\alpha - \mathbf{y} = 0$$

which is a structured convex constrained optimization problem and can be solved by the ADM method. Let $\mathbf{z}$ be the Lagrangian multiplier and $0 < \rho \leqslant 1$ be the augmented Lagrangian parameter for the linear constraint $Q_*^T\mathbf{x} - \mathbf{y} = 0$, then the augmented lagrangian function of (4.21) is

$$L(\mathbf{x}, \mathbf{y}, \mathbf{z}) = \frac{1}{2}\|A\alpha + Q\beta - \mathbf{f}\|_2^2 + \lambda\|\mathbf{y}\|_1 - \mathbf{z}^T(Q_*^T\alpha - \mathbf{y}) + \frac{\rho}{2}\|Q_*^T\alpha - \mathbf{y}\|_2^2. \tag{4.22}$$

Then a framework of the alternating direction method for problem (4.20) could be given as Algorithm 4.2.

Algorithm 4.2: ADM for the l_1–regularized hybrid approximation problem

Step 0: Initialization. Make an initial guess $\mathbf{v}^0 = (\mathbf{y}^0, \mathbf{z}^0)$.

Step 1: Find a new x. For given $(\mathbf{y}^k, \mathbf{z}^k)$, solve the convex quadratic programming

$$\mathbf{x}^{k+1} = \begin{pmatrix} \alpha^{k+1} \\ \beta^{k+1} \end{pmatrix} = \arg\min \left\{ \frac{1}{2}\|A\alpha + Q\beta - \mathbf{f}\|_2^2 - (\mathbf{z}^k)^T(Q_*^T\alpha - \mathbf{y}^k) + \frac{\rho}{2}\|Q_*^T\alpha - \mathbf{y}^k\|_2^2 \right\}. \tag{4.23}$$

Step 3: Find a new y. Use $\mathbf{z}^k$ and the obtained $\mathbf{x}^{k+1}$ to solve the convex separable quadratic programming

$$\mathbf{y}^{k+1} = \arg\min \left\{ \lambda\|\mathbf{y}\|_1 - (\mathbf{z}^k)^T(Q_*^T\alpha^{k+1} - \mathbf{y}) + \frac{\rho}{2}\|Q_*^T\alpha^{k+1} - \mathbf{y}\|_2^2 \right\}. \tag{4.24}$$

Step 4: Update the lagrangian operator. Update $\mathbf{z}^k$ as $\mathbf{z}^{k+1} = \mathbf{z}^k - \rho(Q_*^T\alpha^{k+1} - \mathbf{y}^{k+1})$ and go back to step 2 until convergence.

In step 2, by deriving its first-order optimality condition, solving (4.23) could lead to seeking the solution of the following linear system:

$$\begin{bmatrix} A^TA + \rho Q_*Q_*^T & A^TQ \\ Q^TA & Q^TQ \end{bmatrix} \begin{bmatrix} \alpha^{k+1} \\ \beta^{k+1} \end{bmatrix} = \begin{bmatrix} A^T\mathbf{f} + \rho Q_*\mathbf{y}^k + Q_*\mathbf{z}^k \\ Q^T\mathbf{f} \end{bmatrix}. \tag{4.25}$$

Now we denote by

$$M = \begin{bmatrix} A & Q \end{bmatrix}, \quad \mathbf{x} = \begin{bmatrix} \alpha \\ \beta \end{bmatrix}, \quad B = \begin{bmatrix} Q_*^T & 0 \end{bmatrix}$$

and

$$J = \begin{bmatrix} M \\ B \end{bmatrix} = \begin{bmatrix} A & Q \\ Q_*^T & 0 \end{bmatrix}$$

where $M \in \mathbb{R}^{N\times(N_*+(L+1)^2)}$, $B \in \mathbb{R}^{(L+1)^2\times(N_*+(L+1)^2)}$ and $J \in \mathbb{R}^{(N+(L+1)^2)\times(N_*+(L+1)^2)}$.

Lemma 4.5. *Linear system (4.25) has a unique solution if*

$$\operatorname{rank}(J) = N_* + (L+1)^2.$$

Proof. For (4.25) we could obtain that

$$\begin{bmatrix} A^TA+\rho Q_*Q_*^T & A^TQ \\ Q^TA & Q^TQ \end{bmatrix} = \begin{bmatrix} A^T \\ Q^T \end{bmatrix} \begin{bmatrix} A & Q \end{bmatrix} + \rho \begin{bmatrix} Q_* \\ 0 \end{bmatrix} \begin{bmatrix} Q_*^T & 0 \end{bmatrix} = M^TM + \rho B^TB.$$

The above matrix is invertible if and only if the zero vector is the unique solution of the system

$$J\mathbf{x} = 0.$$

Then we can get that

$$N_* + (L+1)^2 \leqslant \operatorname{rank}(J) \leqslant N_* + (L+1)^2.$$

□

Now we consider the subproblem (4.24) in step 3. The format of problem (4.20) could be simplified as

$$\min_{\mathbf{x}} \frac{1}{2}\|M\mathbf{x}-\mathbf{f}\|_2^2 + \lambda\|B\mathbf{x}\|_1 \tag{4.26}$$

$$\text{s.t.} \quad B\mathbf{x}-\mathbf{y} = 0.$$

We denote by $(B\mathbf{x}^{k+1})_i$ as the ith column of the vector $B\mathbf{x}^{k+1}$. Then problem (4.24) can be reformulated as

$$\begin{aligned} \mathbf{y}^{k+1} &= \arg\min \left\{ \lambda \sum_{i=1}^{(L+1)^2} |\mathbf{y}_i| - \sum_{i=1}^{(L+1)^2} (\mathbf{z}^k)_i((B\mathbf{x}^{k+1})_i - \mathbf{y}_i) \right. \\ &\quad \left. + \frac{\rho}{2} \sum_{i=1}^{(L+1)^2} ((B\mathbf{x}^{k+1})_i - \mathbf{y}_i)^2 \right\} \qquad (4.27) \\ &= \arg\min \left\{ \sum_{i=1}^{(L+1)^2} (\lambda|\mathbf{y}_i| - (\mathbf{z}^k)_i((B\mathbf{x}^{k+1})_i - \mathbf{y}_i) + \frac{\rho}{2}((B\mathbf{x}^{k+1})_i - \mathbf{y}_i)^2) \right\} \end{aligned}$$

We see that (4.27) is a separable optimization problem. Then the problem can be separated to $(L+1)^2$ one-dimension subproblems as

$$\mathbf{y}_i^{k+1} = \arg\min \left\{ \lambda|\mathbf{y}_i| + (\mathbf{z}^k)_i \mathbf{y}_i + \frac{\rho}{2}((B\mathbf{x}^{k+1})_i - \mathbf{y}_i)^2 \right\} \tag{4.28}$$

and by the first order optimal condition, we have that

$$0 \in \lambda \partial(|\mathbf{y}_i|) - \mathbf{z}_i^k - \rho(B\mathbf{x}^{k+1})_i + \rho \mathbf{y}_i,$$

where $\partial(|\mathbf{y}_i|)$ denotes the subdifferential of the nondifferentiable convex function $|\mathbf{y}_i|$. We could note that this step is equivalent to a scalar shrinkage process and the following theorem is developed based on the relative conclusion in [68].

Remark 4.6. *The solution of (4.28) could be given by the formulation*

$$\begin{aligned} \mathbf{y}_i^{k+1} =& \frac{1}{\rho} \left(\max\left\{0, \rho(B\mathbf{x}^{k+1})_i + (\mathbf{z}^k)_i - \lambda \right\} \right. \\ & \left. - \max\left\{0, -\rho(B\mathbf{x}^{k+1})_i - (\mathbf{z}^k)_i - \lambda \right\} \right). \end{aligned} \tag{4.29}$$

Now we consider the stopping criterion of the proposed algorithm. By deriving the first-order optimality condition (4.21), we have

$$\begin{cases} M^T M\mathbf{x} - M^T\mathbf{f} - B^T\mathbf{z} = 0, \\ 0 \in \lambda \partial(\|\mathbf{y}\|_1) + \mathbf{z}, \\ B\mathbf{x} - \mathbf{y} = 0. \end{cases} \tag{4.30}$$

Hence problem (4.21) has the following variational inequality characterization: find $\omega \in \Omega := \mathbb{R}^{N_*+3(L+1)^2}$ such that

$$\omega \in \Omega, \quad \lambda(|\mathbf{y}'| - |\mathbf{y}|) + \langle \omega' - \omega, F(\omega) \rangle \geqslant 0, \quad \forall \omega' \in \Omega, \tag{4.31}$$

where

$$\omega = \begin{pmatrix} \mathbf{x} \\ \mathbf{y} \\ \mathbf{z} \end{pmatrix} \quad and \quad F(\omega) = \begin{pmatrix} M^T M\mathbf{x} - M^T\mathbf{f} - B^T\mathbf{z} \\ \mathbf{z} \\ B\mathbf{x} - \mathbf{y} \end{pmatrix}. \tag{4.32}$$

Let $(\mathbf{x}^{k+1}, \mathbf{y}^{k+1}, \mathbf{z}^{k+1}) \in \Omega$ be generated by Algorithm 1. We denote by $\Omega^* = \{(\mathbf{x}^*, \mathbf{y}^*, \mathbf{z}^*)\}$ the solution set of problem (4.21). Note that system (4.25) is equivalent to find an $\mathbf{x}^{k+1}$ satisfying

$$\left\langle \mathbf{x}' - \mathbf{x}^{k+1}, M^T M\mathbf{x}^{k+1} - M^T\mathbf{f} - B^T\mathbf{z}^k + \rho B^T B\mathbf{x}^{k+1} - \rho B^T\mathbf{y}^k \right\rangle \geqslant 0,$$

$$\forall \mathbf{x}' \in \mathbb{R}^{N_*+(L+1)^2}.$$

Simultaneously, we have

$$\begin{aligned}\lambda(|\mathbf{y}'| - |\mathbf{y}^{k+1}|) - \left\langle \begin{pmatrix} \mathbf{x}' - \mathbf{x}^{k+1} \\ \mathbf{y}' - \mathbf{y}^{k+1} \\ \mathbf{z}' - \mathbf{z}^{k+1} \end{pmatrix}, \right. \\ \left. \begin{pmatrix} M^T M\mathbf{x}^{k+1} - M^T\mathbf{f} - B^T\mathbf{z}^{k+1} \\ \mathbf{z}^{k+1} \\ \rho(B\mathbf{x}^{k+1} - \mathbf{y}^{k+1}) \end{pmatrix} + \begin{pmatrix} \rho B^T(\mathbf{y}^{k+1} - \mathbf{y}^k) \\ 0 \\ \mathbf{z}^{k+1} - \mathbf{z}^k \end{pmatrix} \right\rangle \geqslant 0\end{aligned} \tag{4.33}$$

for any $(\mathbf{x}', \mathbf{y}', \mathbf{z}') \in \Omega$. Therefore, $(\mathbf{x}^{k+1}, \mathbf{y}^{k+1}, \mathbf{z}^{k+1})$ is a solution of (4.21) if and only if $\mathbf{y}^k = \mathbf{y}^{k+1}$ and $\mathbf{z}^{k+1} = \mathbf{z}^k$. Then we could establish a stopping criterion for Algorithm 1 according to this conclusion:

$$\max\{\|\mathbf{y}^k - \mathbf{y}^{k+1}\|_2, \|\mathbf{z}^k - \mathbf{z}^{k+1}\|_2\} \leqslant \epsilon, \tag{4.34}$$

where $\epsilon > 0$.

4.3 Numerical results

In this section we establish some numerical experiments to test the efficiency of the approximation models proposed in the above section. The codes of the ADM are written by Matlab 2011b, and all the numerical experiments are done on a Lenovo Thinkcenter PC equipped with Intel Core i7-3770 3.4G Hz CPU, 8 GB RAM running Windows 7.

In this thesis we do not pay much attention to the choice of regularized parameter λ in (4.19). We know that choosing a suitable parameter is an important process in regularized models. It may influence the result of approximation directly and how to choose a "good" λ is still an open problem. As a part of remedy of that, we would try several different selections of λ, as $\lambda = 10^{-6}, 10^{-5}, \cdots, 10^{6}$, and record the best case among them into the table.

In the coming numerical experiment, to test the two models (4.1) and (4.20) mentioned in previous sections in this chapter, three functions with the different property are tested.

1. Franke function:

$$\begin{aligned} f(\mathbf{x}) = & f(x,y,z) = 0.75\exp(-(9x-2)^2/4 - (9y-2)^2/4 - (9z-2)^2/4) \\ & + 0.75\exp(-(9x+1)^2/49 - (9y+1)/10 - (9z+1)/10) \\ & + 0.5\exp(-(9x-7)^2/4 - (9y-3)^2/4 - (9z-5)^2/4) \\ & - 0.2\exp(-(9x-4)^2 - (9y-7)^2 - (9z-5)^2),\ (x,y,z) \in \mathbb{S}^2. \end{aligned} \tag{4.35}$$

2. Franke function with noise added:

$$f^{\delta}(\mathbf{x}) = f(\mathbf{x}) + \delta(\mathbf{x}), \tag{4.36}$$

   where for each $\mathbf{x}$, $\delta(\mathbf{x})$ is a sample of a normal random variable with mean 0 and standard deviation $\sigma = 0.1$.

3. Franke function plus a cap function:

$$f_{cap}(\mathbf{x}) = f(\mathbf{x}) + g(\mathbf{x}) = f(\mathbf{x}) + \begin{cases} \rho\cos\left(\frac{\pi \arccos(\mathbf{x}_c\cdot\mathbf{x})}{2r}\right), & \mathbf{x} \in \mathcal{C}(\mathbf{x}_c, r), \\ 0, & \text{otherwise}, \end{cases} \tag{4.37}$$

   where $\mathbf{x}_c = (-0.5, 0.5, \sqrt{0.5})^T$, and $r = 0.5$ and $\rho = \frac{1}{r}$.

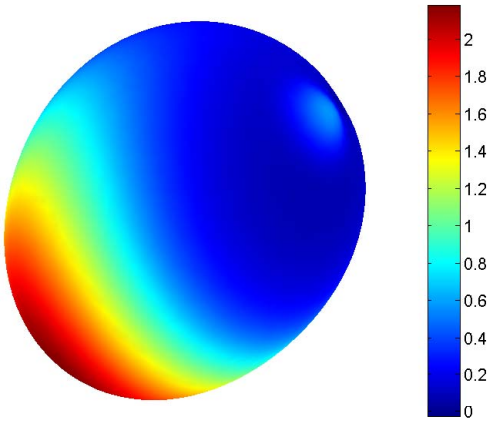

(a) f

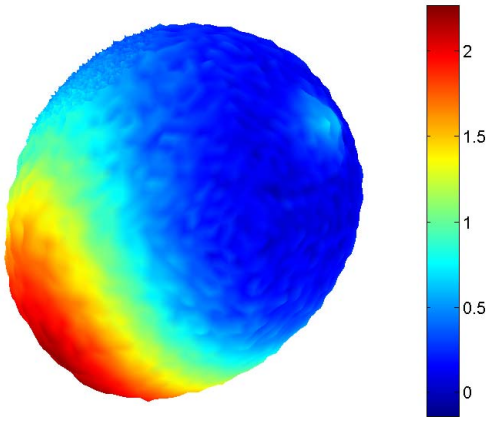

(b) f^{δ}

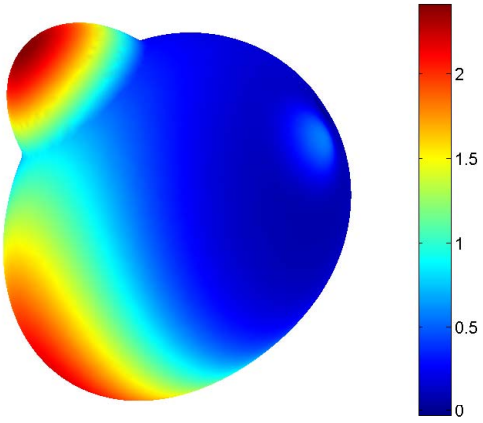

(c) f_{cap}

Figure 4.1: Shapes of f, f^{δ} and f_{cap}

The Franke Function f, which is modified by Renka [56] is continuous differentiable on $\mathbb{S}^2$. The second function f^δ presents a noised data with its original function as a continuous differentiable function. The third function f_{cap} is a continuous but non-differentiable function on $\mathbb{S}^2$. The shapes of the three functions are shown in Figure 4.1.

4.3.1 Regularized weighted least square polynomial approximation using spherical t_ϵ-designs

In this section we will test the model (4.1) proposed in Section 4.1. We will use the spherical t_ϵ-designs found by the STRF algorithm proposed in Section 3.2 as the data point sets. For comparison, we will also implement the model (1.48) proposed in [3] using spherical t-designs proposed in [64] as data point sets.

In this experiment we will use the spherical $t_{0.1}$-designs which are found in Section 3.2 and the spherical t-design proposed in [64] as the point set for polynomial approximation. We will record the uniform errors and $\mathbb{L}_2$ errors to measure the approximation quality. We all know that it is a complicated and time-consuming process to calculate the precise value of the uniform norm and $\mathbb{L}_2$ norm of a function on the sphere. Here we choose a large-scaled and well distributed point set $X_t \subset \mathbb{S}^2$ to be the test set and use it to estimate the errors. Then the uniform error and $\mathbb{L}_2$ error of the approximation are estimated by

$$\|f - p_{L,N}\|_{C(\mathbb{S}^2)} \approx \max_{\mathbf{x}\in X_t} |f(\mathbf{x}) - p_{L,N}(\mathbf{x})|, \tag{4.38}$$

and

$$\|f - p_{L,N}\|_{\mathbb{L}_2} \approx \left(\frac{4\pi}{N_t}\sum_{i=1}^{N_t}(f(\mathbf{x}_i) - p_{L,N}(\mathbf{x}_i))^2\right)^{\frac{1}{2}}, \tag{4.39}$$

where N_t denotes the number of points in X_t. In this experiment, we choose X_t to be an equal area partitioning point set [57] with 10^5 points.

For both spherical t_ϵ-designs and spherical t-designs we always let $L = \lfloor t/2 \rfloor$. Under this setting the solution of model (4.1) can be directly obtained by formula (4.6). Fig. 4.2 shows the errors of for the least squares approximation of f with $\mathcal{R}_L = \mathbf{0}$ (or $\lambda = 0$).

From the figure it can be seen that, the $\mathbb{L}_2$ errors using spherical t_ϵ-designs decay faster than the ones using spherical t-designs, although the uniform errors of them look close to each other.

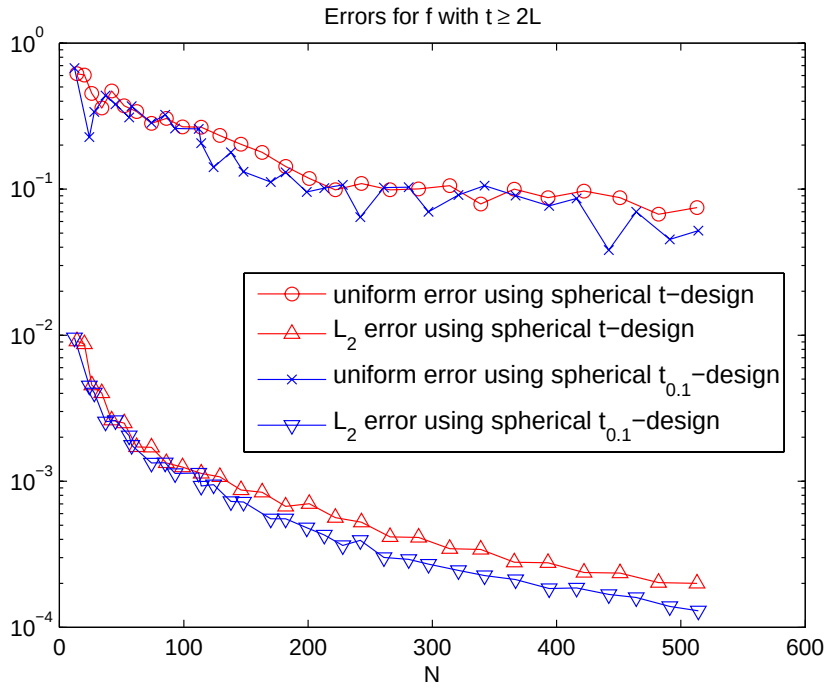

Figure 4.2: Errors for least square approximation of f with zero regularization operator

Fig. 4.2 shows the errors for least squares approximation of f^δ with Laplace-Beltrami operators with $\lambda = 0, 10^{-6}$ using spherical t_ϵ-designs. From the figure we can see that when $\lambda = 10^{-6}$, both the uniform errors and $\mathbb{L}_2$ errors are smaller than the case with $\lambda = 0$, which implies that Laplace-Beltrami regularization can improve the approximation quality for noisy case.

4.3.2 Regularized hybrid approximation using spherical t_ϵ-designs

In this section we will examine the approximation quality of propose model (4.20) in Section 4.2. In this experiment, we apply the "Wendland" function [72] as the kernel of RBFs, which is a kind of piece wise function with compact support to approximate it. It has been proved to be positive definite on $\mathbb{S}^2$. The function is defined as

$$\phi(\mathbf{x}, \mathbf{y}) = \psi(|\mathbf{x} - \mathbf{y}|) = \psi(\sqrt{2 - 2\mathbf{x} \cdot \mathbf{y}}), \quad \mathbf{x}, \mathbf{y} \in \mathbb{S}^2,$$

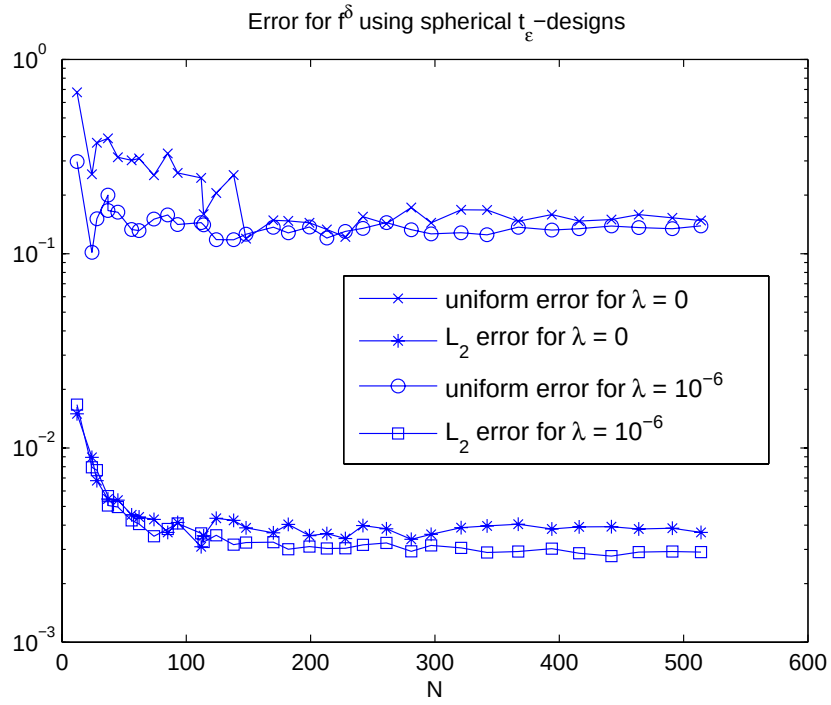

Figure 4.3: Errors for least square approximation of f^δ with Laplace-Beltrami regularization operator

where $\psi(r)$ could be one of the three choices as

$$\psi_0(r) = (1-r)_+^2 \in C^0(\mathbb{R}), \tag{4.40}$$

$$\psi_2(r) = (1-r)_+^4(4r+1) \in C^2(\mathbb{R}), \tag{4.41}$$

$$\psi_4(r) = (1-r)_+^6(35r^2+18r+3) \in C^4(\mathbb{R}), \tag{4.42}$$

where $\psi_i, i = 0, 2, 4$ are all continuous but only ψ_2, ψ_4 are differentiable on $\mathbb{R}$. In our experiment, numerical tests have proved that approximation residuals do not vary so much by choosing different RBFs, so here we will only apply the kernel ψ_2 which is continuous differentiable on $\mathbb{R}$ to construct the RBFs. Sometimes scaling of the compact support is employed to improve the approximation, but scaling also results in large condition number of A, which will lead to long solving time, which will influence the solving time for each different method in different extent. Hence for fairness of the comparison we will not use scaling in this experiment if nothing announced.

We choose two different types of point sets as the data set and center point set for RBFs. One type is a set with its points (approximately) uniformly distributed on the whole sphere. The minimal energy [57], extremal spherical design [29] and well conditioned

spherical t-design [2] systems are all uniformly distributed point systems. Here we will use the spherical t_ϵ-designs proposed in our thesis as the data point set and the center point set. In this experiment we will set $\epsilon = 0.1$ to construct the spherical t_ϵ-designs and denote these sets as "WD" (well distributed) set for brevity of notations.

The other type is a non-uniformly distributed set with points distributed densely in a small cap region and relatively sparsely in the rest region of the sphere. Obviously, this kind of point sets will lead to ill conditioned matrix and cost more solving time. We will generate this set X_N using equal area partitioning (EAP) method, see [57]. The basic scheme is that we first generate some points densely and uniformly in a cap region using EAP and then generate points sparsely in the rest region. We set the proportion of density between the dense region and sparse region are five. In each time of test, we apply the same type of the data set and center point set. That means if a non-uniformly distributed point set is selected as data point set in one test, then the center point set will also be selected as non-uniformly with the same cap region and vice versa. We should also note that the theory of keeping matrix M of full column rank is still not studied. But in practical tests it is not difficult to choose the data set and center set to make this condition hold.

Now we consider using the model (4.20) to approximate the Franke function. We choose the both two types of point set mentioned above: scattered data systems (SD), which represent the non-uniformly distributed point sets, and spherical t_ϵ-designs, which represent the uniformly distributed point sets.

We denote $\Lambda_{p,q}$ as the approximation obtained by problem (4.19) and then the residual could be obtained as

$$R_{p,q} = \|\Lambda_{p,q} f - f\|_{C(\mathbb{S}^2)} \approx \max_{\mathbf{x}\in X_t} |\Lambda_{p,q} f(\mathbf{x}) - f(\mathbf{x})|.$$

Simultaneously, we present the residual norm when we apply the saddle point system (1.70) to get approximation, as

$$R_{X,L} = \|\Lambda_{X,L} f - f\|_{C(\mathbb{S}^2)} \approx \max_{\mathbf{x}\in X_t} |\Lambda_{X,L} f(\mathbf{x}) - f(\mathbf{x})|$$

Table 4.1: Residuals ($R_{\cdot,\cdot}$) and CPU time ($T_{\cdot,\cdot}$) with different models for hybrid approximation with $L = 10$

Type(N,N_*)	$R_{2,1}(T_{2,1})$	$R_{2,2}(T_{2,2})$	$R_{1,1}(T_{1,1})$	$R_{X,L}(T_{X,L})$
Methods	ADM	MINRES	SDPT3	MINRES
WD(2000,400)	0.0433(0.02)	0.0471(0.05)	0.687(55)	0.0446(0.01)
WD(4000,800)	0.0165(0.23)	0.0360(0.14)	0.0305(198)	0.0221(0.08)
WD(6000,1200)	0.0068(0.25)	0.0372(0.39)	0.0076(490)	0.0095(0.25)
WD(8000,1600)	0.0040(0.56)	0.0377(0.81)	0.0076(927)	0.0071(0.63)
WD(10000,2000)	0.0018(0.69)	0.0368(0.87)	0.0031(2438)	0.0031(0.69)
SD(1993,399)	0.0535(0.03)	0.0563(0.06)	0.0845(46)	0.0514(0.04)
SD(3979,801)	0.0261(0.13)	0.0450(0.22)	0.0336(216)	0.0336(0.10)
SD(5974,1194)	0.0109(0.27)	0.0437(0.79)	0.0162(698)	0.0150(0.52)
SD(7964,1592)	0.0080(0.57)	0.0438(1.5)	0.0151(1132)	0.0126(1.39)
SD(9954,1993)	0.0040(0.95)	0.0438(2.5)	0.0076(1828)	0.0071(2.47)

in the table, of which both the center point set and data set are X_{N_*}. Here we use an equal area partitioning point set [57] with 10^6 points distributed uniformly on the sphere to deal with this process. We collect the infinity norms of the approximation residuals and CPU time in seconds for solving process for each model as presented in Table 4.1.

The other three models are the $l_2 - l_2$ problem (4.17), $l_1 - l_1$, which simply change all the norm $\|\cdot\|_2$ in (4.17) to $\|\cdot\|_1$, and the saddle point system (1.70). Since the $l_2 - l_2$ case can be reformulated as a linear system, we will solve it by the minimal residual method (MINRES), as what is applied to equation (1.70). For $l_1 - l_1$ we would employ an existing software or package to solve it. There are many popular methods and packages to solve a convex problem, such as the SPG [13], which is written in Fortran 77 and is proved to be efficient for many continuous differentiable optimization problems.

In our experiment we would apply a package called CVX which is written by Matlab for convenience. The SDPT3 solver [69] is chosen in this package, which employs an infeasible primal-dual predictor-corrector path-following method and could deal with varieties of convex problem.

We can obtain some other interesting conclusions from the table. It is natural to see that all residuals $R_{2,1}$, $R_{2,2}$, $R_{1,1}$ and $R_{X,L}$ generally decrease when N_* turns larger, which means that the approximation is more accurate. For the same scale it is obvious to see that $R_{2,1}$ is always the smallest among the residuals. Also we could see that ADM is an efficient solver for our model. For same scale and same type of point sets, ADM needs the least time to solve the $l_2 - l_1$ model. For similar scale but different types of point sets, $l_2 - l_1$ model using ADM costs similar time for both the SD and the WD case, whereas other models need much more time to solve for SD case than the WD case.

In the next experiment we will approximate f using noised data f^δ defined by (4.36). The saddle point model (1.70) will also be compared with (4.19) for restoration of the original function. The approximate infinity norms of residuals are still recorded to measure the approximation quality. Since we have found that the equal area partition point systems behave well in Table 4.1, in this experiment we only choose the spherical $t_{0.1}$-designs for test. The infinity norms of the residual are still recorded to measure the quality of the approximation.

The residuals of approximating f^δ using different models in different scales of point systems are presented in the Table 4.2.

From the table we could find that for noisy case, the regularized models, including $l_2 - l_1$, $l_2 - l_2$ and $l_1 - l_1$, process more accurate restoration for the original target function. Especially, the $l_2 - l_1$, $l_2 - l_2$ model still own similar residuals and perform better than the $l_1 - l_1$ model.

In Figure 4.4 we present the shapes of Franke function f and the noisy function f^δ. Restorations using model appearing in the above tables are also given in the figure. From Table 4.2 we have already seen that the residuals using $l_2 - l_1$ and $l_2 - l_2$ models are smaller than other model.

Table 4.2: Residuals of approximation for f^δ

N,N_*,L	$R_{2,1}$	$R_{2,2}$	$R_{1,1}$	$R_{X,L}$
121,36,5	0.3312	0.3187	0.3915	0.3968
441,121,5	0.1129	0.1129	0.1708	0.1646
961,256,5	0.1035	0.1035	0.1134	0.1395
961,256,10	0.1039	0.1039	0.1152	0.1449
1681,441,5	0.0959	0.0959	0.1179	0.1585
1681,441,10	0.0861	0.0861	0.1255	0.1591

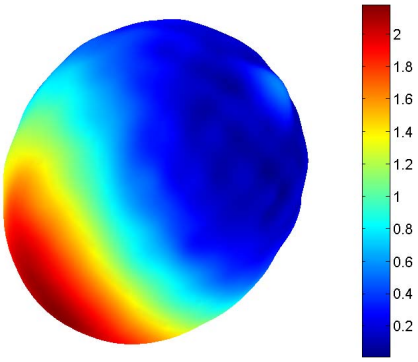

(a) restoration by $\ell_2 - \ell_1$

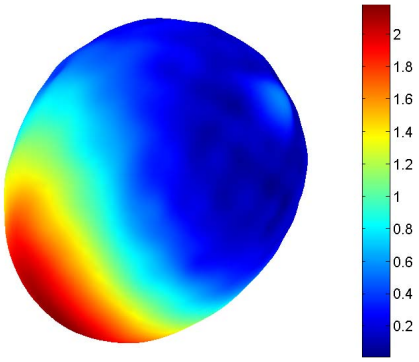

(b) restoration by $\ell_2 - \ell_2$

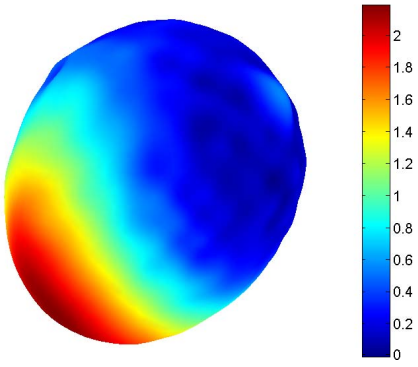

(c) restoration by $\ell_1 - \ell_1$

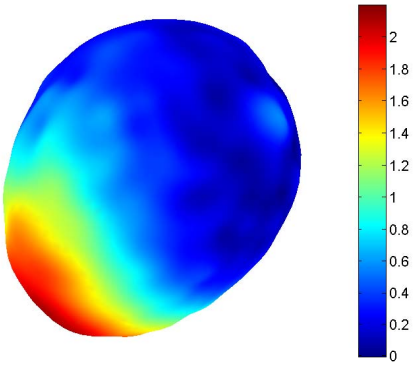

(d) restoration by saddle point system

Figure 4.4: Shapes of f, f^δ and its restoration

Table 4.3: Residuals of approximation for f_{cap} with $L = 10$

N,N_*	$R_{2,1}$	$R_{2,2}$	$R_{1,1}$	$R_{X,L}$
1993,399	0.1007	0.1040	0.1456	0.1467
2987,598	0.0708	0.0836	0.1096	0.1232
3979,801	0.0673	0.0814	0.0793	0.1101
4980,994	0.0565	0.0745	0.0826	0.0925
5974,1194	0.0490	0.0749	0.0625	0.0745

The third experiment is supposed to approximate the Franke function plus cap function, denoted by f_{cap}.

Note that f_{cap} is a continuous but non-differentiable function on the sphere. Thus, when approximating f_{cap} using differentiable functions, errors near the cap boundary often are much larger than other parts. To get a close estimate of the uniform residual for this case, we choose the test set X_t to be a type with points distributed densely around the cap boundary. Similarly, to obtain better approximation, we will choose points denser in the cap region than the rest region. Also we should note that in each region the points could be uniformly distributed, which may lead to good approximation. In this sense, we apply the SD point systems as the center point set and data point set.

In this experiment we set the scaling parameter $\sigma = 0.5$, which means that in the RBFs kernel $\psi_i(r)$ the variable r is replaced by $\frac{r}{\sigma}$ to reduce the compact support area of each function.

Table 4.3 shows that for any scale of point set we choose, the $l_2 - l_1$ model keeps the best approximation among the four models. In this sense, we could say that our model (4.20) is suitable for the hybrid approximation on the sphere.

Chapter 5

Conclusions and Future Work

5.1 Conclusions

In this thesis we basically studied the spherical t_ϵ-designs on the two-sphere $\mathbb{S}^2$, which is a generalization of spherical t-design with $0 \leqslant \epsilon < 1$. Due to the flexibility of choice for the weights, the number of points in the integration rule can be less for making the exact integral for any polynomial of degree at most t than spherical t-design. In Chapter 2 we prove that all the point sets arbitrarily chosen in the interval enclosures proposed by Chen, Frommer and Lang in 2010 are spherical t_ϵ-designs and give an upper bound of ϵ. We then study the variational characterization and the worst-case error of spherical t_ϵ-design. Based on the reproducing kernel theory and its relationship with the geodesic distance, we propose a way to compute the worst-case error for numerical integration using spherical t_ϵ-design in Sobolev space.

In Chapter 3 we propose an approach for finding spherical t_ϵ-designs. We show that finding a spherical t_ϵ-design can be reformulated as a system of polynomial equations with box constraints. Using the projection operator, the system can be written as a nonsmooth nonconvex least squares problem with zero residual. We propose a smoothing trust region filter algorithm for solving such problems. We present convergence theorems of the proposed algorithm to a Clarke stationary point or a global minimizer of the objective function under certain conditions. Preliminary numerical experiments show the efficiency of the proposed algorithm for finding spherical t_ϵ-designs.

In Chapter 4 we consider two regularized least squares problems: regularized poly-

nomial approximation on the sphere using spherical t_ϵ-designs, and regularized hybrid approximation on the sphere using both radial basis functions and spherical polynomials using spherical t_ϵ-designs. For the first problem we apply the l_2 regularized form and give an approximation quality estimation, and for the second one we study its l_1 regularized form and solve the problem using alternating direction method with multipliers. Numerical experiments are given to demonstrate the effectiveness of these two models.

5.2 Future work

In this thesis we propose a new concept named spherical t_ϵ-design, which is a generalization of spherical t-design with all its quadrature weight to be positive. We investigates this new concept from multiple aspects and achieve some results, but there are still some problems which are interesting to study in the future.

In Chapter 3, we propose the STRF algorithm for finding spherical t_ϵ-design. The STRF is applicable for solving nonsmooth nonconvex least squares problem with zero residual and have many applications besides finding spherical t_ϵ-designs. We propose its global convergence theory in Chapter 3, and we wish to study its local convergence property in the future.

As is shown in Section 3.4, we have found some spherical t_ϵ designs with different ϵ and t. And the points we need to construct spherical t_ϵ-designs are less than spherical t-designs. And based on the Figure 3.4 we can see that for spherical t_ϵ design minimal number of points N decays with the increase of ϵ but the theory of the relationship between each other is not constructed. In the future we will try to establish some theory to explain this phenomenon.

Another work which is worthy to study in the future is that we seek to find spherical t_ϵ-designs which possess a smaller worst-case error in Sobolev spaces. Following the result in Section 3.3, minimizing a worst-case error among spherical t_ϵ-designs leads to solving an optimization problem

$$\min_{w, X_N \subset \mathbb{S}^2} \sum_{i=1}^{N} \sum_{j=1}^{N} w_i w_j (-1)^{L+1} |\mathbf{x}_i - \mathbf{x}_j|^{2s-2}$$

$$\text{s.t.} \begin{cases} \sum_{i=1}^{N} w_i Y_{\ell,k}(\mathbf{x}_i) = 0, \ \ell = 1, \ldots, t, \ k = 1, \ldots, 2\ell + 1, \\ \\ w - \text{mid}(a, w, b) = 0. \end{cases} \tag{5.1}$$

The problem is non-differentiable expect when $s = 2$. With the flexibility of the weight w, a smaller minimal wosrt-case error than spherical t-design is expected.

Bibliography

[1] M. Abramowitz and I. A. Stegun. *Handbook of mathematical functions*, volume 1. Dover New York, 1972.

[2] C. An, X. Chen, I. H. Sloan, and R. S. Womersley. Well conditioned spherical designs for integration and interpolation on the two-sphere. *SIAM J. Numer. Anal.*, 48(6):2135–2157, 2010.

[3] C. An, X. Chen, I. H. Sloan, and R. S. Womersley. Regularized least squares approximations on the sphere using spherical designs. *SIAM J. Numer. Anal.*, 50(3):1513–1534, 2012.

[4] N. Aronszajn. Theory of reproducing kernels. *Trans. Amer. Math. Soc.*, pages 337–404, 1950.

[5] K. Atkinson and W. Han. *Spherical harmonics and approximations on the unit sphere: an introduction*. Springer, 2012.

[6] B. Bajnok. Construction of spherical t-designs. *Geom. Dedicata*, 43(2):167–179, 1992.

[7] E. Bannai. On tight spherical designs. *J. Comb. Theo., Series A*, 26(1):38–47, 1979.

[8] E. Bannai and E. Bannai. A survey on spherical designs and algebraic combinatorics on spheres. *European J. Combin.*, 30(6):1392–1425, 2009.

[9] E. Bannai and E. Bannai. Remarks on the concepts of t-designs. *J. Appl. Math. Comput.*, 40(1-2):195–207, 2012.

[10] E. BANNAI and R. M. DAMERELL. Tight spherical designs, i. *Journal of the Mathematical Society of Japan*, 31(1):199–207, 01 1979.

[11] B. J. C. Baxter and S. Hubbert. Radial basis functions for the sphere. In *Recent Progress in Multivariate Approximation*, pages 33–47. Springer, 2001.

[12] W. Bian and X. Chen. Neural network for nonsmooth, nonconvex constrained minimization via smooth approximation. *IEEE T. Neur. Net. Lear.*, 25(3):545–556, March 2014.

[13] E. G. Birgin, J. Martínez, and M. Raydan. Algorithm 813: Spg—software for convex-constrained optimization. *ACM Trans. Math. Softw.*, 27(3):340–349, September 2001.

[14] A. Bondarenko, D. Radchenko, and M. Viazovska. Optimal asymptotic bounds for spherical designs. *Ann. Math.*, 178:443–452, 2013.

[15] A. Bondarenko, D. Radchenko, and M. Viazovska. Well-separated spherical designs. *Constr. Approx.*, pages 1–20, 2013.

[16] P. Borwein. *Polynomials and polynomial inequalities*. Springer, 1995.

[17] L. Brandolini, C. Choirat, L. Colzani, G. Gigante, R. Seri, and G. Travaglini. Quadrature rules and distribution of points on manifolds. *arXiv preprint arXiv:1012.5409*, 2010.

[18] J. S. Brauchart and Ke. Hesse. Numerical integration over spheres of arbitrary dimension. *Constru. Approx.*, 25(1):41–71, 2007.

[19] J. S. Brauchart, E. B. Saff, I. H. Sloan, and R. S. Womersley. Qmc designs: optimal order quasi monte carlo integration schemes on the sphere. *arXiv preprint arXiv:1208.3267*, 2012.

[20] J. V. Burke and T. Hoheisel. Epi-convergent smoothing with applications to convex composite functions. *SIAM J. Opti.*, 23(3):1457–1479, 2013.

[21] J. V. Burke, T. Hoheisel, and C. Kanzow. Gradient consistency for integral-convolution smoothing functions. *Set-Valued Var. Anal.*, 21(2):359–376, 2013.

[22] M. Caliari, S. De Marchi, and M. Vianello. Hyperinterpolation in the cube. *Comput. Math. Appl.*, 55(11):2490–2497, 2008.

[23] C. Cartis, N. I. M. Gould, and P. L. Toint. *How Much Patience to You Have?: A Worst-case Perspective on Smooth Noncovex Optimization*. Science and Technology Facilities Council, 2012.

[24] X. Chen. Smoothing methods for nonsmooth, nonconvex minimization. *Math. Program.*, 134(1):71–99, 2012.

[25] X. Chen, A. Frommer, and B. Lang. Computational existence proofs for spherical t-designs. *Numer. Math.*, 117(2):289–305, 2011.

[26] X. Chen, L. Niu, and Y. Yuan. Optimality conditions and a smoothing trust region newton method for nonlipschitz optimization. *SIAM J. Opti.*, 23(3):1528–1552, 2013.

[27] X. Chen and Z. Wang. Convergence of regularized time-stepping methods for differential variational inequalities. *SIAM J. Opti.*, 23(3):1647–1671, 2013.

[28] X. Chen and R. S. Womersley. Existence of solutions to systems of underdetermined equations and spherical designs. *SIAM J. Numer. Anal.*, 44(6):2326–2341, 2006.

[29] X. Chen, R. S. Womersley, and J. J. Ye. Minimizing the condition number of a gram matrix. *SIAM J. Opti.*, 21(1):127–148, 2011.

[30] X. Chen, F. Xu, and Y. Ye. Lower bound theory of nonzero entries in solutions of $\ell_2 - \ell_p$ minimization. *SIAM J. Sci. Comp.*, 32(5):2832–2852, 2010.

[31] E. W. Cheney. *Multivariate approximation theory: Selected topics*. SIAM, 1986.

[32] F. H. Clarke. *Optimization and nonsmooth analysis*, volume 5. SIAM, 1990.

[33] H. Cohn and A. Kumar. Universally optimal distribution of points on spheres. *J. Amer. Math. Soci.*, 20(1):99–148, 2007.

[34] A. R. Conn, N. I. M. Gould, and P. L. Toint. *Trust region methods*, volume 1. SIAM, 2000.

[35] J. H. Conway and N. J. Sloane. Sphere packings, lattices and groups, 1993.

[36] P. Delsarte, J. Goethals, and J. J. Seidel. Spherical codes and designs. *Geometriae Dedicata*, 6(3):363–388, 1977.

[37] J. Ding. Perturbation of systems of linear algebraic equations. *Linear Multilinear A.*, 47(2):119–127, 2000.

[38] R. Fletcher, S. Leyffer, and P. L. Toint. On the global convergence of a filter–sqp algorithm. *SIAM J. Opti.*, 13(1):44–59, 2002.

[39] W. Freeden, T. Gervens, and M. Schreiner. *Constructive approximation on the sphere: with applications to geomathematics*. Clarendon Press Oxford, 1998.

[40] R. Garmanjani and L. N. Vicente. Smoothing and worst-case complexity for direct-search methods in nonsmooth optimization. *IMA J. Numer. Anal.*, 33(3):1008–1028, 2013.

[41] N. I. M. Gould, S. Leyffer, and P. L. Toint. A multidimensional filter algorithm for nonlinear equations and nonlinear least-squares. *SIAM J. Opti.*, 15(1):17–38, 2004.

[42] M. Gräf, S. Kunis, and D. Potts. On the computation of nonnegative quadrature weights on the sphere. *Appl. Comput. Harmon. A.*, 27(1):124–132, 2009.

[43] R. H. Hardin and N. J. A. Sloane. Mclarens improved snub cube and other new spherical designs in three dimensions. *Discrete Comput. Geom.*, 15(4):429–441, 1996.

[44] K. Hesse and I. H. Sloan. Worst-case errors in a sobolev space setting for cubature over the sphere s^2. *Bull. Austr. Math. Soci.*, 71(01):81–105, 2005.

[45] K. Hesse and I. H. Sloan. Cubature over the sphere s^2 in sobolev spaces of arbitrary order. *J. Approx. Theo.*, 141(2):118–133, 2006.

[46] Hesse K. and Leopardi P. The coulomb energy of spherical designs on s^2. *Adv. Comput. Math.*, 1(28):331–354, 2008.

[47] J. Korevaar and J. L. H. Meyers. Spherical faraday cage for the case of equal point charges and chebyshev-type quadrature on the sphere. *Intger. Transf. Spec. F.*, 1(2):105–117, 1993.

[48] Q. T. Le Gia, I. H. Sloan, and A. J. Wathen. Stability and preconditioning for a hybrid approximation on the sphere. *Numer. Math.*, 118(4):695–711, 2011.

[49] R. G. Michael and D. S. Johnson. *Computers and Intractability: A guide to the theory of NP-completeness*. 1979.

[50] I. P. Mysovsskikh. On the construction of cubature formulas with fewest nodes. *Soviet Math. Dokl.*, 9:277–280, 1968.

[51] B. K. Natarajan. Sparse approximate solutions to linear systems. *SIAM J. Comp.*, 24(2):227–234, 1995.

[52] J. Nocedal and S. J. Wright. *Numerical optimization*. Springer New York, 2nd edition, 2006.

[53] D. L. Ragozin. Constructive polynomial approximation on spheres and projective spaces. *T. Am. Math. Soc.*, 162:157–170, 1971.

[54] E. A. Rakhmanov, E. B. Saff, and Y. Zhou. Minimal discrete energy on the sphere. *Math. Res. Lett*, 1(6):647–662, 1994.

[55] M. Reimer. Quadrature rules for the surface integral of the unit sphere based on extremal fundamental systems. *Math. Nachr.*, 169(1):235–241, 1994.

[56] R. J. Renka. Multivariate interpolation of large sets of scattered data. *ACM Tran. Math. Soft. (TOMS)*, 14(2):139–148, 1988.

[57] E. B. Saff and A. B. J. Kuijlaars. Distributing many points on a sphere. *The Mathematical Intelligencer*, 19(1):5–11, 1997.

[58] I. J. Schoenberg. Positive definite functions on spheres. *Duke Math. J.*, 1:172, 1988.

[59] L. L. Schumaker. *Spline functions: basic theory*. Wiley New York, 1981.

[60] P. D. Seymour and T. Zaslavsky. Averaging sets: a generalization of mean values and spherical designs. *Adv. Math.*, 52(3):213–240, 1984.

[61] I. H. Sloan. Polynomial interpolation and hyperinterpolation over general regions. *J. Approx. Theo.*, 83(2):238–254, 1995.

[62] I. H. Sloan and A. Sommariva. Approximation on the sphere using radial basis functions plus polynomials. *Advances in Comp. Math.*, 29(2):147–177, 2008.

[63] I. H. Sloan and R. S. Womersley. Extremal systems of points and numerical integration on the sphere. *Adv. Comput. Math.*, 21(1-2):107–125, 2004.

[64] I. H. Sloan and R. S. Womersley. A variational characterisation of spherical designs. *J. Approx. Theo.*, 159(2):308–318, 2009.

[65] I. H. Sloan and R. S. Womersley. Filtered hyperinterpolation: a constructive polynomial approximation on the sphere. *GEM-Intern. J. Geomath.*, 3(1):95–117, 2012.

[66] J. Sun and G. W. Stewart. *Matrix perturbation theory*. Computer science and scientific computing. Academic Press, 1990.

[67] G. Szegö. *Orthogonal polynomials*, volume 23. American Mathematical Society New York, 1959.

[68] R. Tibshirani. Regression shrinkage and selection via the lasso. *J. Roy. Stat. Soc. B*, 58:267–288, 1996.

[69] K. C. Toh, R. H. Tutuncu, and M. J. Todd. On the implementation of sdpt3 (version 3.1)-a matlab software package for semidefinite-quadratic-linear programming. In *Computer Aided Control Systems Design (2004)*.

[70] D. Varshalovich, A. Moskalev, and V. Khersonskii. *Quantum theory of angular momentum*. World Scientific, 1988.

[71] M. Von Golitschek and L. L. Schumaker. Data fitting by penalized least squares. In *Algorithms for approximation II*, pages 210–227. Springer, 1990.

[72] H. Wendland. *Scattered data approximation*, volume 17. Cambridge University Press, 2005.

[73] Y. Xu and E. W. Cheney. Strictly positive definite functions on spheres. *P. Am. Math. Soc.*, 116:977–981, 1992.